Tennessee Valley Authority (TVA) Regional Operations Center (Courtesy of TVA)

6

POWER FLOWS

Successful power system operation under normal balanced three-phase steady-state conditions requires the following:

1. Generation supplies the demand (load) plus losses.
2. Bus voltage magnitudes remain close to rated values.
3. Generators operate within specified real and reactive power limits.
4. Transmission lines and transformers are not overloaded.

The power-flow computer program (sometimes called *load flow*) is the basic tool for investigating these requirements. This program computes the voltage magnitude and angle at each bus in a power system under balanced three-phase steady-state conditions. It also computes real and reactive power flows for all equipment interconnecting the buses, as well as equipment losses.

Both existing power systems and proposed changes including new generation and transmission to meet projected load growth are of interest.

Conventional nodal or loop analysis is not suitable for power-flow studies because the input data for loads are normally given in terms of power, not impedance. Also, generators are considered as power sources, not voltage or current sources. The power-flow problem is therefore formulated as a set of nonlinear algebraic equations suitable for computer solution.

In Sections 6.1–6.3 we review some basic methods, including direct and iterative techniques for solving algebraic equations. Then in Sections 6.4–6.6 we formulate the power-flow problem, specify computer input data, and present two solution methods, Gauss–Seidel and Newton–Raphson. Means for controlling power flows are discussed in Section 6.7. Sections 6.8 and 6.9 introduce sparsity techniques and a fast decoupled power-flow method, while Section 6.10 discusses the dc power flow, and Section 6.11 considers the power-flow representation of wind turbine generators.

Since balanced three-phase steady-state conditions are assumed, we use only positive-sequence networks in this chapter. Also, all power-flow equations and input/output data are given in per-unit.

CASE STUDY

Power-flow programs are used to analyze large transmission grids and the complex interaction between transmission grids and the power markets. Historically, these transmission grids were designed primarily by local utilities to meet the needs of their own customers. But increasingly there is a need for coordinated transmission system planning to create coordinated, continent-spanning grids. The following article details some of the issues associated with such large-scale system planning.

Future Vision: The Challenge of Effective Transmission Planning

BY DONALD J. MORROW AND RICHARD E. BROWN

Exceptional forces are changing the use of the transmission infrastructure in the United States. There are high expectations that the transmission system will support and enable national-level economic, renewable energy, and other emerging policy issues.

The U. S. transmission system was developed in a piecemeal fashion. Originally, transmission systems connected large generation facilities in remote areas to users of the electricity they produced. Shortly thereafter, utilities started to interconnect their systems in order to realize the benefits of improved reliability that larger systems offer and to get access to lower cost energy in other systems. Subsequent transmission lines were typically added incrementally to the network, primarily driven by the needs of the local utility and without wide-area planning considerations.

Opportunistic usage of the transmission system beyond its design occurred early in the U. S. electric system. The need for coordinated transmission planning among utilities soon followed. As early as 1925, small power pools formed to take advantage of the economies of developing larger, more cost-effective power plants that were made possible by the expanding transmission network. By today's standards, these power pools were rather simple affairs made up of localized pockets of utilities that shared the expenses of fuel and operation and maintenance of shared units.

Today, the transmission system is increasingly being called upon to serve as the platform to enable sophisticated and complex energy and financial transactions. New market systems have been developed that allow transactions interconnection-wide. Today, a utility can purchase power without knowing the seller. These same market systems have the ability to enable transactions to be interconnection-wide and will soon accommodate the ability of load-serving entities to bid in their loads.

As the barriers to participate in electricity markets start to disappear, the U. S. electric system starts to look small from the perspective of market participants. In his book *The World is Flat*, author Thomas Friedman states, "The world is flat." That is, the location of producers and consumers no longer matters in the world. It is the expectation of wholesale electricity market participants that they can soon claim, "The transmission system is flat." That is, the transmission system is such that the location of power producers and power purchasers does not matter in terms of participation in national electricity markets.

Unfortunately, the vast majority of transmission infrastructure was not designed for this purpose. The existing transmission infrastructure is aging, and new transmission investment hasn't kept pace with other development. This article discusses these challenges and then presents a vision for the future where effective planning can address the transmission expectations of today.

BENEFITS OF TRANSMISSION

The primary function of transmission is to transport bulk power from sources of desirable generation to bulk power delivery points. Benefits have traditionally included lower electricity costs, access to renewable energy such as wind and hydro, locating power plants away from large population centers, and access to alternative generation sources when primary sources are not available.

Historically, transmission planning has been done by individual utilities with a focus on local benefits. However, proponents of nationwide transmission policies now view the transmission system as an "enabler" of energy policy objectives at even the national level. This is an understandable expectation since a well-planned transmission grid has the potential to enable the following:

- **Efficient bulk power markets.** Bulk power purchasers should almost always be able to purchase from the lowest cost generation. Today, purchasers are often forced to buy higher-cost electricity to avoid violating transmission loading constraints. The difference between the actual price of electricity at the point of consumption and the lowest price on the grid is called the "congestion" cost.
- **Hedge against generation outages.** The transmission system should typically allow access to alternative economic energy sources to replace lost resources. This is especially critical when long-term, unplanned outages of large generation units occur.
- **Hedge against fuel price changes.** The transmission system should allow purchasers to economically access generation from diversified fuel resources as a hedge against fuel disruptions that may occur from strikes, natural disasters, rail interruptions, or natural fuel price variation.
- **Low-cost access to renewable energy.** Many areas suitable for producing electricity from renewable resources are not near transmission with spare capacity. The transmission system should usually allow developers to build renewable sources of energy without the need for expensive transmission upgrades (Figure 1).
- **Operational flexibility.** The transmission system should allow for the economic scheduling of maintenance outages and for the economic reconfiguration of the grid when unforeseen events occur.

Many of these benefits are available on a local level, since transmission systems have been planned by the local utility with these objectives in mind. However, these benefits are not fully realized on a regional or national level, since planning has traditionally been focused on providing these benefits at the local level.

AGING TRANSMISSION SYSTEM

Even at a local level, transmission benefits are in jeopardy. For the past 20 years, the growth of electricity demand has far outpaced the growth of transmission capacity. With limited new transmission capacity available, the loading of existing transmission lines has dramatically increased (Figure 2). North American Reliability Corporation (NERC) reliability criteria have still been maintained for the most part, but the transmission system is far more vulnerable to multiple contingencies and cascading events.

A large percentage of transmission equipment was installed in the postwar period between the mid-1950s and

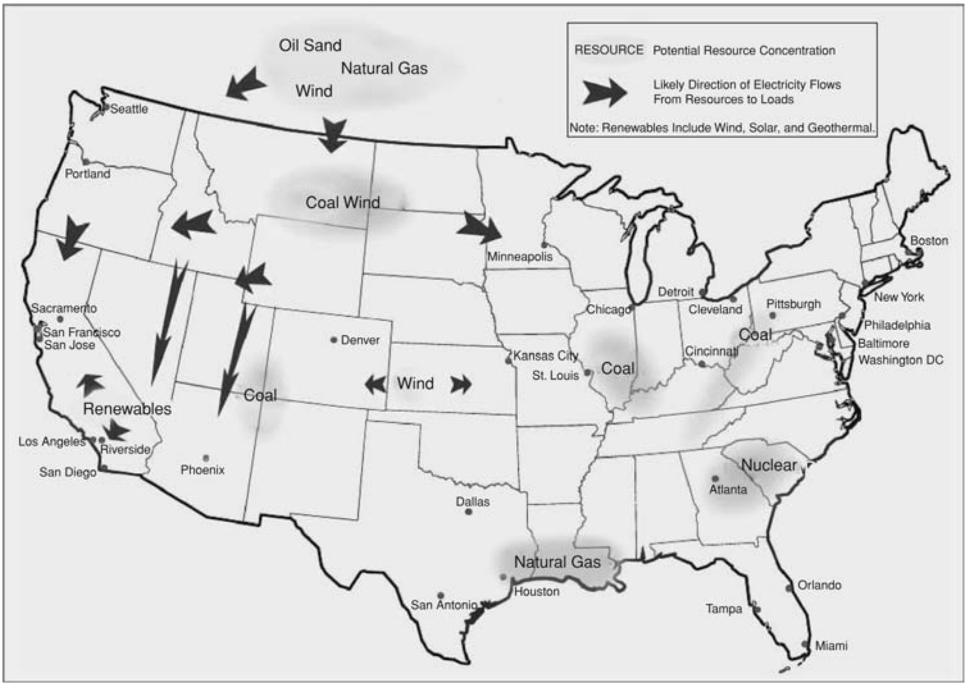

Figure 1
Potential sources of renewable energy concentrations (U.S. Department of Energy, *National Electric Transmission Congestion Study,* 2006)

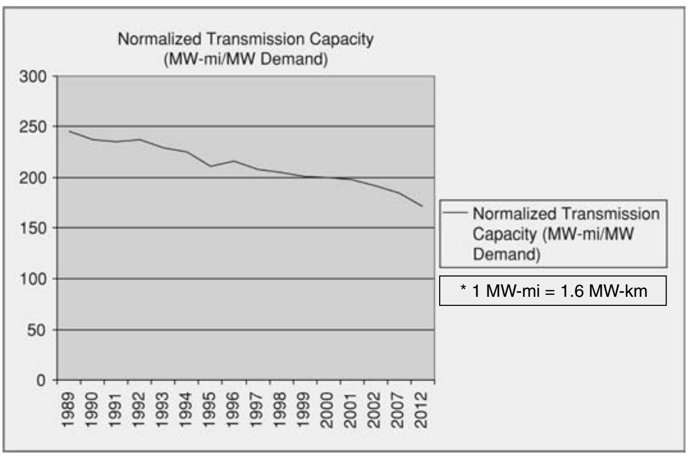

Figure 2
Transmission capacity normalized over MW demand (E. Hurst, *U.S. Transmission Capacity: Present Status and Future Prospects,* prepared for EEI and DOE, Aug. 2004)

the mid-1970s, with limited construction in the past 20 years. The equipment installed in the postwar period is now between 30 and 50 years old and is at the end of its expected life (Figure 3). Having a large amount of old and aging equipment typically results in higher probabilities of failure, higher maintenance costs, and higher replacement costs. Aging equipment will eventually have to be replaced, and this replacement should be planned and coordinated with capacity additions.

According to Fitch Ratings, 70% of transmission lines and power transformers in the United States are 25 years old or older. Their report also states that 60% of high-voltage circuit breakers are 30 years old or older. It is this aging infrastructure that is being asked to bear the burden of increased market activity and to support policy developments such as massive wind farm deployment.

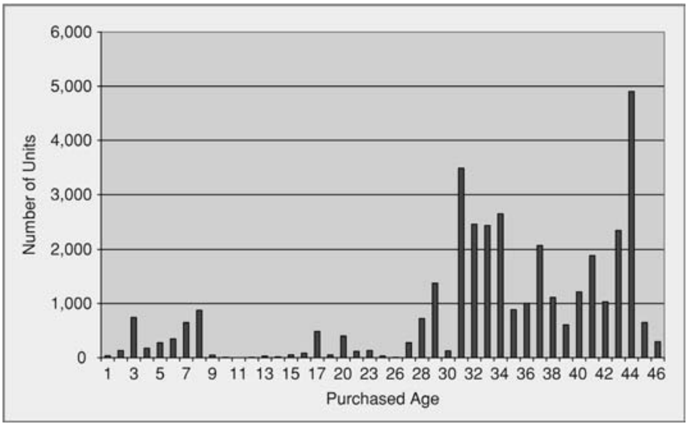

Figure 3
The age distribution of wood transmission poles for a Midwestern utility. Most of these structures are over 30 years old

Transmission interconnections to neighboring utilities for the purposes of importing and exporting bulk power and the development of transmission projects that spanned multiple utilities were also the responsibility of the vertically integrated utility. They were negotiated projects that often took years of effort to ensure that ownership shares and cost allocations were acceptable to each party and that no undue burden was placed on the affected systems.

Planning coordination eventually emerged, facilitated through the regional reliability councils (RRCs). Committees were formed that performed aggregate steady-state and dynamic analysis on the total set of transmission owner (TO) plans. These studies were performed under the direction of committee members, facilitated by RRC staff, to ensure that NERC planning policies (the predecessor to today's NERC standards) and regional planning guidelines were satisfied. Insights from these studies were used by planners to adjust their projects if necessary. Some regions still follow this process for their coordinated planning activities.

Today, the industry is beginning to spend more money on new transmission lines and on upgrading existing transmission lines. It is critical that this new transmission construction be planned well, so that the existing grid can be systematically transformed into a desired future state rather than becoming a patchwork of incremental decisions and uncoordinated projects.

PLANNING CHALLENGES

As the transmission system becomes flatter, the processes to analyze and achieve objectives on a regional or interconnection-wide basis have lagged. Current planning processes simply do not have the perspective necessary to keep pace with the scope of the economic and policy objectives being faced today. While the planners of transmission owners often recognize these needs, addressing these needs exceeds the scope of their position. Regional transmission organizations exist today, but these organizations do not have the ability to effectively plan for interconnect-wide objectives.

PLANNING BEFORE OPEN ACCESS

Before access to the electric system was required by the Federal Energy Regulatory Commission (FERC) in 1996, a vertically integrated utility would plan for generation and transmission needs within its franchise territory. This allowed for a high degree of certainty because the decisions regarding the timing and location of new generation and transmission were controlled by the utility. These projects were developed to satisfy the utility's reliability and economic needs.

PLANNING AFTER OPEN ACCESS

The Open Access Tariff of 1996 (created through FERC Order 888) requires functional separation of generation and transmission within a vertically integrated utility. A generation queue process is now required to ensure that generation interconnection requests are processed in a nondiscriminatory fashion and in a first-come, first-served order. FERC Order 889, the companion to Order 888, establishes the OASIS (Open Access Same-time Information System) process that requires transmission service requests, both external and internal, to be publicly posted and processed in the order in which they arc entered. Order 889 requires each utility to ensure nonpreferential treatment of its own generation plan. Effectively, generation and transmission planning, even within the same utility, are not allowed to be coordinated and integrated. This has been done to protect nondiscriminatory, open access to the electric system for all parties.

These landmark orders have removed barriers to market participation by entities such as independent power producers (IPPs) and power marketers. They force utilities to follow standardized protocols to address their needs and allow, for the most part, market forces to drive the addition of new generation capacity.

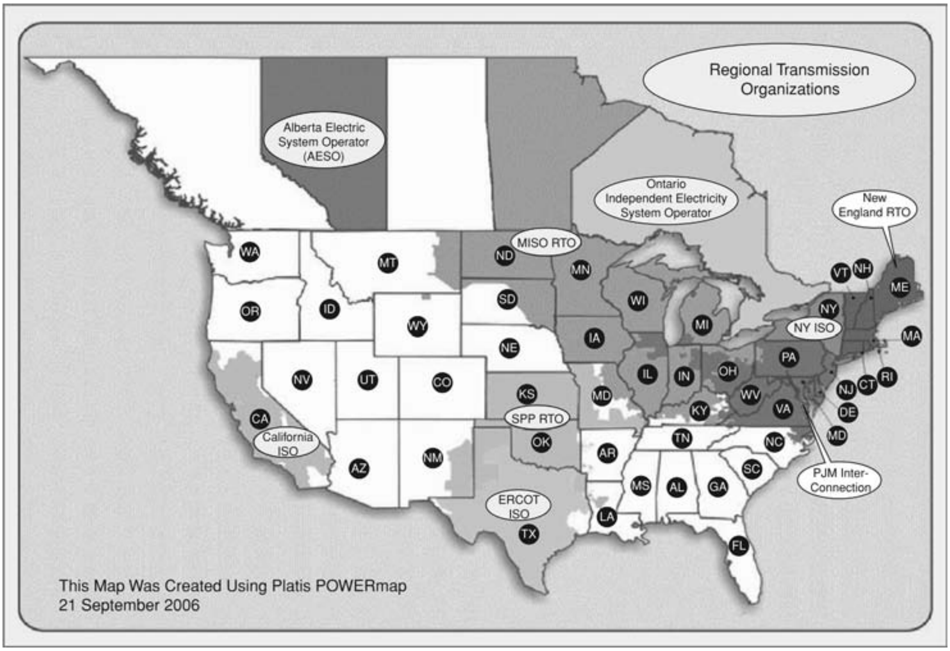

Figure 4
Regional transmission organizations in the United Stated and Canada

These orders also complicated the planning process, since information flow within planning departments becomes one-directional. Transmission planners know all the details of proposed generation planners through the queue process, but not vice versa. A good transmission plan is now supposed to address the economic objectives of all users of the transmission grid by designing plans to accommodate generation entered into the generation queue and to ensure the viability of long-term firm transmission service requests entered through OASIS. However, utility transmission planners continue to design their transmission systems largely to satisfy their own company's reliability objectives.

These planning processes designed the electric system in the Eastern United States and Canada that existed on 13 August 2003. The blackout that occurred that day which interrupted more the 50 million customers made it clear what planners were beginning to suspect-that the margins within the system were becoming dangerously small. The comprehensive report performed by the U. S.—Canada Power System Outage Task Force summarizes the situation as follows:

> A smaller transmission margin for reliability makes the preservation of system reliability a harder job than it used to be. The system is being operated closer to the edge of reliability than it was just a few years ago.

PLANNING IN THE ERA OF THE RTO

Well before the 2003 blackout, FERC realized that better coordination among transmission owners is required for efficient national electricity markets. FERC Order 2000 issued in December 1999 established the concept of the regional transmission operator (RTO) and requires transmission operators to make provisions to form and participate in these organizations.

In this order, FERC establishes the authority of an RTO to perform regional planning and gives it the ultimate responsibility for planning within its region. Order 2000 allowed a 3-year phase-in to allow the RTO to develop the processes and capabilities to perform this function. For the first time in its history, the U. S. electric system has the potential for a coordinated, comprehensive regional planning process (Figure 4 shows the existing RTOs in the United States and Canada).

Despite the advance of developing planning organizations that aligned with the scope of the reliability and economic needs of a region, a significant gap was introduced between planning a system and implementing the plan. Order 2000 recognizes this gap with the following statement:

> We also note that the RTO's implementation of this general standard requires addressing many specific design questions, including who decides which projects should be built and how the costs and benefits of the project should be allocated.

Determining who decides which project should be built is a difficult problem. Does the RTO decide which projects are to be built since it has planned the system? Does the TO decide which projects are to be built since it bears the project development risks such as permitting, regulatory approval, right-of-way acquisition financing, treatment of allowance for funds used during construction (AFUDC), construction, cost escalation, and prudency reviews?

If the issue of project approval is not properly addressed, it is easy to envision a situation where planners spend significant efforts and costs to design a grid that satisfies critical economic and policy objectives. This plan ultimately languishes on the table because no TO wants to build it, no TO has the ability to build it, or no state regulator will approve it. To their credit, RTOs and their member transmission owners recognize this gap and have begun to take steps to resolve it.

TECHNICAL CHALLENGES

The main technical criteria that should drive transmission planning are reliability and congestion. Reliability relates to unexpected transmission contingencies (such as faults) and the ability of the system to respond to these contingencies without interrupting load. Congestion occurs when transmission reliability limitations result in the need to use higher-cost generation than would be the case without any reliability constraints. Both reliability and congestion are of critical importance and present difficult technical challenges.

Transmission reliability is tracked and managed by NERC, which as of 20 July 2006 now serves as the federal electric reliability organization (ERO) under the jurisdiction of FERC. For decades, the primary reliability consideration used by NERC for transmission planning has been "*N*-l." For a system consisting of N major components, the *N*-1 criterion is satisfied if the system can perform properly with only *N*-1 components in service. An *N*-1 analysis consists of a steady-state and a dynamic component. The steady-state analysis checks to see if the transmission system can withstand the loss of any single major piece of equipment (such as a transmission line or a transformer) without violating voltage or equipment loading limits. The dynamic analysis checks to see if the system can retain synchronism after all potential faults.

N-1 has served the industry well but has several challenges when applied to transmission planning today. The first is its deterministic nature; all contingencies are treated equal regardless of how likely they are to occur or the severity of consequences. The second, and more insidious, is the inability of *N*-1 (and *N*-2) to account for the increased risk associated with a more heavily interconnected system and a more heavily loaded system.

When a system is able to withstand any single major contingency, it is termed "*N*-l secure." For a moderately loaded *N*-l secure system, most single contingencies can be handled even if the system response to the contingency is not perfect. When many components of a transmission system are operated close to their thermal or stability limits, a single contingency can significantly stress the system and can lead to problems unless all protection systems and remedial actions operate perfectly. In this sense, moderately loaded systems are "resilient" and can often absorb multiple contingencies and/or cascading events. Heavily loaded systems are brittle and run the risk of widespread outages if an initiating event is followed by a protection system failure or a mistake in remedial actions. Since blackouts invariably involve multiple contingencies and/or cascading events, *N*-1 and *N*-2 are not able to effectively plan for wide-area events.

N-1 secure systems are, by design, not able to withstand certain multiple contingencies. When equipment failure rates are low, this is a minor problem. When equipment failure rates increase due to aging and higher loading, this problem becomes salient. Consider the likelihood of two pieces of equipment experiencing outages that overlap. If the outages are independent, the probability of overlap increases with the square of outage rate. Similarly, the probability of three outages overlapping (exceeding *N*-2) increases with the cube of outage rate. Blackouts typically result from three or more simultaneous contingencies. If transmission failure rates double due to aging and higher loading, the likelihood of a third-order event increases by a factor of eight or more. Today's transmission systems may remain *N*-1 or *N*-2 secure, but the risk of wide-area events is much higher than a decade ago.

Computationally it is difficult to plan for wide-area events. This is due to large system models, a high number of potential contingencies, and convergence difficulties.

Consider the eastern interconnected system, which would require over 150,000 major components in a power flow model. This size exceeds the useful capabilities of present planning software, even when exploring only a few cases. To plan for all triple contingencies, more than 3 sextillion (thousand trillion) cases must be considered. Even if only one out of every million of cases is considered, more than 3 billion simulations must be performed. Each simulation is also at risk for nonconvergence, since a system under multiple contingencies will often have a solution very different from the base case.

In addition to reliability planning, it is becoming increasingly important to plan for congestion (the 2006 Department of Energy congestion study reports that two constraints alone in PJM Interconnection resulted in congestion costs totaling US$1. 2 billion in 2005). Basic congestion planning tools work as follows. First, hourly loads for an entire year are assigned to each bulk power delivery point. Second, a load flow is performed for each hour (accounting for scheduled generation and transmission maintenance). If transmission reliability criteria are violated, remedial actions such as generation re-dispatch is performed until the constraints are relieved. The additional energy costs resulting from these remedial actions is assigned to congestion cost (sophisticated tools will also incorporate generation bidding strategies and customer demand curves). Each case examined in a congestion study is computationally intensive.

There are many ways to address existing congestion problems, but it difficult from a technical perspective to combine congestion planning with reliability planning. Imagine a tool with the capability to compute both the reliability and congestion characteristics of a system. A congestion simulation is still required, but unplanned contingencies must now be considered. To do this, each transmission component is checked in each hour of the simulation to see if a random failure occurs. If so, this component is removed from the system until it is repaired, potentially resulting in increased congestion costs. Since each simulated year will only consider a few random transmission failures, many years must be simulated (typically 1,000 or more) for each case under consideration. These types of tools are useful when only the existing transmission system is of interest, such as for energy traders or for dealing with existing congestion problems. For transmission planners that need to consider many scenarios and many project alternatives, these types of tools are insufficient at this time.

The last major technical challenge facing transmission planning is the application of new technologies such as phasor measurements units, real-time conductor ratings, and power electronic devices. Proper application of these devices to address a specific problem already requires a specialist familiar with the technology. Considering each new technology as part of an overall proactive planning process would require new tools, new processes, and transmission planners familiar with the application of all new technologies.

Perhaps the biggest technical challenge to transmission planning is overcoming the traditional mindset of planners. Traditionally a utility transmission planner was primarily concerned with the transport of bulk generation to load centers without violation of local constraints. In today's environment, effective transmission planning requires a wide-area perspective, aging infrastructure awareness, a willingness to coordination extensively, an economic mindset, and an ability to effectively integrate new technologies with traditional approaches.

INFRASTRUCTURE DEVELOPMENT CHALLENGES

Developing transmission projects has been a daunting affair in recent years, and significant roadblocks still exist. A partial list of these roadblocks includes:

- NIMBY mentality (Not In My Back Yard)
- organized public opposition
- environmental concerns
- lack of institutional knowledge
- regulatory risk
- uncontrolled cost increases
- political pressures
- financing risks.

Perhaps the biggest impediment to transmission infrastructure development is the risk of cost recovery. AFUDC rate treatment is the present norm for transmission project financing. This allows the accrued cost of financing for development of a utility project to be included in rates for cost recovery. Recovery is typically only allowed after a project is completed and after state regulatory prudency review on the project. The effect is a substantial risk of cost nonrecovery that discourages transmission investment. If a project fails during development or is judged to be imprudent, AFUDC recovery may not be allowed and the shareholders then bear the financial risk. Without assurances for cost recovery, it will be very difficult to build substantial amounts of new transmission. Minimizing development risks becomes of paramount importance when developing the types of projects necessary for regional and national purposes.

VISION FOR THE FUTURE

The challenges facing effective transmission planning are daunting, but pragmatic steps can be taken today to help the industry move toward a future vision capable of meeting these challenges. The following are suggestions that address the emerging economic and policy issues of today and can help to plan for a flexible transmission system that can effectively serve a variety of different future scenarios.

DEVELOP AN ALIGNED PLANNING PROCESS

Effective planning requires processes and methodologies that align well with the specific objectives being addressed. A good process should "de-clutter" a planning problem and align planning activity with the geographic scope of the goals. The process should push down the planning problem to the lowest possible level to reduce analytical requirements and organizational burden to a manageable size.

If the planning goal is to satisfy the reliability needs for communities in a tight geographic area, planning efforts should be led by the associated TO. This type of planning can be considered "bottom up" planning since it starts with the specific needs of specific customers. If the planning goal is to address regional market issues, planning efforts should be led by the associated RTO. This type of planning can be considered "top down" since it addresses the general requirements of the transmission system itself (in this case the ability to be an efficient market maker).

Typically, RTOs have drawn a demarcation line at an arbitrary voltage level (100 kV is typical). Below this line, TOs are responsible for the transmission plan. Above the line, RTOs are responsible for the transmission plan. This criterion can run counter to the "de-cluttering" principle. Very often, local planning requires solutions that go above 100 kV, and regional solutions may require the need to reach below 100 kV.

TOs and RTOs can effectively address planning issues corresponding to local and regional areas, respectively, but what about issues of national scope? Consider the current issue of renewable energy. For example, many states in the Northeast are beginning to set renewable energy portfolio targets that will require access to renewable energy concentrations in other parts of the country. Access to these resources will require crossing multiple RTO boundaries and/or transmission systems currently without RTO oversight.

Individual RTOs and TOs do not have the geographic perspective necessary to effectively address these types of broader issues. Who then should play this national role? RTOs working together could potentially be effective if the process is perceived as fair and equitable for all regions. However, if it is perceived that one region's objectives are beginning to take precedence over others, then a new national organization may be required.

If such a national step were taken, the role of the RTO must shift toward integrating member TO plans necessary to meet local load serving needs, integrating the EHV plan to address the national policy, and creating the regional plan that necessarily results to accommodate the regional objectives. The role would implement the strategic national plan and enables the tactical at the regional and local levels.

ADDRESSING THE REGULATORY NEED

The gap between planning a system and getting it developed needs to be closed. Planners should recognize that regulators are the ultimate decision makers. They decide whether or not a project is developed, not the planner. Therefore, planners must perform their work in a way that maximizes the probability of regulatory approval for their projects.

The regulatory oversight role is to ensure that transmission investment is prudent. It also ensures that public impacts are minimized. Planners need to recognize these roles and address these concerns early in and throughout the planning processes.

To address the prudency question, transmission planning processes should be open to stakeholder participation and permit stakeholders to have influence on a project. This ensures that a broadly vetted set of goals and objectives are being addressed by the process.

The objectives of an open planning process are:

- Transparency: the ability of affected stakeholders to observe and influence the planning processes and decisions
- Traceable: the ability for all parties to track the flow of planning effort throughout the life cycle of a project or overall plan
- Defendable: the appropriateness and completeness of the process from the perspective of key decision

makers such as RTO management, TOs, and regulators
- Dynamic: the ability to adjust the process for good reasons.

For planning at the regional or national levels, regulators expect that plans balance the benefits across the footprint and that stakeholder needs are addressed in an unbiased way. By design, RTOs do not own the facilities they plan and operate. By de-coupling the financial benefit of the transmission plan from the RTO, FERC hoped to ensure that plans were forwarded only driven by the needs of the stakeholders and designed in such a way as to minimize the overall cost regardless of the ownership boundaries. This independence is used by regulators to help make the prudency assessment since a project will, at least theoretically, only be approved for the "right" reasons.

To address the impacts on the public, planning processes need to encourage public involvement preferably early on in the process. Use of techniques such as press releases, community meetings, public planning meetings, open houses, and interactions with community development groups, economic development commissions, and regional planning commissions are extremely effective in addressing the public concerns in a meaningful way.

The effect is significant. First, the feedback provided can significantly aid in route selection and allow the planner and ultimate developer to better predict the costs of a project. Second, and equally important, if the public feels it has been heard and has had a meaningful chance to influence the results, the opposition is significantly muted. If not, the opposition is empowered and is able to recruit support from a much wider audience. The public tends to fear the unknown more than the known.

Many TOs know that these efforts are critical to the success of their projects, and some have successfully incorporated this outreach into their planning and infrastructure development efforts.

However, RTOs seem less aware of the importance of the public outreach step. A search of RTO Web sites shows significant efforts expended to bring certain stakeholders into their processes (highly commendable and necessary) but little efforts to bring in the public. There is a need for the public to be appropriately involved in the process. If regional and national transmission projects are to be planned in a way that maximizes the likelihood of approval, then the public input must be meaningfully provided. While difficult, creative thought needs to be applied to determine how to meaningfully bring the public into the regional and national forums.

ADDRESSING THE NEEDS OF THE DEVELOPER

At the RTO level, the regulatory need for an independent plan makes it more difficult to incorporate the needs of developers. The perception of independence needs to be protected to ensure the RTO appropriately plays its FERC-appointed role.

However, by bringing the stakeholders and the public into the planning process, developers have greater assurance that a project will be approved, that costs have been more accurately estimated, and that opposition has been minimized. Meaningfully addressing these issues in the RTO process are significant steps in encouraging developers to come forward.

ENHANCED PROJECT JUSTIFICATION

The advent of electricity markets illustrates the need for a richer understanding of the economic benefits of transmission projects. New facilities can have significant energy price impacts and, therefore, affect the underlying value of financial transmission rights. The evolving electricity markets are creating new winners and losers. As a result, it has become more critical to understand the economic benefits of transmission projects, especially at regional and national levels.

Project justification during the planning process needs to incorporate the pricing information available from these developing markets. Energy price history is now available to calibrate the analysis (Figure 5). Analysis tools that merge production cost analysis with transmission system constraints now exist to aid the planning in getting insights into the economic value of projects. As discussed above, these tools are difficult to use when considering myriads of alternative projects. However, they can be extremely effective in selecting between a narrowed-down set of alternatives.

For planning on a regional or national level, probabilistic methods show promise in managing the scope of studies necessary to perform *N*-2 or higher contingency analysis. At the regional or national level, decluttering still results in a network of significant scope. At the national level, the dynamics of an interconnect-wide system are poorly understood by any one planning entity.

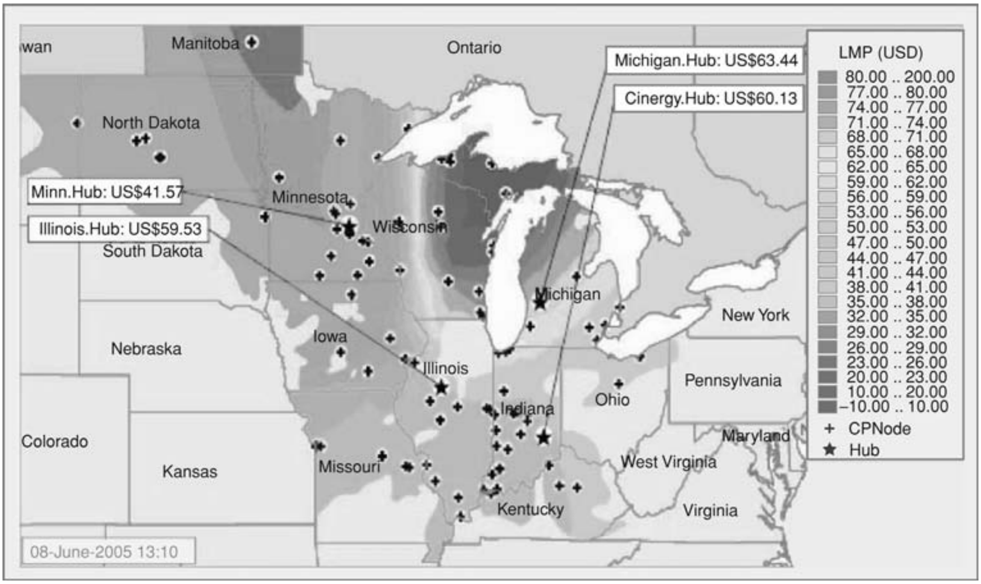

Figure 5
Examples of locational marginal price (LMP) information

Two things are certain; the United States needs to build more transmission capacity and it needs to begin to deal with aging transmission infrastructure. There are many challenges, but better transmission planning is needed to effectively address these issues in an integrated and cost-effective manner.

FOR FURTHER READING

B. Beck, *Interconnections: The History of the Mid-Continent Area Power Pool.* Minneapolis, MN: The Pool, 1988.

U.S. Department of Energy, *National Electric Transmission Congestion Study,* 2006, [Online]. Available: http://nietc.anl.gov/documents/docs/Congestion_Study_2006-9MB.pdf

E. Hirst, *U.S. Transmission Capacity: Present Status and Future Prospects,* EEI and DOE, Aug. 2004. [Online]. Available: http://www.oe.energy.gov/DocumentsandMedia/transmission_capacity.pdf

Fitch Ratings, *Frayed Wires: U.S. Transmission System Shows Its Age,* Oct. 25, 2006.

U.S.-Canada Power System Outage Task Force, *Causes of the August 14 2003 Blackout in the United States and Canada,* 2003.

BIOGRAPHIES

Donald. J. Morrow is vice president with the Technology Division of InfraSource. Morrow has extensive experience in transmission system planning, system operations, and transmission development. In his previous role, he was director of system planning and protection at American Transmission Company, a stand-alone transmission company in the upper Midwest. In this capacity he managed a US$3 billion/year capital budget portfolio. Morrow has been actively involved in many industry organizations including NERC and MISO. He has a B.S.E.E. and an executive M.B.A., both from the University of Wisconsin, Madison. He is a registered professional engineer in Wisconsin and a member of the IEEE.

Richard E. Brown is a vice president with the Technology Division of InfraSource. Brown has published more than 70 technical papers related to power system reliability and asset management, is author of the book *Electric Power Distribution Reliability*, and has provided consulting services to most major utilities in the United States. He is an IEEE Fellow and vice-chair of the Planning and Implementation Committee. Dr. Brown has a B.S.E.E., M.S.E.E., and Ph.D. from the University of Washington, Seattle, and an M.B.A. from the University of North Carolina, Chapel Hill.

Characteristics of Wind Turbine Generators for Wind Power Plants: IEEE PES Wind Plant Collector System Design Working Group

CONTRIBUTING MEMBERS: E. H. CAMM, M. R. BEHNKE, O. BOLADO, M. BOLLEN, M. BRADT, C. BROOKS, W. DILLING, M. EDDS, W. J. HEJDAK, D. HOUSEMAN, S. KLEIN, F. LI, J. LI, P. MAIBACH, T. NICOLAI, J. PATIÑO, S. V. PASUPULATI, N. SAMAAN, S. SAYLORS, T. SIEBERT, T. SMITH, M. STARKE, R. WALLING

Abstract—This paper presents a summary of the most important characteristics of wind turbine generators applied in modern wind power plants. Various wind turbine generator designs, based on classification by machine type and speed control capabilities, are discussed along with their operational characteristics, voltage, reactive power, or power factor control capabilities, voltage ride-through characteristics, behavior during short circuits, and reactive power capabilities.

Index Terms—Wind turbine generator, voltage ride-through, wind power plants.

I. INTRODUCTION

Modern wind power plants (WPPs), comprised of a large number of wind turbine generators (WTGs), a collector system, collector and/or interconnect substation utilize machines that are designed to optimize the generation of power using the energy in the wind. WTGs have developed from small machines with output power ratings on the order of kilowatts to several megawatts, and from machines with limited speed control and other capabilities to machines with variable speed control capabilities over a wide speed range and sophisticated control capabilities using modern power electronics [1].

The application of WTGs in modern WPPs requires an understanding of a number of different aspects related to the design and capabilities of the machines involved. This paper, authored by members of the Wind Plant Collector Design Working Group of the IEEE, is intended to provide insight into the various wind turbine generator designs, based on classification by machine type and speed control capabilities, along with their operational characteristics, voltage, reactive power, or power factor control capabilities, voltage ride-through characteristics, behavior during short circuits, and reactive power capabilities.

II. TURBINE CHARACTERISTICS

The principle of wind turbine operation is based on two well-known processes. The first one involves the conversion of kinetic energy of moving air into mechanical energy. This is accomplished by using aerodynamic rotor blades and a variety of methodologies for mechanical power control. The second process is the electromechanical energy conversion through a generator that is transmitted to the electrical grid.

Wind turbines can be classified by their mechanical power control, and further divided by their speed control. All turbine blades convert the motion of air across the air foils to torque, and then regulate that torque in an attempt to capture as much energy as possible, yet prevent damage. At the top level turbines can be classified as either stall regulated (with active stall as an improvement) or pitch regulated.

Stall regulation is achieved by shaping the turbine blades such that the airfoil generates less aerodynamic force at high wind speed, eventually stalling, thus reducing the turbine's torque-this is a simple, inexpensive and robust mechanical system. Pitch regulation, on the other hand, is achieved through the use of pitching devices in the turbine hub, which twist the blades around their own axes. As the wind speed changes, the blade quickly pitches to the optimum angle to control torque in order to capture the maximum energy or self-protect, as needed. Some turbines now are able to pitch each blade independently to achieve more balanced torques on the rotor shaft given wind speed differences at the top and bottom of the blade arcs.

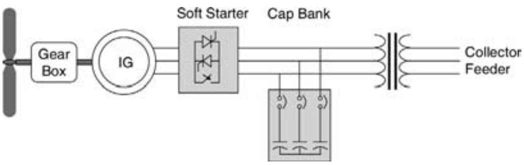

Figure 1
Typical Configuration of a Type 1 WTG

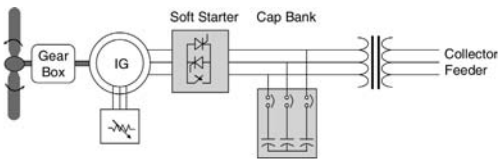

Figure 3
Typical Configuration of a Type 2 WTG

Beyond mechanical power regulation, turbines are further divided into fixed speed (Type 1), limited variable speed (Type 2), or variable speed with either partial (Type 3) or full (Type 4) power electronic conversion. The different speed control types are implemented via different rotating ac machines and the use of power electronics. There is one other machine type that will be referred to as Type 5 in which a mechanical torque converter between the rotor's low-speed shaft and the generator's high-speed shaft controls the generator speed to the electrical synchronous speed. This type of machine then uses a synchronous machine directly connected to the medium voltage grid.

The Type 1 WTG is implemented with a squirrel-cage induction generator (SCIG) and is connected to the step-up transformer directly. See Figure 1. The turbine speed is fixed (or nearly fixed) to the electrical grid's frequency, and generates real power (P) when the turbine shaft rotates faster than the electrical grid frequency creating a negative slip (positive slip and power is motoring convention).

Figure 2 shows the power flow at the SCIG terminals. While there is a bit of variability in output with the slip of the machine, Type 1 turbines typically operate at or very close to a rated speed. A major drawback of the induction machine is the reactive power that it consumes for its excitation field and the large currents the machine can draw when started "across-the-line." To ameliorate these effects the turbine typically employs a soft starter and discrete steps of capacitor banks within the turbine.

In Type 2 turbines, wound rotor induction generators arc connected directly to the WTG step-up transformer in a fashion similar to Type 1 with regards to the machines stator circuit, but also include a variable resistor in the rotor circuit. See Figure 3. This can be accomplished with a set of resistors and power electronics external to the rotor with currents flowing between the resistors and rotor via slip rings. Alternately, the resistors and electronics can be mounted on the rotor, eliminating the slip rings—this is the Weier design. The variable resistors are connected into the rotor circuit softly and can control the rotor currents quite rapidly so as to keep constant power even during gusting conditions, and can influence the machine's dynamic response during grid disturbances.

By adding resistance to the rotor circuit, the real power curve, which was shown in Figure 2, can be "stretched" to the higher slip and higher speed ranges. See Figure 4. That is to say that the turbine would have

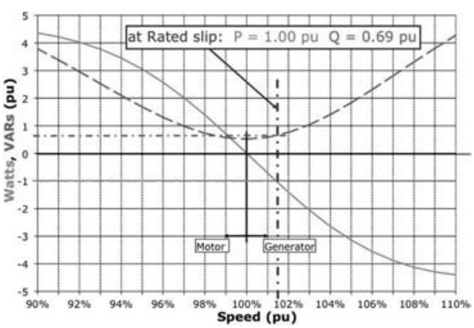

Figure 2
Variation of Real and Reactive Power for SCIG

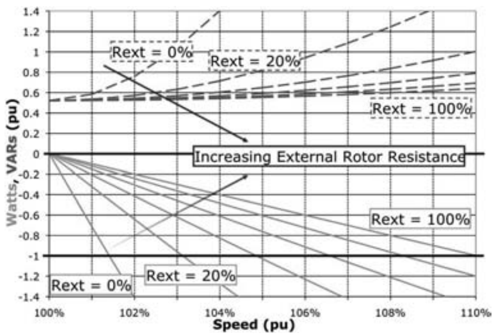

Figure 4
Variation of Real and Reactive Power with External Rotor Resitor in a Type 2 WTG

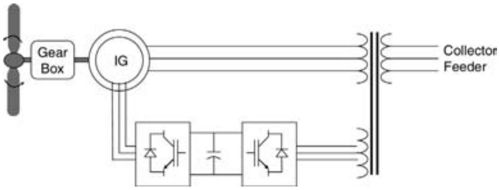

Figure 5
Typical Configuration of a Type 3 WTG

to spin faster to create the same output power, for an added rotor resistance. This allows some ability to control the speed, with the blades' pitching mechanisms and move the turbines operation to a tip speed ratio (ration of tip speed to the ambient wind speed) to achieve the best energy capture. It is typical that speed variations of up to 10% are possible, allowing for some degree of freedom in energy capture and self protective torque control.

The Type 3 turbine, known commonly as the Doubly Fed Induction Generator (DFIG) or Doubly Fed Asynchronous Generator (DFAG), takes the Type 2 design to the next level, by adding variable frequency ac excitation (instead of simply resistance) to the rotor circuit. The additional rotor excitation is supplied via slip rings by a current regulated, voltage-source converter, which can adjust the rotor currents' magnitude and phase nearly instantaneously. This rotor-side converter is connected back-to-back with a grid side converter, which exchanges power directly with the grid. See Figure 5.

A small amount power injected into the rotor circuit can effect a large control of power in the stator circuit. This is a major advantage of the DFIG—a great deal of control of the output is available with the presence of a set of converters that typically are only 30% of the rating of the machine. In addition to the real power that is delivered to the grid from the generator's stator circuit, power is delivered to the grid through the grid-connected inverter when the generator is moving faster than synchronous speed. When the generator is moving slower than synchronous speed, real power flows from the grid, through both converters, and from rotor to stator. These two modes, made possible by the four-quadrant nature of the two converters, allows a much wider speed range, both above and *below* synchronous speed by up to 50%, although narrower ranges are more common.

The greatest advantage of the DFIG, is that it offers the benefits of separate real and reactive power control, much like a traditional synchronous generator, while being able to run asynchronously. The field of industrial drives has produced and matured the concepts of vector or field oriented control of induction machines. Using these control schemes, the torque producing components of the rotor flux can be made to respond fast enough that the machine remains under relative control, even during significant grid disturbances. Indeed, while more expensive than the Type 1 or 2 machines, the Type 3 is becoming popular due to its advantages.

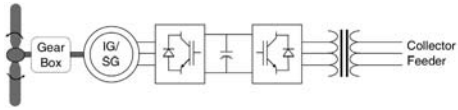

Figure 6
Typical Configuration of a Type 4 WTG

The Type 4 turbine (Figure 6) offers a great deal of flexibility in design and operation as the output of the rotating machine is sent to the grid through a full-scale back-to-back frequency converter. The turbine is allowed to rotate at its optimal aerodynamic speed, resulting in a "wild" ac output from the machine. In addition, the gearbox may be eliminated, such that the machine spins at the slow turbine speed and generates an electrical frequency well below that of the grid. This is no problem for a Type 4 turbine, as the inverters convert the power, and offer the possibility of reactive power supply to the grid, much like a STATCOM. The rotating machines of this type have been constructed as wound rotor synchronous machines, similar to conventional generators found in hydroelectric plants with control of the field current and high pole numbers, as permanent magnet synchronous machines, or as squirrel cage induction machines. However, based upon the ability of the machine side inverter to control real and reactive power flow, any type of machine could be used. Advances in power electronic devices and controls in the last decade have made the converters both responsive and efficient. It does bear mentioning, however, that the power electronic converters have to be sized to pass the full rating of the rotating machine, plus any capacity to be used for reactive compensation.

Type 5 turbines (Figure 7) consist of a typical WTG variable-speed drive train connected to a torque/speed converter coupled with a synchronous generator. The torque/speed converter changes the variable speed of the rotor shaft to a constant output shaft speed. The closely coupled synchronous generator,

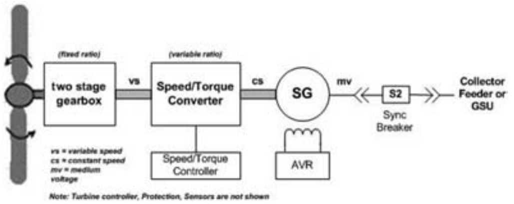

Figure 7
Typical Configuration of a Type 5 WTG

operating at a fixed speed (corresponding to grid frequency), can then be directly connected to the grid through a synchronizing circuit breaker. The synchronous generator can be designed appropriately for any desired speed (typically 6 pole or 4 pole) and voltage (typically medium voltage for higher capacities). This approach requires speed and torque control of the torque/speed converter along with the typical voltage regulator (AVR), synchronizing system, and generator protection system inherent with a grid-connected synchronous generator.

III. VOLTAGE, REACTIVE POWER, AND POWER FACTOR CONTROL CAPABILITIES

The voltage control capabilities of a WTG depend on the wind turbine type. Type 1 and Type 2 WTGs can typically not control voltage. Instead, these WTGs typically use power factor correction capacitors (PFCCs) to maintain the power factor or reactive power output on the low-voltage terminals of the machine to a setpoint. Types 3 through 5 WTGs can control voltage. These WTGs are capable of varying the reactive power at a given active power and terminal voltage, which enables voltage control [2]. In a Type 3 WTG voltage is controlled by changing the direct component of the rotor current (this is the component of the current that is in-line with the stator flux). In a Type 4 WTG voltage control is achieved by varying the quadrature (reactive) component of current at the grid-side converter. To allow voltage control capability, the grid-side converter must be rated above the rated MW of the machine. Since a synchronous generator is used in a Type 5 WTG, an automatic voltage regulator (AVR) is typically needed. Modern AVRs can be programmed to control reactive power, power factor and voltage.

The voltage control capabilities of individual WTGs are typically used to control the voltage at the collector bus or on the high side of the main power transformer. Usually a centralized wind farm controller will manage the control of the voltage through communication with the individual WTGs. A future companion Working Group paper is planned to discuss the WPP SCADA and control capabilities.

IV. REACTIVE POWER CAPABILITIES

The reactive power capabilities of modern WTGs are significant as most grid codes require the WPP to have reactive power capability at the point of interconnect over a specified power factor range, for example 0.95 leading (inductive) to 0.95 lagging (capacitive). Typical interconnect requirements related to total WPP reactive power capabilities are discussed in [3].

As stated earlier, Type 1 and Type 2 WTGs typically use PFCCs to maintain the power factor or reactive power of the machine to a specified setpoint. The PFCCs may be sized to maintain a slightly leading (inductive) power factor of around 0.98 at rated power output. This is often referred to as no-load compensation. With full-load compensation, the PFCCs are sized to maintain unity power factor or, in some cases, a slightly lagging (capacitive) power factor at the machine's rated power output. The PFCCs typically consists of multiple stages of capacitors switched with a low-voltage ac contactor.

Type 3 (DFIG) WTGs typically have a reactive power capability corresponding to a power factor of 0.95 lagging (capacitive) to 0.90 leading (inductive) at the terminals of the machines. Options for these machines include an expanded reactive power capability of 0.90 lagging to 0.90 leading. Some Type 3 WTGs can deliver reactive power even when the turbine is not operating mechanically, while no real power is generated.

As previously stated, Type 4 WTGs can vary the grid-side converter current, allowing control of the effective power factor of the machines over a wide range. Reactive power limit curves for different terminal voltage levels are typically provided. Some Type 4 WTGs can deliver reactive power even when the turbine is not operating mechanically, while no real power is generated.

The synchronous generator in a Type 5 WTG has inherent dynamic reactive power capabilities similar to that of Type 3 and 4 machines. See Figure 8. Depending on the design of the generator, operating power factor ranges at rated output can vary from 0.8 leading to 0.8 lagging.

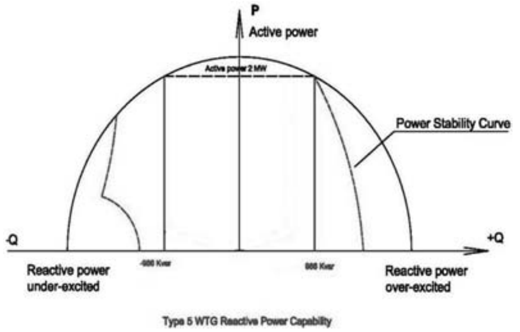

Figure 8
Reactive Power Capabilities of a 2 MW Type 5 WTG

A range of 0.9 leading and lagging is more typical. At power outputs below rated power, the reactive power output is only limited by rotor or stator heating, stability concerns, and local voltage conditions and it is unlikely that PFCCs would be required. As with some Type 3 and 4 WTGs, it is also possible to operate the machine as a synchronous condenser, requiring minimal active power output with adjustable reactive power output levels.

V. VOLTAGE RIDE-THROUOH

The voltage ride-through (VRT) capabilities of WTGs vary widely and have evolved based on requirements in various grid codes. In the United States, low voltage ride-through (LVRT) requirements specified in FERC Order 661-A [5] calls for wind power plants to ride-through a three-phase fault on the high side of the substation transformer for up to 9 cycles, depending on the primary fault clearing time of the fault interrupting circuit breakers at the location. There is no high voltage ride-through (HVRT) requirement in FERC order 661-A, but NERC and some ISO/RTOs are in the process of imposing such requirement. In many European countries WPP are required not to trip for a high voltage level up to 110% of the nominal voltage at the POI [4].

Some of the Type 1 WTGs have limited VRT capability and may require a central reactive power compensation system [4] to meet wind power plant VRT capability. Many of the Types 2, 3, and 4 WTGs have VRT capabilities that may meet the requirements of FERC Order 661, which was issued before FERC Order 661-A (i.e., withstand a three-phase fault for 9 cycles at a voltage as low as 0.15 p.u measured on the high side of the substation transformer). Most WTGs are expected to ultimately meet the FERC 661-A requirements.

The VRT of a Type 5 WTG is very similar to that of standard grid-connected synchronous generators, which are well understood. The capabilities of the excitation system (AVR) and physical design of the generator (machine constants, time constants) will determine the basic performance of a synchronous generator during transient conditions. In order to meet utility VRT requirements, the settings and operation of the turbine control system, excitation system and protection systems must be generally coordinated and then fine-tuned for a specific site.

VI. WTG BEHAVIOR DURING GRID SHORT CIRCUITS

The response of WTGs to short circuits on the grid depends largely on the type of WTG. While the response of Type 1 and Type 2 WTGs are essentially similar to that of large induction machines used in industrial applications, the response of Type 3, 4, and 5 WTGs is dictated by the WTG controls. In short circuit calculations, a Type 1 WTG can be represented as a voltage source in series with the direct axis sub-transient inductance X_d''. This practice is used to consider the maximum short-circuit contribution from the induction generator as it determines the symmetrical current magnitude during the first few cycles after the fault. A Type 1 WTG can contribute short circuit current up to the value of its locked rotor current which is usually on the order of 5 to 6 p.u [6].

Type 2 WTGs employing limited speed control via controlled external rotor resistance are fundamentally induction generators. If, during the fault, the external resistance control were to result in short-circuiting of the generator rotor, the short-circuit behavior would be similar to Type 1. On the other hand, if the control action at or shortly after fault inception were to result in insertion of the full external resistance, the equivalent voltage source-behind-Thevenin impedance representation for the WTG should be modified to include this significant resistance value in series with the equivalent turbine inductance.

Other wind turbine topologies employ some type of power electronic control. Consequently, the behavior during short-circuit conditions cannot be ascertained directly from the physical structure of the electrical generator. Algorithms which control the power electronic switches can have significant influence on the short-circuit currents contributed by the turbine, and the details of these controllers are generally held closely by the turbine manufacturers.

For Type 3 WTGs (DFIG), if during the fault, the rotor power controller remains active, the machine stator currents would be limited between 1.1 to 2.5 p.u. of the machine rated current. Under conditions where protective functions act to "crowbar" the rotor circuit, the short-circuit behavior defaults to 5 to 6 p.u. in the case of a fault applied directly to the WTG terminals. [7]

In turbines employing full-rated power converters as the interface to the grid (Type 4), currents during network faults will be limited to slightly above rated current. This limitation is affected by the power converter control, and is generally necessary to protect the power semiconductor switches.

Type 5 WTGs exhibit typical synchronous generator behavior during grid short circuits. Generator contribution to grid faults can be calculated from the machine constants, obtainable from the generator manufacturer. Fault current contribution for line to ground faults will depend on the type of generator grounding used. Typical generator fault current contribution can range from 4 to more times rated current for close-in bolted three-phase faults. Fault current contribution for single-line to ground faults can range from near zero amps (ungrounded neutral) to more than the three-phase bolted level (depending on the zero sequence impedance of solidly grounded generators.)

A joint Working Group sponsored by the Power Systems Relaying Committee (PSRC) and the T&D Committee on short-circuit contributions from WTGs is currently discussing this topic. It is expected that more specific guidelines on considerations in determining short-circuit contributions from different types of WTGs will be forthcoming.

VII. REFERENCES

[1] Robert Zavadil, Nicholas Miller, Abraham Ellis, and Eduard Muljadi, "Making Connections [Wind Generation Facilities]," *IEEE Power & Energy Magazine,* vol. 3, no. 6, pp. 26-37, Nov.–Dec. 2005.

[2] W.L. Kling, J.G. Slootweg, "Wind Turbines as Power Plants" IEEE/Cigré Workshop on Wind Power and the Impacts on Power Systems, June 2002, Oslo, Norway.

[3] Wind Plant Collector System Design Working Group, "Wind Power Plant Collector System Design Considerations," in *Proc. 2009 IEEE Power and Energy Society General Meeting,* Calgary, Canada, July 2009.

[4] Wind Plant Collector SystemDesign Working Group, "Reactive Power Compensation for Wind Power Plants," in *Proc. 2009 IEEE Power and Energy Society General Meeting,* Calgary, Canada, July 2009.

[5] FERC Order no. 661-A, "Interconnection for Wind Energy," Docket No. RM05-4-001, December 2005.

[6] Nader Samaan, Robert Zavadil. J. Charles Smith and Jose Conto, "Modeling of Wind Power Plants for Short Circuit Analysis in the Transmission Network," in *Proc. of IEEE/PES Transmission and Distribution Conference,* Chicago, USA, April 2008.

[7] J. Morreu, S.W.H. de Haan, "Ridethrough of Wind Turbines with Doubly-Fed Induction Generator During a Voltage Dip," IEEE Transactions on Energy Conversion, vol. 20, no. 2, June 2005.

[8] Ackermann, Thomas, ed. Wind Power in Power Systems. West Sussex, UK: John Wiley & Sons, 2005. ISBN 13: 978-0-470-85508-9.

[9] Hau, Erich. Wind Turbines: Fundamentals. Technologies. Application, Economics. 2nd Edition. Trans. Horst von Renouard. Sidcup, Kent, UK: Springer, 2006. ISBN 13: 978-3-540-24240-6.

6.1

DIRECT SOLUTIONS TO LINEAR ALGEBRAIC EQUATIONS: GAUSS ELIMINATION

Consider the following set of linear algebraic equations in matrix format:

$$\begin{bmatrix} A_{11} & A_{12} & \cdots & A_{1N} \\ A_{21} & A_{22} & \cdots & A_{2N} \\ \vdots & & \vdots & \\ A_{N1} & A_{N2} & \cdots & A_{NN} \end{bmatrix} \begin{bmatrix} x_1 \\ x_2 \\ \vdots \\ x_N \end{bmatrix} = \begin{bmatrix} y_1 \\ y_2 \\ \vdots \\ y_N \end{bmatrix} \tag{6.1.1}$$

or

$$\mathbf{Ax} = \mathbf{y} \tag{6.1.2}$$

where $\mathbf{x}$ and $\mathbf{y}$ are N vectors and $\mathbf{A}$ is an $N \times N$ square matrix. The components of $\mathbf{x}$, $\mathbf{y}$, and $\mathbf{A}$ may be real or complex. Given $\mathbf{A}$ and $\mathbf{y}$, we want to solve for $\mathbf{x}$. We assume the det($\mathbf{A}$) is nonzero, so a unique solution to (6.1.1) exists.

The solution $\mathbf{x}$ can easily be obtained when $\mathbf{A}$ is an upper triangular matrix with nonzero diagonal elements. Then (6.1.1) has the form

$$\begin{bmatrix} A_{11} & A_{12}\ldots & & A_{1N} \\ 0 & A_{22}\ldots & & A_{2N} \\ \vdots & & & \\ 0 & 0\ldots & A_{N-1,N-1} & A_{N-1,N} \\ 0 & 0\ldots 0 & & A_{NN} \end{bmatrix} \begin{bmatrix} x_1 \\ x_2 \\ \vdots \\ x_{N-1} \\ x_N \end{bmatrix} = \begin{bmatrix} y_1 \\ y_2 \\ \vdots \\ y_{N-1} \\ y_N \end{bmatrix} \tag{6.1.3}$$

Since the last equation in (6.1.3) involves only x_N,

$$x_N = \frac{y_N}{A_{NN}} \tag{6.1.4}$$

After x_N is computed, the next-to-last equation can be solved:

$$x_{N-1} = \frac{y_{N-1} - A_{N-1,N}x_N}{A_{N-1,N-1}} \tag{6.1.5}$$

In general, with $x_N, x_{N-1}, \ldots, x_{k+1}$ already computed, the kth equation can be solved

$$x_k = \frac{y_k - \sum_{n=k+1}^{N} A_{kn}x_n}{A_{kk}} \qquad k = N, N-1, \ldots, 1 \tag{6.1.6}$$

This procedure for solving (6.1.3) is called *back substitution*.

If **A** is not upper triangular, (6.1.1) can be transformed to an equivalent equation with an upper triangular matrix. The transformation, called *Gauss elimination*, is described by the following $(N-1)$ steps. During Step 1, we use the first equation in (6.1.1) to eliminate x_1 from the remaining equations. That is, Equation 1 is multiplied by A_{n1}/A_{11} and then subtracted from equation n, for $n = 2, 3, \ldots, N$. After completing Step 1, we have

$$\begin{bmatrix} A_{11} & A_{12} & \cdots & A_{1N} \\ 0 & \left(A_{22} - \frac{A_{21}}{A_{11}}A_{12}\right) & \cdots & \left(A_{2N} - \frac{A_{21}}{A_{11}}A_{1N}\right) \\ 0 & \left(A_{32} - \frac{A_{31}}{A_{11}}A_{12}\right) & \cdots & \left(A_{3N} - \frac{A_{31}}{A_{11}}A_{1N}\right) \\ \vdots & \vdots & & \vdots \\ 0 & \left(A_{N2} - \frac{A_{N1}}{A_{11}}A_{12}\right) & \cdots & \left(A_{NN} - \frac{A_{N1}}{A_{11}}A_{1N}\right) \end{bmatrix} \begin{bmatrix} x_1 \\ x_2 \\ x_3 \\ \vdots \\ x_N \end{bmatrix}$$

$$= \begin{bmatrix} y_1 \\ y_2 - \frac{A_{21}}{A_{11}}y_1 \\ y_3 - \frac{A_{31}}{A_{11}}y_1 \\ \vdots \\ y_N - \frac{A_{N1}}{A_{11}}y_1 \end{bmatrix} \tag{6.1.7}$$

Equation (6.1.7) has the following form:

$$\begin{bmatrix} A_{11}^{(1)} & A_{12}^{(1)} & \cdots & A_{1N}^{(1)} \\ 0 & A_{22}^{(1)} & \cdots & A_{2N}^{(1)} \\ 0 & A_{32}^{(1)} & \cdots & A_{3N}^{(1)} \\ \vdots & \vdots & & \vdots \\ 0 & A_{N2}^{(1)} & \cdots & A_{NN}^{(1)} \end{bmatrix} \begin{bmatrix} x_1 \\ x_2 \\ x_3 \\ \vdots \\ x_N \end{bmatrix} = \begin{bmatrix} y_1^{(1)} \\ y_2^{(1)} \\ y_3^{(1)} \\ \vdots \\ y_N^{(1)} \end{bmatrix} \tag{6.1.8}$$

where the superscript (1) denotes Step 1 of Gauss elimination.

During Step 2 we use the second equation in (6.1.8) to eliminate x_2 from the remaining (third, fourth, fifth, and so on) equations. That is, Equation 2 is multiplied by $A_{n2}^{(1)}/A_{22}^{(1)}$ and subtracted from equation n, for $n = 3, 4, \ldots, N$.

After Step 2, we have

$$\begin{bmatrix} A_{11}^{(2)} & A_{12}^{(2)} & A_{13}^{(2)} & \cdots & A_{1N}^{(2)} \\ 0 & A_{22}^{(2)} & A_{23}^{(2)} & \cdots & A_{2N}^{(2)} \\ 0 & 0 & A_{33}^{(2)} & \cdots & A_{3N}^{(2)} \\ 0 & 0 & A_{43}^{(2)} & \cdots & A_{4N}^{(2)} \\ \vdots & \vdots & \vdots & & \vdots \\ 0 & 0 & A_{N3}^{(2)} & \cdots & A_{NN}^{(2)} \end{bmatrix} \begin{bmatrix} x_1 \\ x_2 \\ x_3 \\ x_4 \\ \vdots \\ x_N \end{bmatrix} = \begin{bmatrix} y_1^{(2)} \\ y_2^{(2)} \\ y_3^{(2)} \\ y_4^{(2)} \\ \vdots \\ y_N^{(2)} \end{bmatrix} \tag{6.1.9}$$

During step k, we start with $\mathbf{A}^{(k-1)}\mathbf{x} = \mathbf{y}^{(k-1)}$. The first k of these equations, already triangularized, are left unchanged. Also, equation k is multiplied by $A_{nk}^{(k-1)}/A_{kk}^{(k-1)}$ and then subtracted from equation n, for $n = k+1, k+2, \ldots, N$.

After $(N-1)$ steps, we arrive at the equivalent equation $\mathbf{A}^{(N-1)}\mathbf{x} = \mathbf{y}^{(N-1)}$, where $\mathbf{A}^{(N-1)}$ is upper triangular.

EXAMPLE 6.1 Gauss elimination and back substitution: direct solution to linear algebraic equations

Solve

$$\left[\begin{array}{c|c} 10 & 5 \\ \hline 2 & 9 \end{array}\right] \begin{bmatrix} x_1 \\ x_2 \end{bmatrix} = \begin{bmatrix} 6 \\ 3 \end{bmatrix}$$

using Gauss elimination and back substitution.

SOLUTION Since $N = 2$ for this example, there is $(N-1) = 1$ Gauss elimination step. Multiplying the first equation by $A_{21}/A_{11} = 2/10$ and then subtracting from the second,

$$\left[\begin{array}{c|c} 10 & 5 \\ \hline 0 & 9 - \dfrac{2}{10}(5) \end{array}\right] \begin{bmatrix} x_1 \\ x_2 \end{bmatrix} = \begin{bmatrix} 6 \\ 3 - \dfrac{2}{10}(6) \end{bmatrix}$$

or

$$\left[\begin{array}{c|c} 10 & 5 \\ \hline 0 & 8 \end{array}\right] \begin{bmatrix} x_1 \\ x_2 \end{bmatrix} = \begin{bmatrix} 6 \\ 1.8 \end{bmatrix}$$

which has the form $\mathbf{A}^{(1)}\mathbf{x} = \mathbf{y}^{(1)}$, where $\mathbf{A}^{(1)}$ is upper triangular. Now, using back substitution, (6.1.6) gives, for $k = 2$:

$$x_2 = \frac{y_2^{(1)}}{A_{22}^{(1)}} = \frac{1.8}{8} = 0.225$$

and, for $k = 1$,

$$x_1 = \frac{y_1^{(1)} - A_{12}^{(1)} x_2}{A_{11}^{(1)}} = \frac{6 - (5)(0.225)}{10} = 0.4875 \qquad \blacksquare$$

EXAMPLE 6.2 Gauss elimination: triangularizing a matrix

Use Gauss elimination to triangularize

$$\begin{bmatrix} 2 & 3 & -1 \\ -4 & 6 & 8 \\ 10 & 12 & 14 \end{bmatrix} \begin{bmatrix} x_1 \\ x_2 \\ x_3 \end{bmatrix} = \begin{bmatrix} 5 \\ 7 \\ 9 \end{bmatrix}$$

SOLUTION There are $(N - 1) = 2$ Gauss elimination steps. During Step 1, we subtract $A_{21}/A_{11} = -4/2 = -2$ times Equation 1 from Equation 2, and we subtract $A_{31}/A_{11} = 10/2 = 5$ times Equation 1 from Equation 3, to give

$$\left[\begin{array}{c|c|c} 2 & 3 & -1 \\ \hline 0 & 6 - (-2)(3) & 8 - (-2)(-1) \\ \hline 0 & 12 - (5)(3) & 14 - (5)(-1) \end{array}\right] \begin{bmatrix} x_1 \\ x_2 \\ x_3 \end{bmatrix} = \begin{bmatrix} 5 \\ 7 - (-2)(5) \\ 9 - (5)(5) \end{bmatrix}$$

or

$$\begin{bmatrix} 2 & 3 & -1 \\ 0 & 12 & 6 \\ 0 & -3 & 19 \end{bmatrix} \begin{bmatrix} x_1 \\ x_2 \\ x_3 \end{bmatrix} = \begin{bmatrix} 5 \\ 17 \\ -16 \end{bmatrix}$$

which is $\mathbf{A}^{(1)}\mathbf{x} = \mathbf{y}^{(1)}$. During Step 2, we subtract $A_{32}^{(1)}/A_{22}^{(1)} = -3/12 = -0.25$ times Equation 2 from Equation 3, to give

$$\left[\begin{array}{c|c|c} 2 & 3 & -1 \\ \hline 0 & 12 & 6 \\ \hline 0 & 0 & 19 - (-.25)(6) \end{array}\right] \begin{bmatrix} x_1 \\ x_2 \\ x_3 \end{bmatrix} = \begin{bmatrix} 5 \\ 17 \\ -16 - (-.25)(17) \end{bmatrix}$$

or

$$\begin{bmatrix} 2 & 3 & -1 \\ 0 & 12 & 6 \\ 0 & 0 & 20.5 \end{bmatrix} \begin{bmatrix} x_1 \\ x_2 \\ x_3 \end{bmatrix} = \begin{bmatrix} 5 \\ 17 \\ -11.75 \end{bmatrix}$$

which is triangularized. The solution $\mathbf{x}$ can now be easily obtained via back substitution. $\blacksquare$

Computer storage requirements for Gauss elimination and back substitution include N^2 memory locations for $\mathbf{A}$ and N locations for $\mathbf{y}$. If there is no further need to retain $\mathbf{A}$ and $\mathbf{y}$, then $\mathbf{A}^{(k)}$ can be stored in the location of $\mathbf{A}$, and $\mathbf{y}^{(k)}$, as well as the solution $\mathbf{x}$, can be stored in the location of $\mathbf{y}$. Additional memory is also required for iterative loops, arithmetic statements, and working space.

Computer time requirements can be evaluated by determining the number of arithmetic operations required for Gauss elimination and back substitution. One can show that Gauss elimination requires $(N^3 - N)/3$ multiplications, $(N)(N-1)/2$ divisions, and $(N^3 - N)/3$ subtractions. Also, back substitution requires $(N)(N-1)/2$ multiplications, N divisions, and $(N)(N-1)/2$ subtractions. Therefore, for very large N, the approximate computer time for solving (6.1.1) by Gauss elimination and back substitution is the time required to perform $N^3/3$ multiplications and $N^3/3$ subtractions.

For example, consider a digital computer with a 2×10^{-9} s multiplication time and 1×10^{-9} s addition or subtraction time. Solving $N = 10{,}000$ equations would require approximately

$$\tfrac{1}{3}N^3(2 \times 10^{-9}) + \tfrac{1}{3}N^3(1 \times 10^{-9}) = \tfrac{1}{3}(10{,}000)^3(3 \times 10^{-9}) = 1000 \quad \text{s}$$

plus some additional bookkeeping time for indexing and managing loops.

Since the power-flow problem often involves solving power systems with tens of thousands of equations, by itself Gauss elimination would not be a good solution. However, for matrixes that have relatively few nonzero elements, known as sparse matrices, special techniques can be employed to significantly reduce computer storage and time requirements. Since all large power systems can be modeled using sparse matrices, these techniques are briefly introduced in Section 6.8.

6.2 ITERATIVE SOLUTIONS TO LINEAR ALGEBRAIC EQUATIONS: JACOBI AND GAUSS–SEIDEL

A general iterative solution to (6.1.1) proceeds as follows. First select an initial guess $\mathbf{x}(0)$. Then use

$$\mathbf{x}(i+1) = \mathbf{g}[\mathbf{x}(i)] \qquad i = 0, 1, 2, \ldots \tag{6.2.1}$$

where $\mathbf{x}(i)$ is the ith guess and $\mathbf{g}$ is an N vector of functions that specify the iteration method. Continue the procedure until the following stopping condition is satisfied:

$$\left| \frac{x_k(i+1) - x_k(i)}{x_k(i)} \right| < \varepsilon \qquad \text{for all } k = 1, 2, \ldots, N \tag{6.2.2}$$

where $x_k(i)$ is the kth component of $\mathbf{x}(i)$ and ε is a specified *tolerance level*.

The following questions are pertinent:

1. Will the iteration procedure converge to the unique solution?
2. What is the convergence rate (how many iterations are required)?
3. When using a digital computer, what are the computer storage and time requirements?

These questions are addressed for two specific iteration methods: *Jacobi* and *Gauss–Seidel*.* The Jacobi method is obtained by considering the kth equation of (6.1.1), as follows:

$$y_k = A_{k1}x_1 + A_{k2}x_2 + \cdots + A_{kk}x_k + \cdots + A_{kN}x_N \tag{6.2.3}$$

Solving for x_k,

$$\begin{aligned} x_k &= \frac{1}{A_{kk}}[y_k - (A_{k1}x_1 + \cdots + A_{k,k-1}x_{k-1} + A_{k,k+1}x_{k+1} + \cdots + A_{kN}x_N)] \\ &= \frac{1}{A_{kk}}\left[y_k - \sum_{n=1}^{k-1} A_{kn}x_n - \sum_{n=k+1}^{N} A_{kn}x_n\right] \end{aligned} \tag{6.2.4}$$

The Jacobi method uses the "old" values of $\mathbf{x}(i)$ at iteration i on the right side of (6.2.4) to generate the "new" value $x_k(i+1)$ on the left side of (6.2.4). That is,

$$x_k(i+1) = \frac{1}{A_{kk}}\left[y_k - \sum_{n=1}^{k-1} A_{kn}x_n(i) - \sum_{n=k+1}^{N} A_{kn}x_n(i)\right] \qquad k = 1, 2, \ldots, N \tag{6.2.5}$$

The Jacobi method given by (6.2.5) can also be written in the following matrix format:

$$\mathbf{x}(i+1) = \mathbf{M}\mathbf{x}(i) + \mathbf{D}^{-1}\mathbf{y} \tag{6.2.6}$$

where

$$\mathbf{M} = \mathbf{D}^{-1}(\mathbf{D} - \mathbf{A}) \tag{6.2.7}$$

and

$$\mathbf{D} = \begin{bmatrix} A_{11} & 0 & 0 & \cdots & 0 \\ 0 & A_{22} & 0 & \cdots & 0 \\ 0 & \vdots & \vdots & & \vdots \\ \vdots & & & & 0 \\ 0 & 0 & 0 & \cdots & A_{NN} \end{bmatrix} \tag{6.2.8}$$

For Jacobi, $\mathbf{D}$ consists of the diagonal elements of the $\mathbf{A}$ matrix.

* The Jacobi method is also called the Gauss method.

EXAMPLE 6.3 Jacobi method: iterative solution to linear algebraic equations

Solve Example 6.1 using the Jacobi method. Start with $x_1(0) = x_2(0) = 0$ and continue until (6.2.2) is satisfied for $\varepsilon = 10^{-4}$.

SOLUTION From (6.2.5) with $N = 2$,

$$k = 1 \qquad x_1(i+1) = \frac{1}{A_{11}}[y_1 - A_{12}x_2(i)] = \frac{1}{10}[6 - 5x_2(i)]$$

$$k = 2 \qquad x_2(i+1) = \frac{1}{A_{22}}[y_2 - A_{21}x_1(i)] = \frac{1}{9}[3 - 2x_1(i)]$$

Alternatively, in matrix format using (6.2.6)–(6.2.8),

$$\mathbf{D}^{-1} = \left[\begin{array}{c|c} 10 & 0 \\ \hline 0 & 9 \end{array}\right]^{-1} = \left[\begin{array}{c|c} \frac{1}{10} & 0 \\ \hline 0 & \frac{1}{9} \end{array}\right]$$

$$\mathbf{M} = \left[\begin{array}{c|c} \frac{1}{10} & 0 \\ \hline 0 & \frac{1}{9} \end{array}\right] \left[\begin{array}{c|c} 0 & -5 \\ \hline -2 & 0 \end{array}\right] = \left[\begin{array}{c|c} 0 & -\frac{5}{10} \\ \hline -\frac{2}{9} & 0 \end{array}\right]$$

$$\begin{bmatrix} x_1(i+1) \\ x_2(i+1) \end{bmatrix} = \left[\begin{array}{c|c} 0 & -\frac{5}{10} \\ \hline -\frac{2}{9} & 0 \end{array}\right] \begin{bmatrix} x_1(i) \\ x_2(i) \end{bmatrix} + \left[\begin{array}{c|c} \frac{1}{10} & 0 \\ \hline 0 & \frac{1}{9} \end{array}\right] \begin{bmatrix} 6 \\ 3 \end{bmatrix}$$

The above two formulations are identical. Starting with $x_1(0) = x_2(0) = 0$, the iterative solution is given in the following table:

JACOBI

i	0	1	2	3	4	5	6	7	8	9	10
$x_1(i)$	0	0.60000	0.43334	0.50000	0.48148	0.48889	0.48683	0.48766	0.48743	0.48752	0.48749
$x_2(i)$	0	0.33333	0.20000	0.23704	0.22222	0.22634	0.22469	0.22515	0.22496	0.22502	0.22500

As shown, the Jacobi method converges to the unique solution obtained in Example 6.1. The convergence criterion is satisfied at the 10th iteration, since

$$\left|\frac{x_1(10) - x_1(9)}{x_1(9)}\right| = \left|\frac{0.48749 - 0.48752}{0.48749}\right| = 6.2 \times 10^{-5} < \varepsilon$$

and

$$\left|\frac{x_2(10) - x_2(9)}{x_2(9)}\right| = \left|\frac{0.22500 - 0.22502}{0.22502}\right| = 8.9 \times 10^{-5} < \varepsilon \qquad \blacksquare$$

The Gauss–Seidel method is given by

$$x_k(i+1) = \frac{1}{A_{kk}}\left[y_k - \sum_{n=1}^{k-1} \mathrm{A}_{kn}x_n(i+1) - \sum_{n=k+1}^{N} \mathrm{A}_{kn}x_n(i)\right] \tag{6.2.9}$$

Comparing (6.2.9) with (6.2.5), note that Gauss–Seidel is similar to Jacobi except that during each iteration, the "new" values, $x_n(i+1)$, for $n<k$ are used on the right side of (6.2.9) to generate the "new" value $x_k(i+1)$ on the left side.

The Gauss–Seidel method of (6.2.9) can also be written in the matrix format of (6.2.6) and (6.2.7), where

$$\mathbf{D} = \begin{bmatrix} \mathrm{A}_{11} & 0 & 0 & \cdots & 0 \\ \mathrm{A}_{21} & \mathrm{A}_{22} & 0 & \cdots & 0 \\ \vdots & \vdots & & & \vdots \\ \mathrm{A}_{N1} & \mathrm{A}_{N2} & \cdots & & \mathrm{A}_{NN} \end{bmatrix} \tag{6.2.10}$$

For Gauss–Seidel, **D** in (6.2.10) is the lower triangular portion of **A**, whereas for Jacobi, **D** in (6.2.8) is the diagonal portion of **A**.

EXAMPLE 6.4 Gauss–Seidel method: iterative solution to linear algebraic equations

Rework Example 6.3 using the Gauss–Seidel method.

SOLUTION From (6.2.9),

$$k=1 \qquad x_1(i+1) = \frac{1}{\mathrm{A}_{11}}[y_1 - \mathrm{A}_{12}x_2(i)] = \frac{1}{10}[6 - 5x_2(i)]$$

$$k=2 \qquad x_2(i+1) = \frac{1}{\mathrm{A}_{22}}[y_2 - \mathrm{A}_{21}x_1(i+1)] = \frac{1}{9}[3 - 2x_1(i+1)]$$

Using this equation for $x_1(i+1)$, $x_2(i+1)$ can also be written as

$$x_2(i+1) = \frac{1}{9}\left\{3 - \frac{2}{10}[6 - 5x_2(i)]\right\}$$

Alternatively, in matrix format, using (6.2.10), (6.2.6), and (6.2.7):

$$\mathbf{D}^{-1} = \left[\begin{array}{c|c} 10 & 0 \\ \hline 2 & 9 \end{array}\right]^{-1} = \left[\begin{array}{c|c} \frac{1}{10} & 0 \\ \hline -\frac{2}{90} & \frac{1}{9} \end{array}\right]$$

$$\mathbf{M} = \left[\begin{array}{c|c} \frac{1}{10} & 0 \\ \hline -\frac{2}{90} & \frac{1}{9} \end{array}\right] \left[\begin{array}{c|c} 0 & -5 \\ \hline 0 & 0 \end{array}\right] = \left[\begin{array}{c|c} 0 & -\frac{1}{2} \\ \hline 0 & \frac{1}{9} \end{array}\right]$$

$$\begin{bmatrix} x_1(i+1) \\ x_2(i+1) \end{bmatrix} = \left[\begin{array}{c|c} 0 & -\frac{1}{2} \\ \hline 0 & \frac{1}{9} \end{array}\right] \begin{bmatrix} x_1(i) \\ x_2(i) \end{bmatrix} + \left[\begin{array}{c|c} \frac{1}{10} & 0 \\ \hline -\frac{2}{90} & \frac{1}{9} \end{array}\right] \begin{bmatrix} 6 \\ 3 \end{bmatrix}$$

These two formulations are identical. Starting with $x_1(0) = x_2(0) = 0$, the solution is given in the following table:

GAUSS–SEIDEL

i	0	1	2	3	4	5	6
$x_1(i)$	0	0.60000	0.50000	0.48889	0.48765	0.48752	0.48750
$x_2(i)$	0	0.20000	0.22222	0.22469	0.22497	0.22500	0.22500

For this example, Gauss–Seidel converges in 6 iterations, compared to 10 iterations with Jacobi. ■

The convergence rate is faster with Gauss–Seidel for some **A** matrices, but faster with Jacobi for other **A** matrices. In some cases, one method diverges while the other converges. In other cases both methods diverge, as illustrated by the next example.

EXAMPLE 6.5 Divergence of Gauss–Seidel method

Using the Gauss–Seidel method with $x_1(0) = x_2(0) = 0$, solve

$$\left[\begin{array}{c|c} 5 & 10 \\ \hline 9 & 2 \end{array}\right] \begin{bmatrix} x_1 \\ x_2 \end{bmatrix} = \begin{bmatrix} 6 \\ 3 \end{bmatrix}$$

SOLUTION Note that these equations are the same as those in Example 6.1, except that x_1 and x_2 are interchanged. Using (6.2.9),

$$k = 1 \qquad x_1(i+1) = \frac{1}{A_{11}}[y_1 - A_{12}x_2(i)] = \frac{1}{5}[6 - 10x_2(i)]$$

$$k = 2 \qquad x_2(i+1) = \frac{1}{A_{22}}[y_2 - A_{21}x_1(i+1)] = \frac{1}{2}[3 - 9x_1(i+1)]$$

Successive calculations of x_1 and x_2 are shown in the following table:

GAUSS–SEIDEL

i	0	1	2	3	4	5
$x_1(i)$	0	1.2	9	79.2	711	6397
$x_2(i)$	0	−3.9	−39	−354.9	−3198	−28786

The unique solution by matrix inversion is

$$\begin{bmatrix} x_1 \\ x_2 \end{bmatrix} = \left[\begin{array}{c|c} 5 & 10 \\ \hline 9 & 2 \end{array}\right]^{-1} \begin{bmatrix} 6 \\ 3 \end{bmatrix} = \frac{-1}{80} \left[\begin{array}{c|c} 2 & -10 \\ \hline -9 & 5 \end{array}\right] \begin{bmatrix} 6 \\ 3 \end{bmatrix} = \begin{bmatrix} 0.225 \\ 0.4875 \end{bmatrix}$$

As shown, Gauss–Seidel does not converge to the unique solution; instead it diverges. We could show that Jacobi also diverges for this example. ■

If any diagonal element A_{kk} equals zero, then Jacobi and Gauss–Seidel are undefined, because the right-hand sides of (6.2.5) and (6.2.9) are divided by A_{kk}. Also, if any one diagonal element has too small a magnitude, these methods will diverge. In Examples 6.3 and 6.4, Jacobi and Gauss–Seidel converge, since the diagonals (10 and 9) are both large; in Example 6.5, however, the diagonals (5 and 2) are small compared to the off-diagonals, and the methods diverge.

In general, convergence of Jacobi or Gauss–Seidel can be evaluated by recognizing that (6.2.6) represents a digital filter with input $\mathbf{y}$ and output $\mathbf{x}(i)$. The z-transform of (6.2.6) may be employed to determine the filter transfer function and its poles. The output $\mathbf{x}(i)$ converges if and only if all the filter poles have magnitudes less than 1 (see Problems 6.16 and 6.17).

Rate of convergence is also established by the filter poles. Fast convergence is obtained when the magnitudes of all the poles are small. In addition, experience with specific $\mathbf{A}$ matrices has shown that more iterations are required for Jacobi and Gauss–Seidel as the dimension N increases.

Computer storage requirements for Jacobi include N^2 memory locations for the $\mathbf{A}$ matrix and $3N$ locations for the vectors $\mathbf{y}$, $\mathbf{x}(i)$, and $\mathbf{x}(i+1)$. Storage space is also required for loops, arithmetic statements, and working space to compute (6.2.5). Gauss–Seidel requires N fewer memory locations, since for (6.2.9) the new value $x_k(i+1)$ can be stored in the location of the old value $x_k(i)$.

Computer time per iteration is relatively small for Jacobi and Gauss–Seidel. Inspection of (6.2.5) or (6.2.9) shows that N^2 multiplications/divisions and $N(N-1)$ subtractions per iteration are required [one division, $(N-1)$ multiplications, and $(N-1)$ subtractions for each $k = 1, 2, \ldots, N$]. But as was the case with Gauss elimination, if the matrix is sparse (i.e., most of the elements are zero), special sparse matrix algorithms can be used to substantially decrease both the storage requirements and the computation time.

6.3

ITERATIVE SOLUTIONS TO NONLINEAR ALGEBRAIC EQUATIONS: NEWTON–RAPHSON

A set of nonlinear algebraic equations in matrix format is given by

$$\mathbf{f}(\mathbf{x}) = \begin{bmatrix} f_1(\mathbf{x}) \\ f_2(\mathbf{x}) \\ \vdots \\ f_N(\mathbf{x}) \end{bmatrix} = \mathbf{y} \tag{6.3.1}$$

where $\mathbf{y}$ and $\mathbf{x}$ are N vectors and $\mathbf{f}(\mathbf{x})$ is an N vector of functions. Given $\mathbf{y}$ and $\mathbf{f}(\mathbf{x})$, we want to solve for $\mathbf{x}$. The iterative methods described in Section 6.2 can be extended to nonlinear equations as follows. Rewriting (6.3.1),

$$\mathbf{0} = \mathbf{y} - \mathbf{f}(\mathbf{x}) \tag{6.3.2}$$

Adding $\mathbf{Dx}$ to both sides of (6.3.2), where $\mathbf{D}$ is a square $N \times N$ invertible matrix,

$$\mathbf{Dx} = \mathbf{Dx} + \mathbf{y} - \mathbf{f}(\mathbf{x}) \tag{6.3.3}$$

Premultiplying by $\mathbf{D}^{-1}$,

$$\mathbf{x} = \mathbf{x} + \mathbf{D}^{-1}[\mathbf{y} - \mathbf{f}(\mathbf{x})] \tag{6.3.4}$$

The old values $\mathbf{x}(i)$ are used on the right side of (6.3.4) to generate the new values $\mathbf{x}(i+1)$ on the left side. That is,

$$\mathbf{x}(i+1) = \mathbf{x}(i) + \mathbf{D}^{-1}\{\mathbf{y} - \mathbf{f}[\mathbf{x}(i)]\} \tag{6.3.5}$$

For linear equations, $\mathbf{f}(\mathbf{x}) = \mathbf{Ax}$ and (6.3.5) reduces to

$$\mathbf{x}(i+1) = \mathbf{x}(i) + \mathbf{D}^{-1}[\mathbf{y} - \mathbf{Ax}(i)] = \mathbf{D}^{-1}(\mathbf{D} - \mathbf{A})\mathbf{x}(i) + \mathbf{D}^{-1}\mathbf{y} \tag{6.3.6}$$

which is identical to the Jacobi and Gauss–Seidel methods of (6.2.6). For nonlinear equations, the matrix $\mathbf{D}$ in (6.3.5) must be specified.

One method for specifying $\mathbf{D}$, called *Newton–Raphson*, is based on the following Taylor series expansion of $\mathbf{f}(\mathbf{x})$ about an operating point $\mathbf{x}_0$.

$$\mathbf{y} = \mathbf{f}(\mathbf{x}_0) + \left.\frac{d\mathbf{f}}{d\mathbf{x}}\right|_{\mathbf{x}=\mathbf{x}_0} (\mathbf{x} - \mathbf{x}_0) \cdots \tag{6.3.7}$$

Neglecting the higher order terms in (6.3.7) and solving for $\mathbf{x}$,

$$\mathbf{x} = \mathbf{x}_0 + \left[\left. \frac{d\mathbf{f}}{d\mathbf{x}} \right|_{\mathbf{x}=\mathbf{x}_0} \right]^{-1} [\mathbf{y} - \mathbf{f}(\mathbf{x}_0)] \tag{6.3.8}$$

The Newton–Raphson method replaces $\mathbf{x}_0$ by the old value $\mathbf{x}(i)$ and $\mathbf{x}$ by the new value $\mathbf{x}(i+1)$ in (6.3.8). Thus,

$$\mathbf{x}(i+1) = \mathbf{x}(i) + \mathbf{J}^{-1}(i)\{\mathbf{y} - \mathbf{f}[\mathbf{x}(i)]\} \tag{6.3.9}$$

where

$$\mathbf{J}(i) = \left. \frac{d\mathbf{f}}{d\mathbf{x}} \right|_{\mathbf{x}=\mathbf{x}(i)} = \begin{bmatrix} \frac{\partial f_1}{\partial x_1} & \frac{\partial f_1}{\partial x_2} & \cdots & \frac{\partial f_1}{\partial x_N} \\ \frac{\partial f_2}{\partial x_1} & \frac{\partial f_2}{\partial x_2} & \cdots & \frac{\partial f_2}{\partial x_N} \\ \vdots & \vdots & & \vdots \\ \frac{\partial f_N}{\partial x_1} & \frac{\partial f_N}{\partial x_2} & \cdots & \frac{\partial f_N}{\partial x_N} \end{bmatrix}_{\mathbf{x}=\mathbf{x}(i)} \tag{6.3.10}$$

The $N \times N$ matrix $\mathbf{J}(i)$, whose elements are the partial derivatives shown in (6.3.10), is called the Jacobian matrix. The Newton–Raphson method is similar to extended Gauss–Seidel, except that $\mathbf{D}$ in (6.3.5) is replaced by $\mathbf{J}(i)$ in (6.3.9).

EXAMPLE 6.6 Newton–Raphson method: solution to polynomial equations

Solve the scalar equation $f(x) = y$, where $y = 9$ and $f(x) = x^2$. Starting with $x(0) = 1$, use (a) Newton–Raphson and (b) extended Gauss–Seidel with $D = 3$ until (6.2.2) is satisfied for $\varepsilon = 10^{-4}$. Compare the two methods.

SOLUTION

a. Using (6.3.10) with $f(x) = x^2$,

$$\mathbf{J}(i) = \left. \frac{d}{dx}(x^2) \right|_{x=x(i)} = 2x \Big|_{x=x(i)} = 2x(i)$$

Using $\mathbf{J}(i)$ in (6.3.9),

$$x(i+1) = x(i) + \frac{1}{2x(i)}[9 - x^2(i)]$$

Starting with $x(0) = 1$, successive calculations of the Newton–Raphson equation are shown in the following table:

NEWTON–RAPHSON

i	0	1	2	3	4	5
$x(i)$	1	5.00000	3.40000	3.02353	3.00009	3.00000

b. Using (6.3.5) with D = 3, the Gauss–Seidel method is

$$x(i+1) = x(i) + \tfrac{1}{3}[9 - x^2(i)]$$

The corresponding Gauss–Seidel calculations are as follows:

GAUSS–SEIDEL (D = 3)

i	0	1	2	3	4	5	6
$x(i)$	1	3.66667	2.18519	3.59351	2.28908	3.54245	2.35945

As shown, Gauss–Seidel oscillates about the solution, slowly converging, whereas Newton–Raphson converges in five iterations to the solution $x = 3$. Note that if $x(0)$ is negative, Newton–Raphson converges to the negative solution $x = -3$. Also, it is assumed that the matrix inverse $\mathbf{J}^{-1}$ exists. Thus the initial value $x(0) = 0$ should be avoided for this example. ■

EXAMPLE 6.7 Newton–Raphson method: solution to nonlinear algebraic equations

Solve

$$\begin{bmatrix} x_1 + x_2 \\ x_1 x_2 \end{bmatrix} = \begin{bmatrix} 15 \\ 50 \end{bmatrix} \qquad \mathbf{x}(0) = \begin{bmatrix} 4 \\ 9 \end{bmatrix}$$

Use the Newton–Raphson method starting with the above $\mathbf{x}(0)$ and continue until (6.2.2) is satisfied with $\varepsilon = 10^{-4}$.

SOLUTION Using (6.3.10) with $f_1 = (x_1 + x_2)$ and $f_2 = x_1 x_2$,

$$\mathbf{J}(i)^{-1} = \left[\begin{array}{c|c} \dfrac{\partial f_1}{\partial x_1} & \dfrac{\partial f_1}{\partial x_2} \\ \hline \dfrac{\partial f_2}{\partial x_1} & \dfrac{\partial f_2}{\partial x_2} \end{array}\right]^{-1}_{\mathbf{x}=\mathbf{x}(i)} = \left[\begin{array}{c|c} 1 & 1 \\ \hline x_2(i) & x_1(i) \end{array}\right]^{-1} = \frac{\left[\begin{array}{c|c} x_1(i) & -1 \\ \hline -x_2(i) & 1 \end{array}\right]}{x_1(i) - x_2(i)}$$

Using $\mathbf{J}(i)^{-1}$ in (6.3.9),

$$\begin{bmatrix} x_1(i+1) \\ x_2(i+1) \end{bmatrix} = \begin{bmatrix} x_1(i) \\ x_2(i) \end{bmatrix} + \frac{\left[\begin{array}{c|c} x_1(i) & -1 \\ \hline -x_2(i) & 1 \end{array}\right]}{x_1(i) - x_2(i)} \begin{bmatrix} 15 - x_1(i) - x_2(i) \\ 50 - x_1(i)x_2(i) \end{bmatrix}$$

Writing the preceding as two separate equations,

$$x_1(i+1) = x_1(i) + \frac{x_1(i)[15 - x_1(i) - x_2(i)] - [50 - x_1(i)x_2(i)]}{x_1(i) - x_2(i)}$$

$$x_2(i+1) = x_2(i) + \frac{-x_2(i)[15 - x_1(i) - x_2(i)] + [50 - x_1(i)x_2(i)]}{x_1(i) - x_2(i)}$$

Successive calculations of these equations are shown in the following table:

NEWTON–RAPHSON

i	0	1	2	3	4
$x_1(i)$	4	5.20000	4.99130	4.99998	5.00000
$x_2(i)$	9	9.80000	10.00870	10.00002	10.00000

Newton–Raphson converges in four iterations for this example. ■

Equation (6.3.9) contains the matrix inverse $\mathbf{J}^{-1}$. Instead of computing $\mathbf{J}^{-1}$, (6.3.9) can be rewritten as follows:

$$\mathbf{J}(i)\Delta\mathbf{x}(i) = \Delta\mathbf{y}(i) \tag{6.3.11}$$

where

$$\Delta\mathbf{x}(i) = \mathbf{x}(i+1) - \mathbf{x}(i) \tag{6.3.12}$$

and

$$\Delta\mathbf{y}(i) = \mathbf{y} - \mathbf{f}[\mathbf{x}(i)] \tag{6.3.13}$$

Then, during each iteration, the following four steps are completed:

STEP 1 Compute $\Delta\mathbf{y}(i)$ from (6.3.13).

STEP 2 Compute $\mathbf{J}(i)$ from (6.3.10).

STEP 3 Using Gauss elimination and back substitution, solve (6.3.11) for $\Delta\mathbf{x}(i)$.

STEP 4 Compute $\mathbf{x}(i+1)$ from (6.3.12).

EXAMPLE 6.8 Newton–Raphson method in four steps

Complete the above four steps for the first iteration of Example 6.7.

SOLUTION

STEP 1 $\Delta\mathbf{y}(0) = \mathbf{y} - \mathbf{f}[\mathbf{x}(0)] = \begin{bmatrix} 15 \\ 50 \end{bmatrix} - \begin{bmatrix} 4+9 \\ (4)(9) \end{bmatrix} = \begin{bmatrix} 2 \\ 14 \end{bmatrix}$

STEP 2 $\mathbf{J}(0) = \left[\begin{array}{c|c} 1 & 1 \\ \hline x_2(0) & x_1(0) \end{array}\right] = \left[\begin{array}{c|c} 1 & 1 \\ \hline 9 & 4 \end{array}\right]$

STEP 3 Using $\Delta\mathbf{y}(0)$ and $\mathbf{J}(0)$, (6.3.11) becomes

$$\left[\begin{array}{c|c} 1 & 1 \\ \hline 9 & 4 \end{array}\right]\begin{bmatrix} \Delta x_1(0) \\ \Delta x_2(0) \end{bmatrix} = \begin{bmatrix} 2 \\ 14 \end{bmatrix}$$

Using Gauss elimination, subtract $\mathbf{J}_{21}/\mathbf{J}_{11} = 9/1 = 9$ times the first equation from the second equation, giving

$$\left[\begin{array}{c|c} 1 & 1 \\ \hline 0 & -5 \end{array}\right]\begin{bmatrix} \Delta x_1(0) \\ \Delta x_2(0) \end{bmatrix} = \begin{bmatrix} 2 \\ -4 \end{bmatrix}$$

Solving by back substitution,

$$\Delta x_2(0) = \frac{-4}{-5} = 0.8$$

$$\Delta x_1(0) = 2 - 0.8 = 1.2$$

STEP 4 $\mathbf{x}(1) = \mathbf{x}(0) + \Delta\mathbf{x}(0) = \begin{bmatrix} 4 \\ 9 \end{bmatrix} + \begin{bmatrix} 1.2 \\ 0.8 \end{bmatrix} = \begin{bmatrix} 5.2 \\ 9.8 \end{bmatrix}$

This is the same as computed in Example 6.7. ■

Experience from power-flow studies has shown that Newton–Raphson converges in many cases where Jacobi and Gauss–Seidel diverge. Furthermore, the number of iterations required for convergence is independent of the dimension N for Newton–Raphson, but increases with N for Jacobi and Gauss–Seidel. Most Newton–Raphson power-flow problems converge in fewer than 10 iterations [1].

6.4 THE POWER-FLOW PROBLEM

The power-flow problem is the computation of voltage magnitude and phase angle at each bus in a power system under balanced three-phase steady-state conditions. As a by-product of this calculation, real and reactive power flows in equipment such as transmission lines and transformers, as well as equipment losses, can be computed.

The starting point for a power-flow problem is a single-line diagram of the power system, from which the input data for computer solutions can be obtained. Input data consist of bus data, transmission line data, and transformer data.

As shown in Figure 6.1, the following four variables are associated with each bus k: voltage magnitude V_k, phase angle δ_k, net real power P_k, and reactive power Q_k supplied to the bus. At each bus, two of these variables are specified as input data, and the other two are unknowns to be computed by

FIGURE 6.1

Bus variables V_k, δ_k, P_k, and Q_k

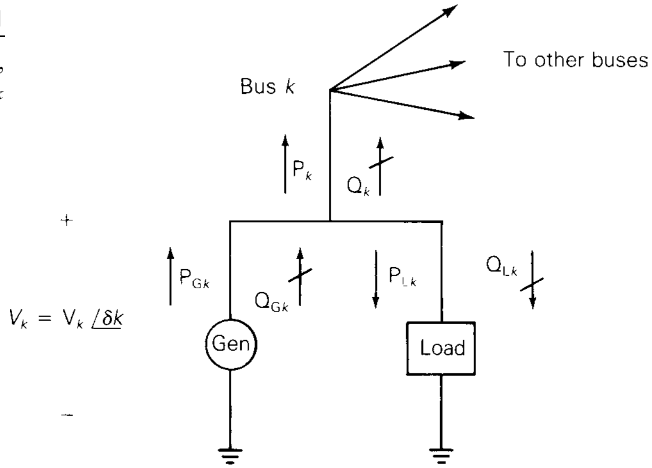

the power-flow program. For convenience, the power delivered to bus k in Figure 6.1 is separated into generator and load terms. That is,

$$P_k = P_{Gk} - P_{Lk}$$
$$Q_k = Q_{Gk} - Q_{Lk} \tag{6.4.1}$$

Each bus k is categorized into one of the following three bus types:

1. Swing bus (or slack bus)—There is only one swing bus, which for convenience is numbered bus 1 in this text. The swing bus is a reference bus for which $V_1\underline{/\delta_1}$, typically $1.0\underline{/0^\circ}$ per unit, is input data. The power-flow program computes P_1 and Q_1.

2. Load (PQ) bus—P_k and Q_k are input data. The power-flow program computes V_k and δ_k. Most buses in a typical power-flow program are load buses.

3. Voltage controlled (PV) bus—P_k and V_k are input data. The power-flow program computes Q_k and δ_k. Examples are buses to which generators, switched shunt capacitors, or static var systems are connected. Maximum and minimum var limits $Q_{Gk\max}$ and $Q_{Gk\min}$ that this equipment can supply are also input data. If an upper or lower reactive power limit is reached, then the reactive power output of the generator is held at the limit, and the bus is modeled as a PQ bus. Another example is a bus to which a tap-changing transformer is connected; the power-flow program then computes the tap setting.

Note that when bus k is a load bus with no generation, $P_k = -P_{Lk}$ is negative; that is, the real power supplied to bus k in Figure 6.1 is negative. If the load is inductive, $Q_k = -Q_{Lk}$ is negative.

Transmission lines are represented by the equivalent π circuit, shown in Figure 5.7. Transformers are also represented by equivalent circuits, as shown in Figure 3.9 for a two-winding transformer, Figure 3.20 for a three-winding transformer, or Figure 3.25 for a tap-changing transformer.

Input data for each transmission line include the per-unit equivalent π circuit series impedance Z' and shunt admittance Y', the two buses to which the line is connected, and maximum MVA rating. Similarly, input data for each transformer include per-unit winding impedances Z, the per-unit exciting branch admittance Y, the buses to which the windings are connected, and maximum MVA ratings. Input data for tap-changing transformers also include maximum tap settings.

The bus admittance matrix $\boldsymbol{Y}_{\text{bus}}$ can be constructed from the line and transformer input data. From (2.4.3) and (2.4.4), the elements of $\boldsymbol{Y}_{\text{bus}}$ are:

$$\begin{aligned} &\text{Diagonal elements:} && Y_{kk} = \text{sum of admittances connected to bus } k \\ &\text{Off-diagonal elements:} && Y_{kn} = -(\text{sum of admittances connected} \\ &&& \qquad\qquad \text{between buses } k \text{ and } n) \\ &&& k \neq n \end{aligned} \tag{6.4.2}$$

EXAMPLE 6.9 Power-flow input data and Y_{bus}

Figure 6.2 shows a single-line diagram of a five-bus power system. Input data are given in Tables 6.1, 6.2, and 6.3. As shown in Table 6.1, bus 1, to which a generator is connected, is the swing bus. Bus 3, to which a generator and a load are connected, is a voltage-controlled bus. Buses 2, 4, and 5 are load buses. Note that the loads at buses 2 and 3 are inductive since $Q_2 = -Q_{L2} = -2.8$ and $-Q_{L3} = -0.4$ are negative.

For each bus k, determine which of the variables V_k, δ_k, P_k, and Q_k are input data and which are unknowns. Also, compute the elements of the second row of $\boldsymbol{Y}_{\text{bus}}$.

SOLUTION The input data and unknowns are listed in Table 6.4. For bus 1, the swing bus, P_1 and Q_1 are unknowns. For bus 3, a voltage-controlled bus,

FIGURE 6.2

Single-line diagram for Example 6.9

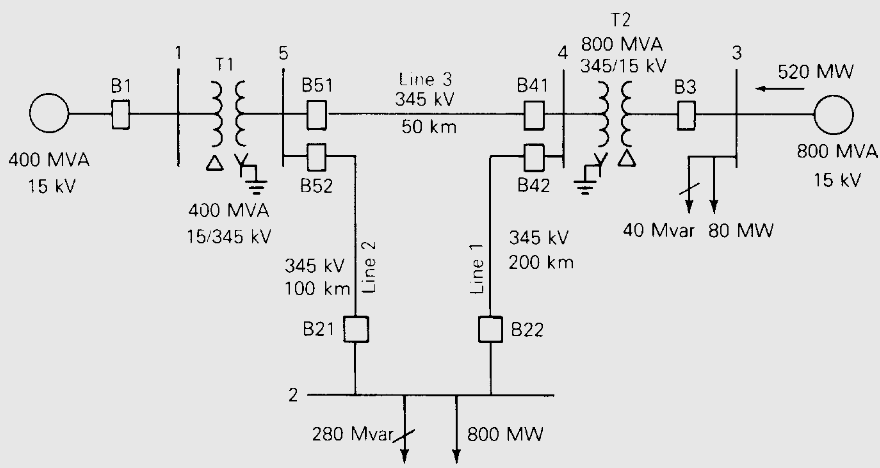

TABLE 6.1

Bus input data for Example 6.9*

Bus	Type	V per unit	δ degrees	P_G per unit	Q_G per unit	P_L per unit	Q_L per unit	Q_{Gmax} per unit	Q_{Gmin} per unit
1	Swing	1.0	0	—	—	0	0	—	—
2	Load	—	—	0	0	8.0	2.8	—	—
3	Constant voltage	1.05	—	5.2	—	0.8	0.4	4.0	−2.8
4	Load	—	—	0	0	0	0	—	—
5	Load	—	—	0	0	0	0	—	—

* $S_{base} = 100$ MVA, $V_{base} = 15$ kV at buses 1, 3, and 345 kV at buses 2, 4, 5

TABLE 6.2

Line input data for Example 6.9

Bus-to-Bus	R' per unit	X' per unit	G' per unit	B' per unit	Maximum MVA per unit
2–4	0.0090	0.100	0	1.72	12.0
2–5	0.0045	0.050	0	0.88	12.0
4–5	0.00225	0.025	0	0.44	12.0

TABLE 6.3

Transformer input data for Example 6.9

Bus-to-Bus	R per unit	X per unit	G_c per unit	B_m per unit	Maximum MVA per unit	Maximum TAP Setting per unit
1–5	0.00150	0.02	0	0	6.0	—
3–4	0.00075	0.01	0	0	10.0	—

TABLE 6.4

Input data and unknowns for Example 6.9

Bus	Input Data	Unknowns
1	$V_1 = 1.0, \delta_1 = 0$	P_1, Q_1
2	$P_2 = P_{G2} - P_{L2} = -8$	V_2, δ_2
	$Q_2 = Q_{G2} - Q_{L2} = -2.8$	
3	$V_3 = 1.05$	Q_3, δ_3
	$P_3 = P_{G3} - P_{L3} = 4.4$	
4	$P_4 = 0, Q_4 = 0$	V_4, δ_4
5	$P_5 = 0, Q_5 = 0$	V_5, δ_5

Q_3 and δ_3 are unknowns. For buses 2, 4, and 5, load buses, V_2, V_4, V_5 and δ_2, δ_4, δ_5 are unknowns.

The elements of $\boldsymbol{Y}_{bus}$ are computed from (6.4.2). Since buses 1 and 3 are not directly connected to bus 2,

$$Y_{21} = Y_{23} = 0$$

Using (6.4.2),

$$Y_{24} = \frac{-1}{R'_{24} + jX'_{24}} = \frac{-1}{0.009 + j0.1} = -0.89276 + j9.91964 \quad \text{per unit}$$

$$= 9.95972\underline{/95.143^\circ} \quad \text{per unit}$$

$$Y_{25} = \frac{-1}{R'_{25} + jX'_{25}} = \frac{-1}{0.0045 + j0.05} = -1.78552 + j19.83932 \quad \text{per unit}$$

$$= 19.9195\underline{/95.143^\circ} \quad \text{per unit}$$

$$Y_{22} = \frac{1}{R'_{24} + jX'_{24}} + \frac{1}{R'_{25} + jX'_{25}} + j\frac{B'_{24}}{2} + j\frac{B'_{25}}{2}$$

$$= (0.89276 - j9.91964) + (1.78552 - j19.83932) + j\frac{1.72}{2} + j\frac{0.88}{2}$$

$$= 2.67828 - j28.4590 = 28.5847\underline{/-84.624^\circ} \quad \text{per unit}$$

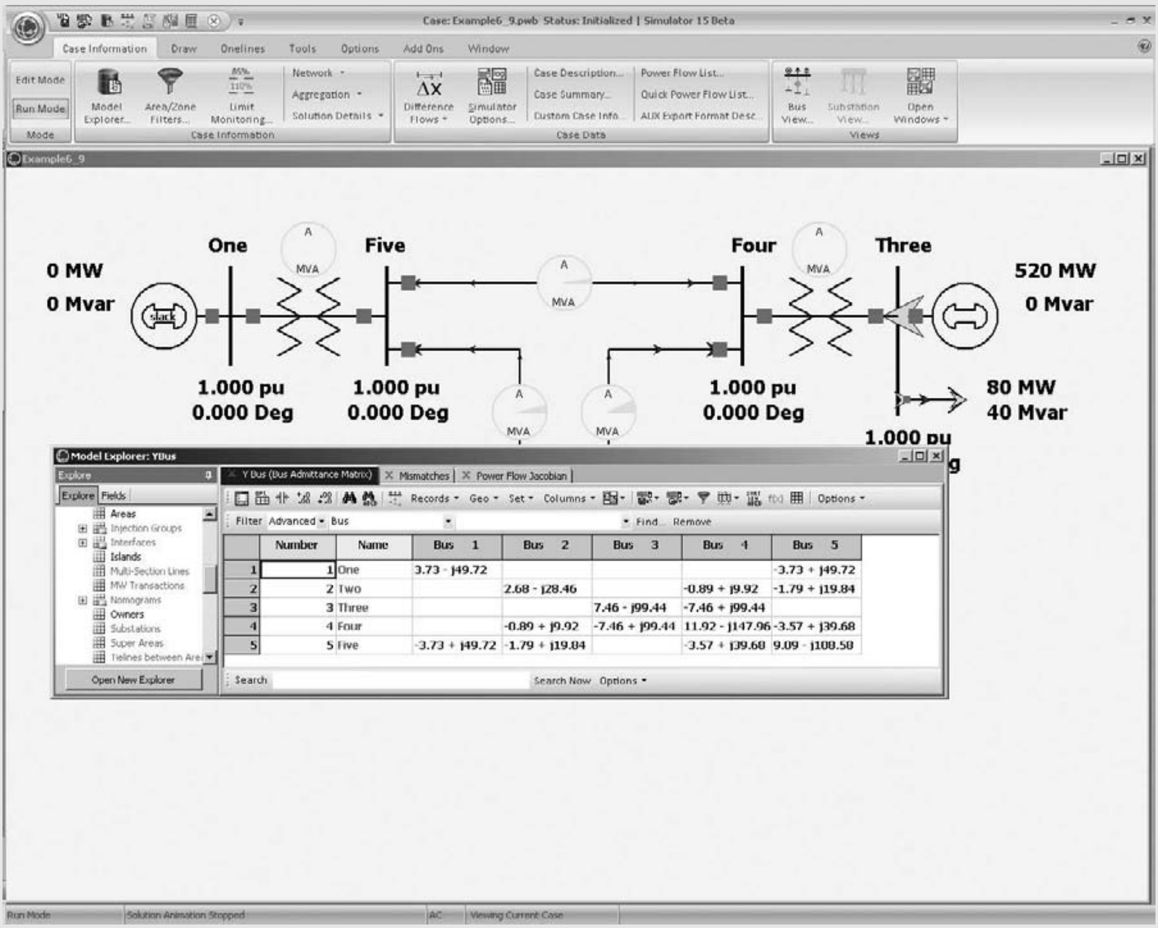

FIGURE 6.3 Screen for Example 6.9

where half of the shunt admittance of each line connected to bus 2 is included in Y_{22} (the other half is located at the other ends of these lines).

This five-bus power system is modeled in PowerWorld Simulator case Example 6_9 (see Figure 6.3). To view the input data, first click on the **Edit Mode** button (on the far left-hand side of the ribbon) to switch into the Edit mode (the Edit mode is used for modifying system parameters). Then by selecting the **Case Information** tab you can view tabular displays showing the various parameters for the system. For example, use **Network, Buses** to view the parameters for each bus, and **Network, Lines and Transformers** to view the parameters for the transmission lines and transformers. Fields shown in blue can be directly changed simply by typing over them, and those shown in green can be toggled by clicking on them. Note that the values shown on these displays match the values from Tables 6.1 to 6.3, except the power values are shown in actual MW/Mvar units.

The elements of Y_{bus} can also be displayed by selecting **Solution Details, $\mathbf{Y_{bus}}$**. Since the Y_{bus} entries are derived from other system parameters, they cannot be changed directly. Notice that several of the entries are blank, indicating that there is no line directly connecting these two buses (a blank entry is equivalent to zero). For larger networks most of the elements of the Y_{bus} are zero since any single bus usually only has a few incident lines (such sparse matrices are considered in Section 6.8). The elements of the Y_{bus} can be saved in a Matlab compatible format by first right-clicking within the Y_{bus} matrix to display the local menu, and then selecting **Save $\mathbf{Y_{bus}}$ in Matlab Format** from the local menu.

Finally, notice that no flows are shown on the one-line because the nonlinear power-flow equations have not yet been solved. We cover the solution of these equations next. ■

Using $\boldsymbol{Y}_{\text{bus}}$, we can write nodal equations for a power system network, as follows:

$$\boldsymbol{I} = \boldsymbol{Y}_{\text{bus}} \boldsymbol{V} \tag{6.4.3}$$

where I is the N vector of source currents injected into each bus and $\boldsymbol{V}$ is the N vector of bus voltages. For bus k, the kth equation in (6.4.3) is

$$I_k = \sum_{n=1}^{N} Y_{kn} V_n \tag{6.4.4}$$

The complex power delivered to bus k is

$$S_k = \mathrm{P}_k + j\mathrm{Q}_k = V_k I_k^* \tag{6.4.5}$$

Power-flow solutions by Gauss–Seidel are based on nodal equations, (6.4.4), where each current source I_k is calculated from (6.4.5). Using (6.4.4) in (6.4.5),

$$\mathrm{P}_k + j\mathrm{Q}_k = V_k \left[\sum_{n=1}^{N} Y_{kn} V_n \right]^* \qquad k = 1, 2, \ldots, N \tag{6.4.6}$$

With the following notation,

$$V_n = \mathrm{V}_n e^{j\delta_n} \tag{6.4.7}$$

$$Y_{kn} = \mathrm{Y}_{kn} e^{j\theta_{kn}} = G_{kn} + jB_{kn} \qquad k, n = 1, 2, \ldots, N \tag{6.4.8}$$

(6.4.6) becomes

$$\mathrm{P}_k + j\mathrm{Q}_k = \mathrm{V}_k \sum_{n=1}^{N} \mathrm{Y}_{kn} \mathrm{V}_n e^{j(\delta_k - \delta_n - \theta_{kn})} \tag{6.4.9}$$

Taking the real and imaginary parts of (6.4.9), we can write the power balance equations as either

$$\mathrm{P}_k = \mathrm{V}_k \sum_{n=1}^{N} \mathrm{Y}_{kn} \mathrm{V}_n \cos(\delta_k - \delta_n - \theta_{kn}) \tag{6.4.10}$$

$$\mathrm{Q}_k = \mathrm{V}_k \sum_{n=1}^{N} \mathrm{Y}_{kn} \mathrm{V}_n \sin(\delta_k - \delta_n - \theta_{kn}) \qquad k = 1, 2, \ldots, N \tag{6.4.11}$$

or when the Y_{kn} is expressed in rectangular coordinates by

$$\mathrm{P}_K = \mathrm{V}_K \sum_{n=1}^{N} V_n [G_{kn} \cos(\delta_k - \delta_n) + B_{kn} \sin(\delta_k - \delta_n)] \tag{6.4.12}$$

$$\mathrm{Q}_K = \mathrm{V}_K \sum_{n=1}^{N} V_n [G_{kn} \sin(\delta_k - \delta_n) - B_{kn} \cos(\delta_k - \delta_n)] \qquad k = 1, 2, \ldots, N \tag{6.4.13}$$

Power-flow solutions by Newton–Raphson are based on the nonlinear power-flow equations given by (6.4.10) and (6.4.11) [or alternatively by (6.4.12) and (6.4.13)].

6.5 POWER-FLOW SOLUTION BY GAUSS–SEIDEL

Nodal equations $\boldsymbol{I} = \boldsymbol{Y}_{\text{bus}} \boldsymbol{V}$ are a set of linear equations analogous to $\boldsymbol{y} = \boldsymbol{A}\boldsymbol{x}$, solved in Section 6.2 using Gauss–Seidel. Since power-flow bus data consists of P_k and Q_k for load buses or P_k and V_k for voltage-controlled buses, nodal equations do not directly fit the linear equation format; the current source vector $\boldsymbol{I}$ is unknown and the equations are actually nonlinear. For each load bus, I_k can be calculated from (6.4.5), giving

$$I_k = \frac{\mathrm{P}_k - j\mathrm{Q}_k}{V_k^*} \tag{6.5.1}$$

Applying the Gauss–Seidel method, (6.2.9), to the nodal equations, with I_k given above, we obtain

$$V_k(i+1) = \frac{1}{Y_{kk}}\left[\frac{P_k - jQ_k}{V_k^*(i)} - \sum_{n=1}^{k-1} Y_{kn}V_n(i+1) - \sum_{n=k+1}^{N} Y_{kn}V_n(i)\right] \quad (6.5.2)$$

Equation (6.5.2) can be applied twice during each iteration for load buses, first using $V_k^*(i)$, then replacing $V_k^*(i)$, by $V_k^*(i+1)$ on the right side of (6.5.2).

For a voltage-controlled bus, Q_k is unknown, but can be calculated from (6.4.11), giving

$$Q_k = V_k(i)\sum_{n=1}^{N} Y_{kn}V_n(i)\sin[\delta_k(i) - \delta_n(i) - \theta_{kn}] \quad (6.5.3)$$

Also,

$$Q_{Gk} = Q_k + Q_{Lk}$$

If the calculated value of Q_{Gk} does not exceed its limits, then Q_k is used in (6.5.2) to calculate $V_k(i+1) = V_k(i+1)\underline{/\delta_k(i+1)}$. Then the magnitude $V_k(i+1)$ is changed to V_k, which is input data for the voltage-controlled bus. Thus we use (6.5.2) to compute only the angle $\delta_k(i+1)$ for voltage-controlled buses.

If the calculated value exceeds its limit $Q_{Gk\max}$ or $Q_{Gk\min}$ during any iteration, then the bus type is changed from a voltage-controlled bus to a load bus, with Q_{Gk} set to its limit value. Under this condition, the voltage-controlling device (capacitor bank, static var system, and so on) is not capable of maintaining V_k as specified by the input data. The power-flow program then calculates a new value of V_k.

For the swing bus, denoted bus 1, V_1 and δ_1 are input data. As such, no iterations are required for bus 1. After the iteration process has converged, one pass through (6.4.10) and (6.4.11) can be made to compute P_1 and Q_1.

EXAMPLE 6.10 Power-flow solution by Gauss–Seidel

For the power system of Example 6.9, use Gauss–Seidel to calculate $V_2(1)$, the phasor voltage at bus 2 after the first iteration. Use zero initial phase angles and 1.0 per-unit initial voltage magnitudes (except at bus 3, where $V_3 = 1.05$) to start the iteration procedure.

SOLUTION Bus 2 is a load bus. Using the input data and bus admittance values from Example 6.9 in (6.5.2),

$$V_2(1) = \frac{1}{Y_{22}}\left\{\frac{P_2 - jQ_2}{V_2^*(0)} - [Y_{21}V_1(1) + Y_{23}V_3(0) + Y_{24}V_4(0) + Y_{25}V_5(0)]\right\}$$

$$= \frac{1}{28.5847\underline{/-84.624^\circ}}\left\{\frac{-8 - j(-2.8)}{1.0\underline{/0^\circ}}\right.$$

$$\left. - [(-1.78552 + j19.83932)(1.0) + (-0.89276 + j9.91964)(1.0)]\right\}$$

$$= \frac{(-8 + j2.8) - (-2.67828 + j29.7589)}{28.5847\underline{/-84.624^\circ}}$$

$$= 0.96132\underline{/-16.543^\circ} \quad \text{per unit}$$

Next, the above value is used in (6.5.2) to recalculate $V_2(1)$:

$$V_2(1) = \frac{1}{28.5847\underline{/-84.624^\circ}}\left\{\frac{-8 + j2.8}{0.96132\underline{/16.543^\circ}}\right.$$

$$\left. - [-2.67828 + j29.75829]\right\}$$

$$= \frac{-4.4698 - j24.5973}{28.5847\underline{/-84.624^\circ}} = 0.87460\underline{/-15.675^\circ} \quad \text{per unit}$$

Computations are next performed at buses 3, 4, and 5 to complete the first Gauss–Seidel iteration.

To see the complete convergence of this case, open PowerWorld Simulator case Example 6_10. By default, PowerWorld Simulator uses the Newton–Raphson method described in the next section. However, the case can be solved with the Gauss–Seidel approach by selecting **Tools, Solve, Gauss–Seidel Power Flow**. To avoid getting stuck in an infinite loop if a case does not converge, PowerWorld Simulator places a limit on the maximum number of iterations. Usually for a Gauss–Seidel procedure this number is quite high, perhaps equal to 100 iterations. However, in this example to demonstrate the convergence characteristics of the Gauss–Seidel method it has been set to a single iteration, allowing the voltages to be viewed after each iteration. To step through the solution one iteration at a time, just repeatedly select **Tools, Solve, Gauss–Seidel Power Flow**.

A common stopping criteria for the Gauss–Seidel is to use the scaled difference in the voltage from one iteration to the next (6.2.2). When this difference is below a specified convergence tolerance ε for each bus, the problem is considered solved. An alternative approach, implemented in PowerWorld Simulator, is to examine the real and reactive mismatch equations, defined as the difference between the right- and left-hand sides of (6.4.10) and (6.4.11). PowerWorld Simulator continues iterating until all the bus mismatches are below an MVA (or kVA) tolerance. When single-stepping through the solution, the bus mismatches can be viewed after each iteration on the **Case**

Information, Mismatches display. The solution mismatch tolerance can be changed on the Power Flow Solution page of the PowerWorld Simulator Options dialog (select **Tools, Simulator Options**, then select the **Power Flow Solution** category to view this dialog); the maximum number of iterations can also be changed from this page. A typical convergence tolerance is about 0.5 MVA. ■

6.6 POWER-FLOW SOLUTION BY NEWTON–RAPHSON

Equations (6.4.10) and (6.4.11) are analogous to the nonlinear equation $\mathbf{y} = \mathbf{f}(\mathbf{x})$, solved in Section 6.3 by Newton–Raphson. We define the $\mathbf{x}$, $\mathbf{y}$, and $\mathbf{f}$ vectors for the power-flow problem as

$$\mathbf{x} = \begin{bmatrix} \boldsymbol{\delta} \\ \mathbf{V} \end{bmatrix} = \begin{bmatrix} \delta_2 \\ \vdots \\ \delta_N \\ \mathrm{V}_2 \\ \vdots \\ \mathrm{V}_N \end{bmatrix}; \quad \mathbf{y} = \begin{bmatrix} \mathbf{P} \\ \mathbf{Q} \end{bmatrix} = \begin{bmatrix} \mathrm{P}_2 \\ \vdots \\ \mathrm{P}_N \\ \mathrm{Q}_2 \\ \vdots \\ \mathrm{Q}_N \end{bmatrix};$$

$$\mathbf{f}(\mathbf{x}) = \begin{bmatrix} \mathbf{P}(\mathbf{x}) \\ \mathbf{Q}(\mathbf{x}) \end{bmatrix} = \begin{bmatrix} \mathrm{P}_2(\mathbf{x}) \\ \vdots \\ \mathrm{P}_N(\mathbf{x}) \\ \mathrm{Q}_2(\mathbf{x}) \\ \vdots \\ \mathrm{Q}_N(\mathbf{x}) \end{bmatrix} \tag{6.6.1}$$

where all V, P, and Q terms are in per-unit and δ terms are in radians. The swing bus variables δ_1 and V_1 are omitted from (6.6.1), since they are already known. Equations (6.4.10) and (6.4.11) then have the following form:

$$\mathrm{y}_k = \mathrm{P}_k = \mathrm{P}_k(\mathbf{x}) = \mathrm{V}_k \sum_{n=1}^{N} \mathrm{Y}_{kn}\mathrm{V}_n \cos(\delta_k - \delta_n - \theta_{kn}) \tag{6.6.2}$$

$$\mathrm{y}_{k+N} = \mathrm{Q}_k = \mathrm{Q}_k(\mathbf{x}) = \mathrm{V}_k \sum_{n=1}^{N} \mathrm{Y}_{kn}\mathrm{V}_n \sin(\delta_k - \delta_n - \theta_{kn})$$

$$k = 2, 3, \ldots, N \tag{6.6.3}$$

TABLE 6.5 Elements of the Jacobian matrix

$n \neq k$

$$J1_{kn} = \frac{\partial P_k}{\partial \delta_n} = V_k Y_{kn} V_n \sin(\delta_k - \delta_n - \theta_{kn})$$
$$J2_{kn} = \frac{\partial P_k}{\partial V_n} = V_k Y_{kn} \cos(\delta_k - \delta_n - \theta_{kn})$$
$$J3_{kn} = \frac{\partial Q_k}{\partial \delta_n} = -V_k Y_{kn} V_n \cos(\delta_k - \delta_n - \theta_{kn})$$
$$J4_{kn} = \frac{\partial Q_k}{\partial V_n} = V_k Y_{kn} \sin(\delta_k - \delta_n - \theta_{kn})$$

$n = k$

$$J1_{kk} = \frac{\partial P_k}{\partial \delta_k} = -V_k \sum_{\substack{n=1\\ n\neq k}}^{N} Y_{kn} V_n \sin(\delta_k - \delta_n - \theta_{kn})$$
$$J2_{kk} = \frac{\partial P_k}{\partial V_k} = V_k Y_{kk} \cos\theta_{kk} + \sum_{n=1}^{N} Y_{kn} V_n \cos(\delta_k - \delta_n - \theta_{kn})$$
$$J3_{kk} = \frac{\partial Q_k}{\partial \delta_k} = V_k \sum_{\substack{n=1\\ n\neq k}}^{N} Y_{kn} V_n \cos(\delta_k - \delta_n - \theta_{kn})$$
$$J4_{kk} = \frac{\partial Q_k}{\partial V_k} = -V_k Y_{kk} \sin\theta_{kk} + \sum_{n=1}^{N} Y_{kn} V_n \sin(\delta_k - \delta_n - \theta_{kn})$$

$k, n = 2, 3, \ldots, N$

The Jacobian matrix of (6.3.10) has the form

$$\mathbf{J} = \begin{array}{c} \qquad\mathbf{J}1 \qquad\qquad\qquad\qquad \mathbf{J}2 \\ \left[\begin{array}{ccc|ccc} \frac{\partial P_2}{\partial \delta_2} & \cdots & \frac{\partial P_2}{\partial \delta_N} & \frac{\partial P_2}{\partial V_2} & \cdots & \frac{\partial P_2}{\partial V_N} \\ \vdots & & & \vdots & & \\ \frac{\partial P_N}{\partial \delta_2} & \cdots & \frac{\partial P_N}{\partial \delta_N} & \frac{\partial P_N}{\partial V_2} & \cdots & \frac{\partial P_N}{\partial V_N} \\ \hline \frac{\partial Q_2}{\partial \delta_2} & \cdots & \frac{\partial Q_2}{\partial \delta_N} & \frac{\partial Q_2}{\partial V_2} & \cdots & \frac{\partial Q_2}{\partial V_N} \\ \vdots & & & \vdots & & \\ \frac{\partial Q_N}{\partial \delta_2} & \cdots & \frac{\partial Q_N}{\partial \delta_N} & \frac{\partial Q_N}{\partial V_2} & \cdots & \frac{\partial Q_N}{\partial V_N} \end{array}\right] \\ \qquad\mathbf{J}3 \qquad\qquad\qquad\qquad \mathbf{J}4 \end{array} \tag{6.6.4}$$

Equation (6.6.4) is partitioned into four blocks. The partial derivatives in each block, derived from (6.6.2) and (6.6.3), are given in Table 6.5.

We now apply to the power-flow problem the four Newton–Raphson steps outlined in Section 6.3, starting with $\mathbf{x}(i) = \begin{bmatrix} \boldsymbol{\delta}(i) \\ \mathbf{V}(i) \end{bmatrix}$ at the ith iteration.

STEP 1 Use (6.6.2) and (6.6.3) to compute

$$\Delta\mathbf{y}(i) = \begin{bmatrix} \Delta\mathbf{P}(i) \\ \Delta\mathbf{Q}(i) \end{bmatrix} = \begin{bmatrix} \mathbf{P} - \mathbf{P}[\mathbf{x}(i)] \\ \mathbf{Q} - \mathbf{Q}[\mathbf{x}(i)] \end{bmatrix} \tag{6.6.5}$$

STEP 2 Use the equations in Table 6.5 to calculate the Jacobian matrix.

STEP 3 Use Gauss elimination and back substitution to solve

$$\left[\begin{array}{c|c} \mathbf{J}1(i) & \mathbf{J}2(i) \\ \hline \mathbf{J}3(i) & \mathbf{J}4(i) \end{array}\right] \begin{bmatrix} \Delta\boldsymbol{\delta}(i) \\ \Delta\mathbf{V}(i) \end{bmatrix} = \begin{bmatrix} \Delta\mathbf{P}(i) \\ \Delta\mathbf{Q}(i) \end{bmatrix} \tag{6.6.6}$$

STEP 4 Compute

$$\mathbf{x}(i+1) = \begin{bmatrix} \boldsymbol{\delta}(i+1) \\ \mathbf{V}(i+1) \end{bmatrix} = \begin{bmatrix} \boldsymbol{\delta}(i) \\ \mathbf{V}(i) \end{bmatrix} + \begin{bmatrix} \Delta\boldsymbol{\delta}(i) \\ \Delta\mathbf{V}(i) \end{bmatrix} \tag{6.6.7}$$

Starting with initial value $\mathbf{x}(0)$, the procedure continues until convergence is obtained or until the number of iterations exceeds a specified maximum. Convergence criteria are often based on $\Delta\mathbf{y}(i)$ (called *power mismatches*) rather than on $\Delta\mathbf{x}(i)$ (phase angle and voltage magnitude mismatches).

For each voltage-controlled bus, the magnitude V_k is already known, and the function $Q_k(\mathbf{x})$ is not needed. Therefore, we could omit V_k from the $\mathbf{x}$ vector and Q_k from the $\mathbf{y}$ vector. We could also omit from the Jacobian matrix the column corresponding to partial derivatives with respect to V_k and the row corresponding to partial derivatives of $Q_k(\mathbf{x})$. Alternatively, rows and corresponding columns for voltage-controlled buses can be retained in the Jacobian matrix. Then during each iteration, the voltage magnitude $V_k(i+1)$ of each voltage-controlled bus is reset to V_k, which is input data for that bus.

At the end of each iteration, we compute $Q_k(\mathbf{x})$ from (6.6.3) and $Q_{Gk} = Q_k(\mathbf{x}) + Q_{Lk}$ for each voltage-controlled bus. If the computed value of Q_{Gk} exceeds its limits, then the bus type is changed to a load bus with Q_{Gk} set to its limit value. The power-flow program also computes a new value for V_k.

EXAMPLE 6.11 Jacobian matrix and power-flow solution by Newton–Raphson

Determine the dimension of the Jacobian matrix for the power system in Example 6.9. Also calculate $\Delta P_2(0)$ in Step 1 and $J1_{24}(0)$ in Step 2 of the first Newton–Raphson iteration. Assume zero initial phase angles and 1.0 per-unit initial voltage magnitudes (except $V_3 = 1.05$).

SOLUTION Since there are $N = 5$ buses for Example 6.9, (6.6.2) and (6.6.3) constitute $2(N-1) = 8$ equations, for which $\mathbf{J}(i)$ has dimension 8×8.

However, there is one voltage-controlled bus, bus 3. Therefore, V_3 and the equation for $Q_3(\mathbf{x})$ could be eliminated, with $\mathbf{J}(i)$ reduced to a 7×7 matrix.

From Step 1 and (6.6.2),

$$\begin{aligned}
\Delta P_2(0) = P_2 - P_2(\mathbf{x}) = P_2 - V_2(0)\{&Y_{21}V_1 \cos[\delta_2(0) - \delta_1(0) - \theta_{21}] \\
&+ Y_{22}V_2 \cos[-\theta_{22}] + Y_{23}V_3 \cos[\delta_2(0) - \delta_3(0) - \theta_{23}] \\
&+ Y_{24}V_4 \cos[\delta_2(0) - \delta_4(0) - \theta_{24}] \\
&+ Y_{25}V_5 \cos[\delta_2(0) - \delta_5(0) - \theta_{25}]\}
\end{aligned}$$

$$\begin{aligned}
\Delta P_2(0) &= -8.0 - 1.0\{28.5847(1.0) \cos(84.624^\circ) \\
&\quad + 9.95972(1.0) \cos(-95.143^\circ) \\
&\quad + 19.9159(1.0) \cos(-95.143^\circ)\} \\
&= -8.0 - (-2.89 \times 10^{-4}) = -7.99972 \quad \text{per unit}
\end{aligned}$$

From Step 2 and J1 given in Table 6.5

$$\begin{aligned}
J1_{24}(0) &= V_2(0)Y_{24}V_4(0) \sin[\delta_2(0) - \delta_4(0) - \theta_{24}] \\
&= (1.0)(9.95972)(1.0) \sin[-95.143^\circ] \\
&= -9.91964 \quad \text{per unit}
\end{aligned}$$

To see the complete convergence of this case, open PowerWorld Simulator case Example 6_11 (see Figure 6.4). Select **Case Information, Network, Mismatches** to see the initial mismatches, and **Case Information, Solution Details, Power Flow Jacobian** to view the initial Jacobian matrix. As is common in commercial power flows, PowerWorld Simulator actually includes rows in the Jacobian for voltage-controlled buses. When a generator is regulating its terminal voltage, this row corresponds to the equation setting the bus voltage magnitude equal to the generator voltage setpoint. However, if the generator hits a reactive power limit, the bus type is switched to a load bus.

To step through the New-Raphson solution, from the **Tools** Ribbon select **Solve, Single Solution—Full Newton**. Ordinarily this selection would perform a complete Newton-Raphson iteration, stopping only when all the mismatches are less than the desired tolerance. However, for this case, in order to allow you to see the solution process, the maximum number of iterations has been set to 1, allowing the voltages, mismatches and the Jacobian to be viewed after each iteration. To complete the solution, continue to select **Single Solution—Full Newton** until the solution convergence to the values shown in Tables 6.6, 6.7 and 6.8 (in about three iterations).

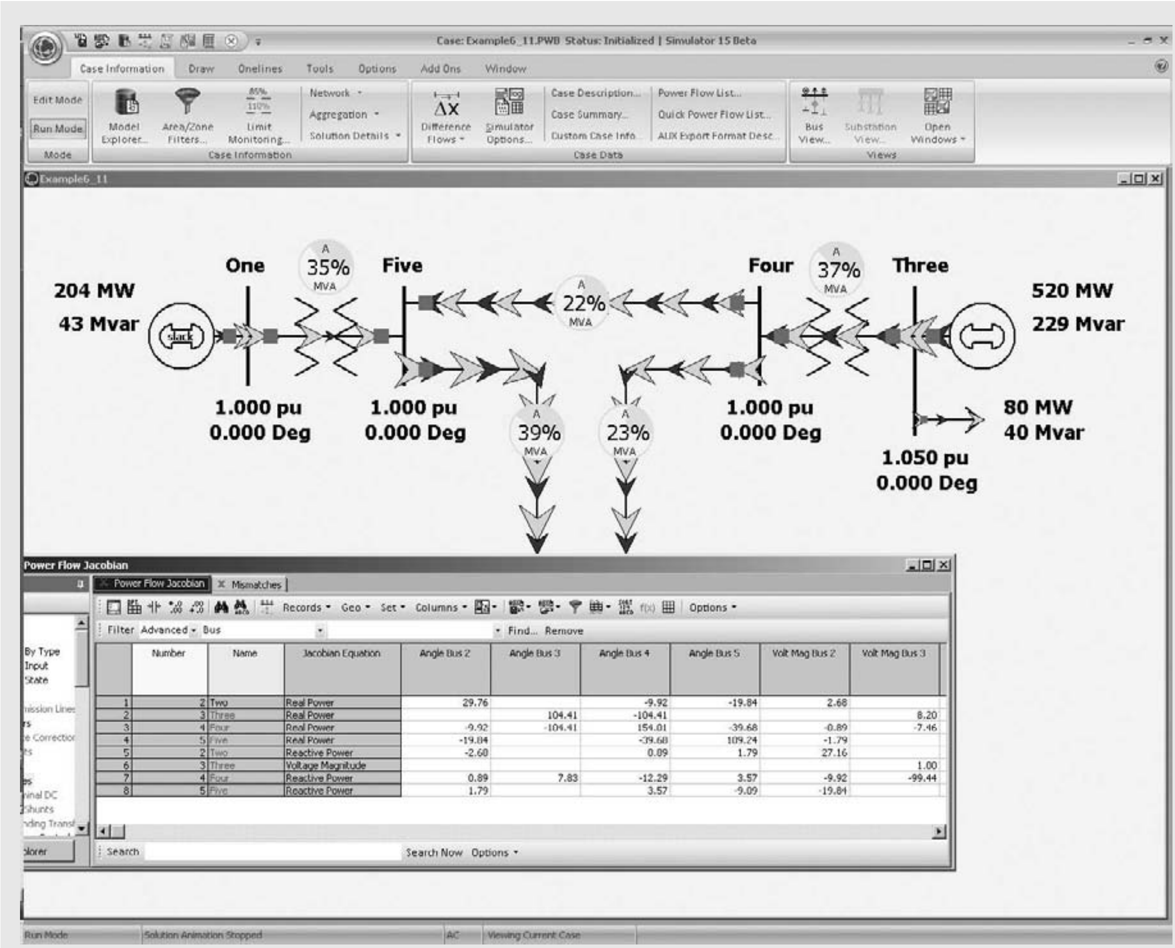

FIGURE 6.4 Screen for Example 6.11 showing Jacobian matrix at first iteration ■

TABLE 6.6

Bus output data for the power system given in Example 6.9

Bus #	Voltage Magnitude (per unit)	Phase Angle (degrees)	Generation PG (per unit)	Generation QG (per unit)	Load PL (per unit)	Load QL (per unit)
1	1.000	0.000	3.948	1.144	0.000	0.000
2	0.834	−22.407	0.000	0.000	8.000	2.800
3	1.050	−0.597	5.200	3.376	0.800	0.400
4	1.019	−2.834	0.000	0.000	0.000	0.000
5	0.974	−4.548	0.000	0.000	0.000	0.000
		TOTAL	9.148	4.516	8.800	3.200

TABLE 6.7

Line output data for the power system given in Example 6.9

Line #	Bus to Bus		P	Q	S
1	2	4	−2.920	−1.392	3.232
	4	2	3.036	1.216	3.272
2	2	5	−5.080	−1.408	5.272
	5	2	5.256	2.632	5.876
3	4	5	1.344	1.504	2.016
	5	4	−1.332	−1.824	2.260

TABLE 6.8

Transformer output data for the power system given in Example 6.9

Tran. #	Bus to Bus		P	Q	S
1	1	5	3.948	1.144	4.112
	5	1	−3.924	−0.804	4.004
2	3	4	4.400	2.976	5.312
	4	3	−4.380	−2.720	5.156

EXAMPLE 6.12 Power-flow program: change in generation

Using the power-flow system given in Example 6.9, determine the acceptable generation range at bus 3, keeping each line and transformer loaded at or below 100% of its MVA limit.

SOLUTION Load PowerWorld Simulator case Example 6.9. Select **Single Solution-Full Newton** to perform a single power-flow solution using the Newton–Raphson approach. Then view the **Case Information** displays to verify that the PowerWorld Simulator solution matches the solution shown in Tables 6.6, 6.7, and 6.8. Additionally, the pie charts on the one-lines show the percentage line and transformer loadings. Initially transformer T1, between buses 1 and 5, is loaded at about 68% of its maximum MVA limit, while transformer T2, between buses 3 and 4, is loaded at about 53%.

Next, the bus 3 generation needs to be varied. This can be done a number of different ways in PowerWorld Simulator. The easiest (for this example) is to use the bus 3 generator MW one-line field to manually change the generation (see Figure 6.5). Right-click on the "520 MW" field to the right of the bus 3 generator and select '**Generator Field Information**' dialog to view the '**Generator Field Options**' dialog. Set the "Delta Per Mouse Click" field to 10 and select OK. Small arrows are now visible next to this field on the one-line; clicking on the up arrow increases the generator's MW output by 10 MW, while clicking on the down arrow decreases the generation by 10 MW. Select **Tools, Play** to begin the simulation. Increase the generation until the pie chart for the transformer from bus 3 to 4 is loaded to 100%. This occurs at about 1000 MW. Notice that as the bus 3 generation is increased the bus 1 slack generation decreases by a similar amount. Repeat the process, except

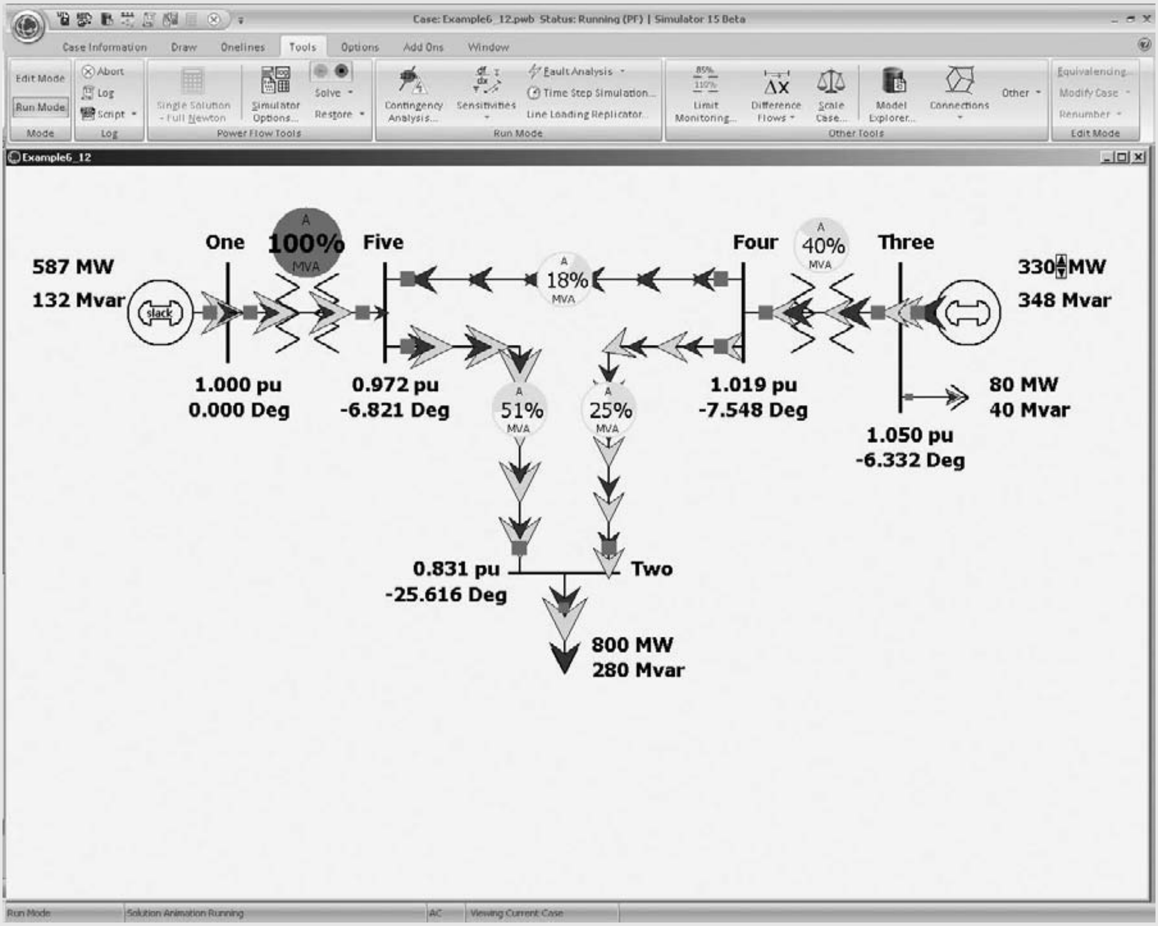

FIGURE 6.5 Screen for Example 6.12, Minimum Bus 3 Generator Loading

now decreasing the generation. This unloads the transformer from bus 3 to 4, but increases the loading on the transformer from bus 1 to bus 5. The bus 1 to 5 transformer should reach 100% loading with the bus 3 generation equal to about 330 MW. ■

Voltage-controlled buses to which tap-changing or voltage-regulating transformers are connected can be handled by various methods. One method is to treat each of these buses as a load bus. The equivalent π circuit parameters (Figure 3.25) are first calculated with tap setting $c = 1.0$ for starting. During each iteration, the computed bus voltage magnitude is compared with the desired value specified by the input data. If the computed voltage is low (or high), c is increased (or decreased) to its next setting, and the parameters of the equivalent π circuit as well as $\boldsymbol{Y}_{\text{bus}}$ are recalculated. The procedure continues until the computed bus voltage magnitude equals the desired value within a specified tolerance, or until the high or low tap-setting limit is reached. Phase-shifting transformers can be handled in a similar way by using a complex turns ratio $c = 1.0\underline{/\alpha}$, and by varying the phase-shift angle α.

A method with faster convergence makes c a variable and includes it in the $\mathbf{x}$ vector of (6.6.1). An equation is then derived to enter into the Jacobian matrix [4].

In comparing the Gauss-Seidel and Newton-Raphson algorithms, experience from power-flow studies has shown that Newton-Raphson converges in many cases where Jacobi and Gauss-Seidel diverge. Furthermore, the number of iterations required for convergence is independent of the number of buses N for Newton-Raphson, but increases with N for Jacobi and Gauss-Seidel. The principal advantage of the Jacobi and Gauss-Seidel methods had been their more modest memory storage requirements and their lower computational requirements per iteration. However, with the vast increases in low-cost computer memory over the last several decades, coupled with the need to solve power-flow problems with tens of thousands of buses, these advantages have been essentially eliminated. Therefore the Newton-Raphson, or one of the derivative methods discussed in Sections 6.9 and 6.10, are the preferred power-flow solution approaches.

EXAMPLE 6.13 Power-flow program: 37-bus system

To see a power-flow example of a larger system, open PowerWorld Simulator case Example 6_13 (see Figure 6.6). This case models a 37-bus, 9-generator power system containing three different voltage levels (345 kV, 138 kV, and 69 kV) with 57 transmission lines or transformers. The one-line can be panned by pressing the arrow keys, and it can be zoomed by pressing the ⟨ctrl⟩ with the up arrow key to zoom in or with the down arrow key to zoom out. Use **Tools, Play** to animate the one-line and **Tools, Pause** to stop the animation.

Determine the lowest per-unit voltage and the maximum line/transformer loading both for the initial case and for the case with the line from bus TIM69 to HANNAH69 out of service.

SOLUTION Use single solution to initially solve the power flow, and then **Case Information, Network, Buses...** to view a listing of all the buses in the case. To quickly determine the lowest per-unit voltage magnitude, left-click on the PU Volt column header to sort the column (clicking a second time reverses the sort). The lowest initial voltage magnitude is 0.9902 at bus DEMAR69. Next, select **Case Information, Network, Lines and Transformers...** to view the Line and Transformer Records display. Left-click on % of Max Limit to sort the lines by percentage loading. Initially the highest percentage loading is 64.9% on the line from UIUC69 to BLT69 circuit 1.

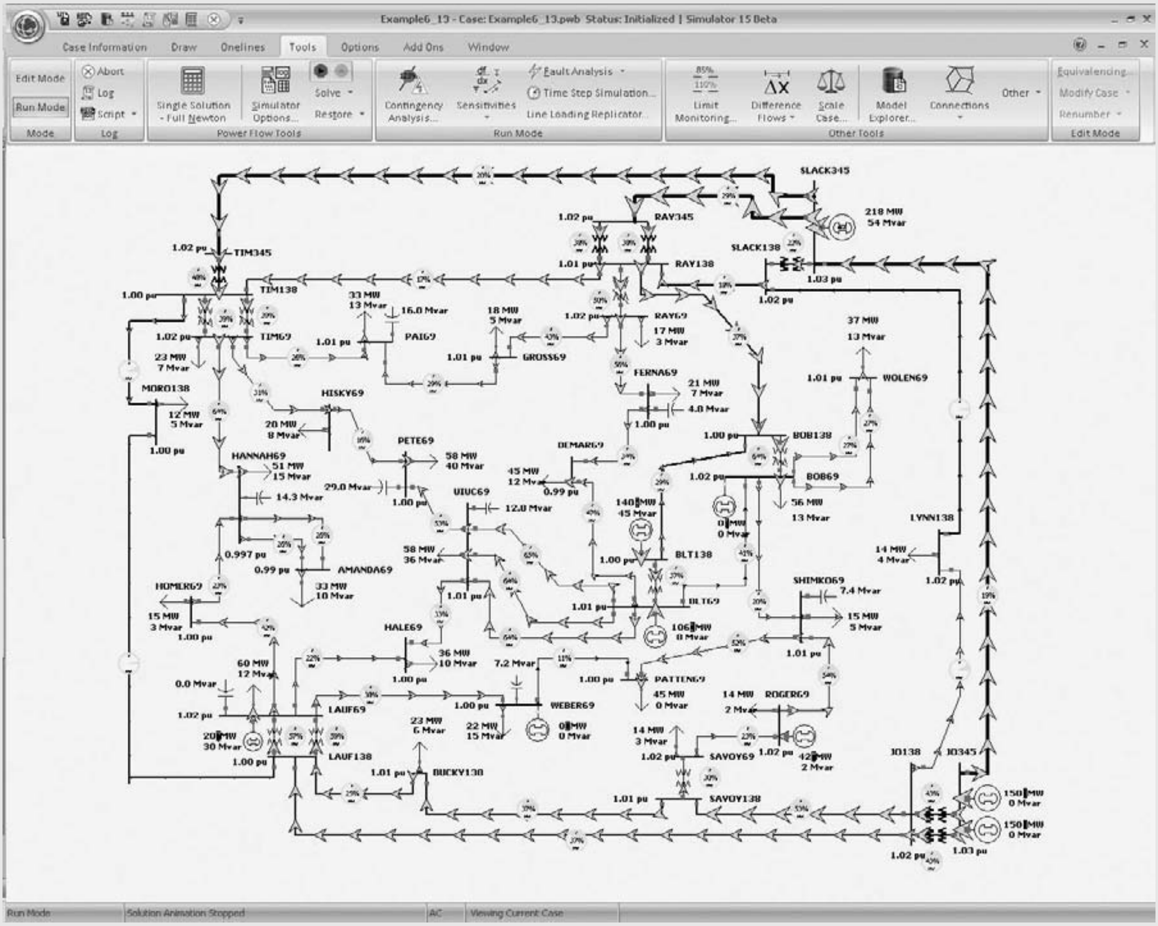

FIGURE 6.6 Screen for Example 6.13 showing the initial flows

There are several ways to remove the TIM69 to HANNAH69 line. One approach is to locate the line on the Line and Transformer Records display and then double-click on the Status field to change its value. An alternative approach is to find the line on the one-line (it is in the upper-lefthand portion) and then click on one of its circuit breakers. Once the line is removed, use single solution to resolve the power flow. The lowest per-unit voltage is now 0.9104 at AMANDA69 and the highest percentage line loading is 134.8%, on the line from HOMER69 to LAUF69. Since there are now several bus and line violations, the power system is no longer at a secure operating point. Control actions and/or design improvements are needed to correct these problems. Design Project 1 discusses these options. ■

6.7

CONTROL OF POWER FLOW

The following means are used to control system power flows:

1. Prime mover and excitation control of generators.
2. Switching of shunt capacitor banks, shunt reactors, and static var systems.
3. Control of tap-changing and regulating transformers.

A simple model of a generator operating under balanced steady-state conditions is the Thévenin equivalent shown in Figure 6.7. V_t is the generator terminal voltage, E_g is the excitation voltage, δ is the power angle, and X_g is the positive-sequence synchronous reactance. From the figure, the generator current is

$$I = \frac{E_g e^{j\delta} - V_t}{jX_g} \tag{6.7.1}$$

and the complex power delivered by the generator is

$$S = P + jQ = V_t I^* = V_t\left(\frac{E_g e^{-j\delta} - V_t}{-jX_g}\right)$$

$$= \frac{V_t E_g (j\cos\delta + \sin\delta) - jV_t^2}{X_g} \tag{6.7.2}$$

The real and reactive powers delivered are then

$$P = \text{Re}\, S = \frac{V_t E_g}{X_g}\sin\delta \tag{6.7.3}$$

$$Q = \text{Im}\, S = \frac{V_t}{X_g}(E_g\cos\delta - V_t) \tag{6.7.4}$$

Equation (6.7.3) shows that the real power P increases when the power angle δ increases. From an operational standpoint, when the prime mover increases the power input to the generator while the excitation voltage is held constant, the rotor speed increases. As the rotor speed increases, the power angle δ also increases, causing an increase in generator real power output P. There is also a decrease in reactive power output Q, given by (6.7.4). However, when δ is

FIGURE 6.7

Generator Thévenin equivalent

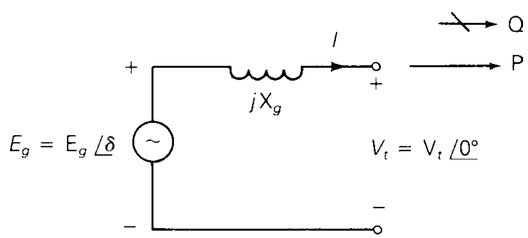

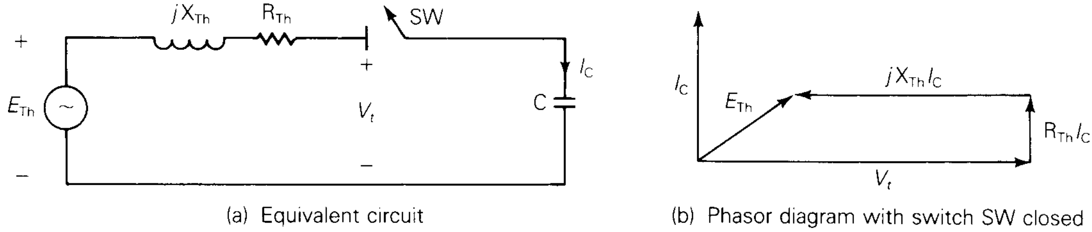

FIGURE 6.8 Effect of adding a shunt capacitor bank to a power system bus

less than 15°, the increase in P is much larger than the decrease in Q. From the power-flow standpoint, an increase in prime-move power corresponds to an increase in P at the constant-voltage bus to which the generator is connected. The power-flow program computes the increase in δ along with the small change in Q.

Equation (6.7.4) shows that reactive power output Q increases when the excitation voltage E_g increases. From the operational standpoint, when the generator exciter output increases while holding the prime-mover power constant, the rotor current increases. As the rotor current increases, the excitation voltage E_g also increases, causing an increase in generator reactive power output Q. There is also a small decrease in δ required to hold P constant in (6.7.3). From the power-flow standpoint, an increase in generator excitation corresponds to an increase in voltage magnitude at the constant-voltage bus to which the generator is connected. The power-flow program computes the increase in reactive power Q supplied by the generator along with the small change in δ.

Figure 6.8 shows the effect of adding a shunt capacitor bank to a power system bus. The system is modeled by its Thévenin equivalent. Before the capacitor bank is connected, the switch SW is open and the bus voltage equals E_{Th}. After the bank is connected, SW is closed, and the capacitor current I_C leads the bus voltage V_t by 90°. The phasor diagram shows that V_t is larger than E_{Th} when SW is closed. From the power-flow standpoint, the addition of a shunt capacitor bank to a load bus corresponds to the addition of a negative reactive load, since a capacitor absorbs negative reactive power. The power-flow program computes the increase in bus voltage magnitude along with the small change in δ. Similarly, the addition of a shunt reactor corresponds to the addition of a positive reactive load, wherein the power-flow program computes the decrease in voltage magnitude.

Tap-changing and voltage-magnitude-regulating transformers are used to control bus voltages as well as reactive power flows on lines to which they are connected. Similarly, phase-angle regulating transformers are used to control bus angles as well as real power flows on lines to which they are connected. Both tap-changing and regulating transformers are modeled by a transformer with an off-nominal turns ratio c (Figure 3.25). From the power-flow standpoint, a change in tap setting or voltage regulation corresponds to a change in c. The power-flow program computes the changes in $\boldsymbol{Y}_{\text{bus}}$, bus voltage magnitudes and angles, and branch flows.

Besides the above controls, the power-flow program can be used to investigate the effect of switching in or out lines, transformers, loads, and generators. Proposed system changes to meet future load growth, including new transmission, new transformers, and new generation can also be investigated. Power-flow design studies are normally conducted by trial and error. Using engineering judgment, adjustments in generation levels and controls are made until the desired equipment loadings and voltage profile are obtained.

EXAMPLE 6.14 Power-flow program: effect of shunt capacitor banks

Determine the effect of adding a 200-Mvar shunt capacitor bank at bus 2 on the power system in Example 6.9.

SOLUTION Open PowerWorld Simulator case Example 6_14 (see Figure 6.9). This case is identical to Example 6.9 except that a 200-Mvar shunt capacitor

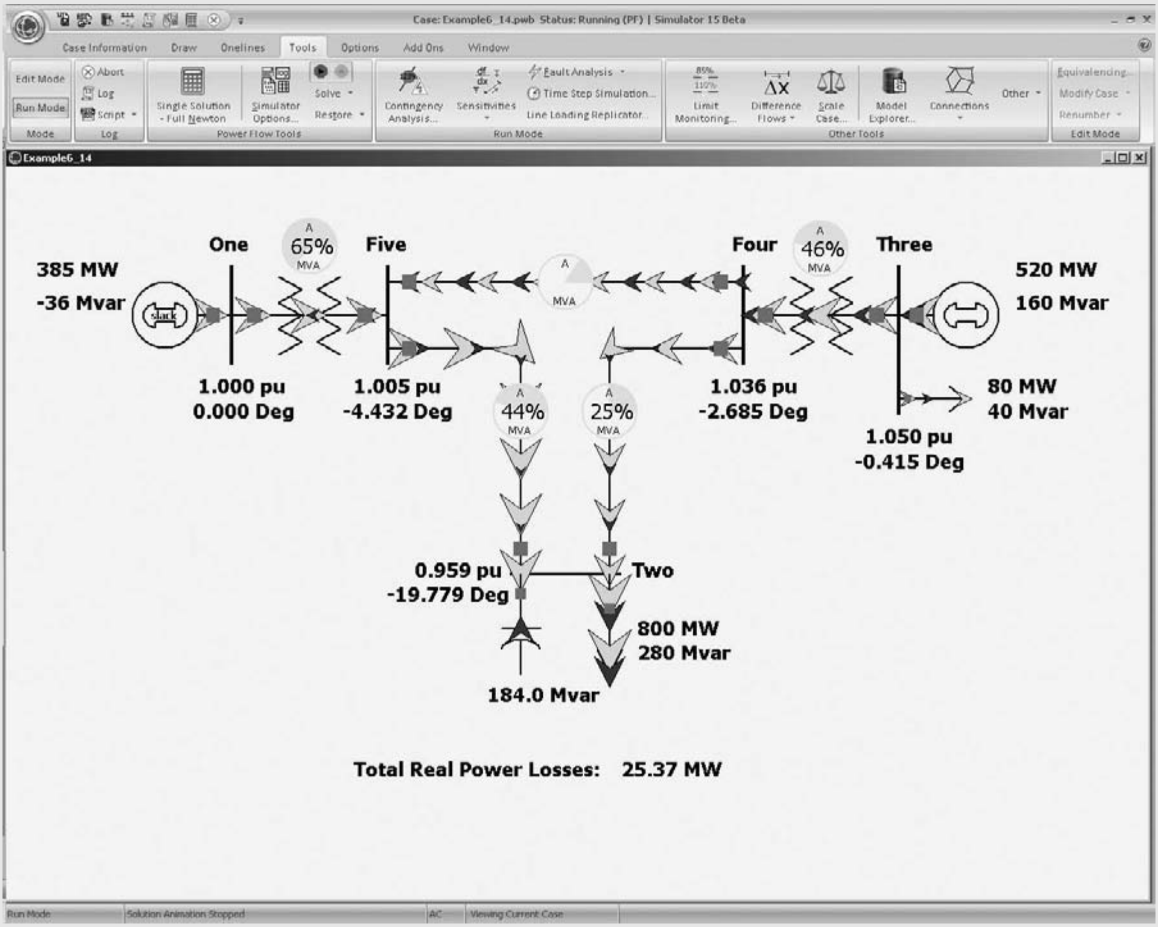

FIGURE 6.9 Screen for Example 6.14

bank has been added at bus 2. Initially this capacitor is open. Click on the capacitor's circuit to close the capacitor and then solve the case. The capacitor increases the bus 2 voltage from 0.834 per unit to a more acceptable 0.959 per unit. The insertion of the capacitor has also substantially decreased the losses, from 34.84 to 25.37 MW.

Notice that the amount of reactive power actually supplied by the capacitor is only 184 Mvar. This discrepancy arises because a capacitor's reactive output varies with the square of the terminal voltage, $Q_{cap} = V_{cap}^2/X_c$ (see 2.3.5). A capacitor's Mvar rating is based on an assumed voltage of 1.0 per unit. ■

EXAMPLE 6.15

PowerWorld Simulator Case Example 6_15 (see Figure 6.10), which modifies the Example 6.13 case by (1) opening one of the 138/69 kV transformers at the LAUF substation, and (2) opening the 69 kV transmission line between

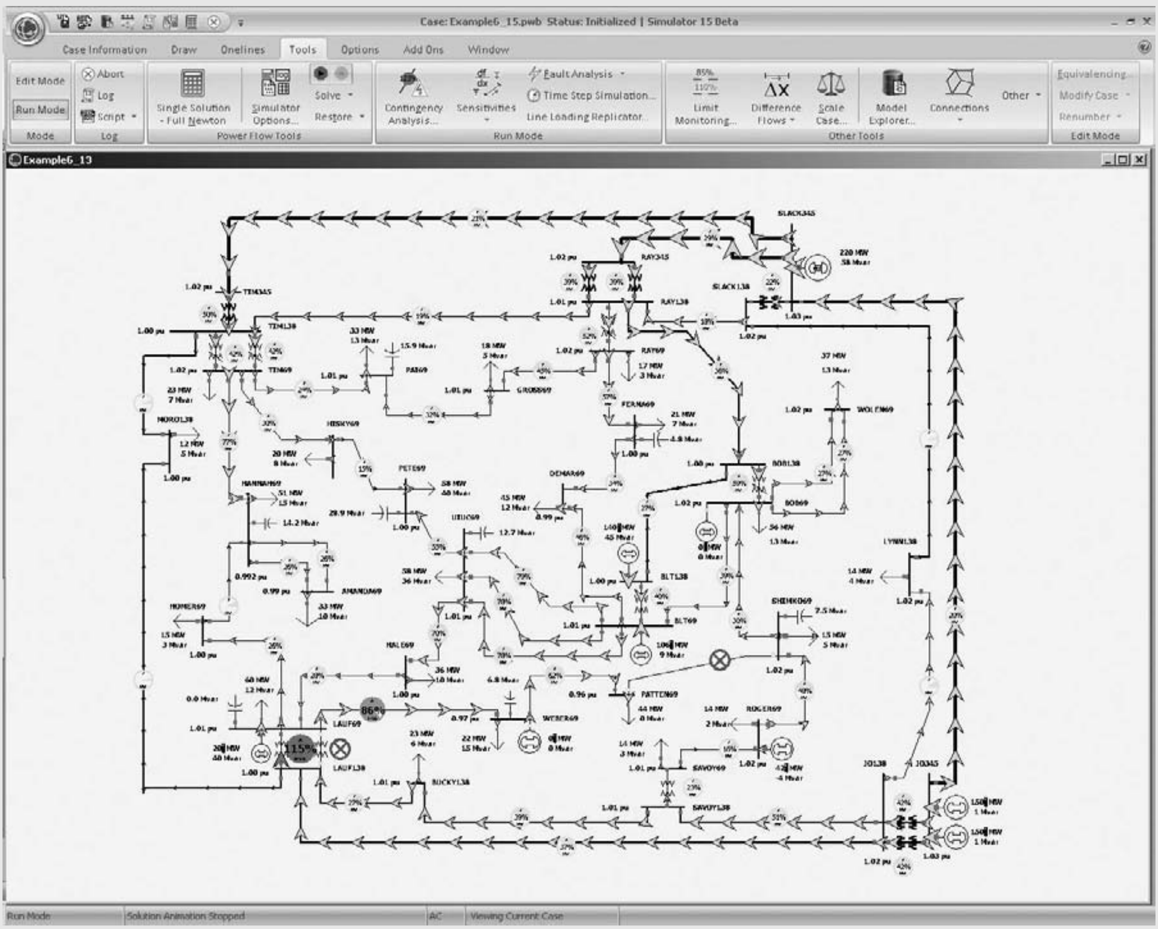

FIGURE 6.10 Screen for Example 6.15

PATTEN69 and SHIMKO69. This causes a flow of 116.2 MVA on the remaining 138/69 kV transformer at LAUF. Since this transformer has a limit of 101 MVA, it results in an overload at 115%. Redispatch the generators in order to remove this overload.

SOLUTION There are a number of solutions to this problem, and several solution techniques. One solution technique would be to use engineering intuition, along with a trial and error approach (see Figure 6.11). Since the overload is from the 138 kV level to the 69 kV level, and there is a generator directly connected to at the LAUF 69 kV bus, it stands to reason that increasing this generation would decrease the overload. Using this approach, we can remove the overload by increasing the Lauf generation until the transformer flow is reduced to 100%. This occurs when the generation is increased from 20 MW to 51 MW. Notice that as the generation is increased, the swing bus (SLACK345) generation automatically decreases in order to satisfy the requirement that total system load plus losses must be equal to total generation.

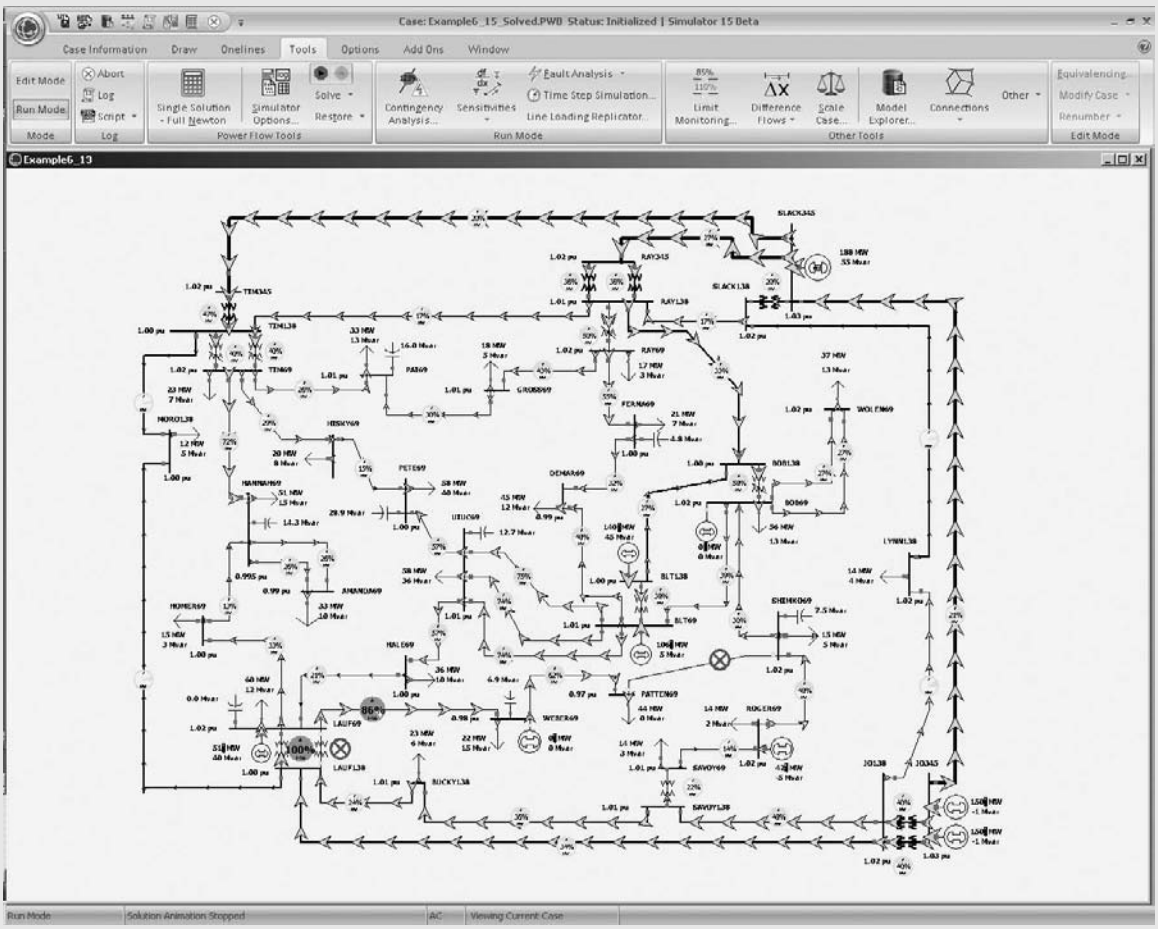

FIGURE 6.11 A solution to Example 6.15

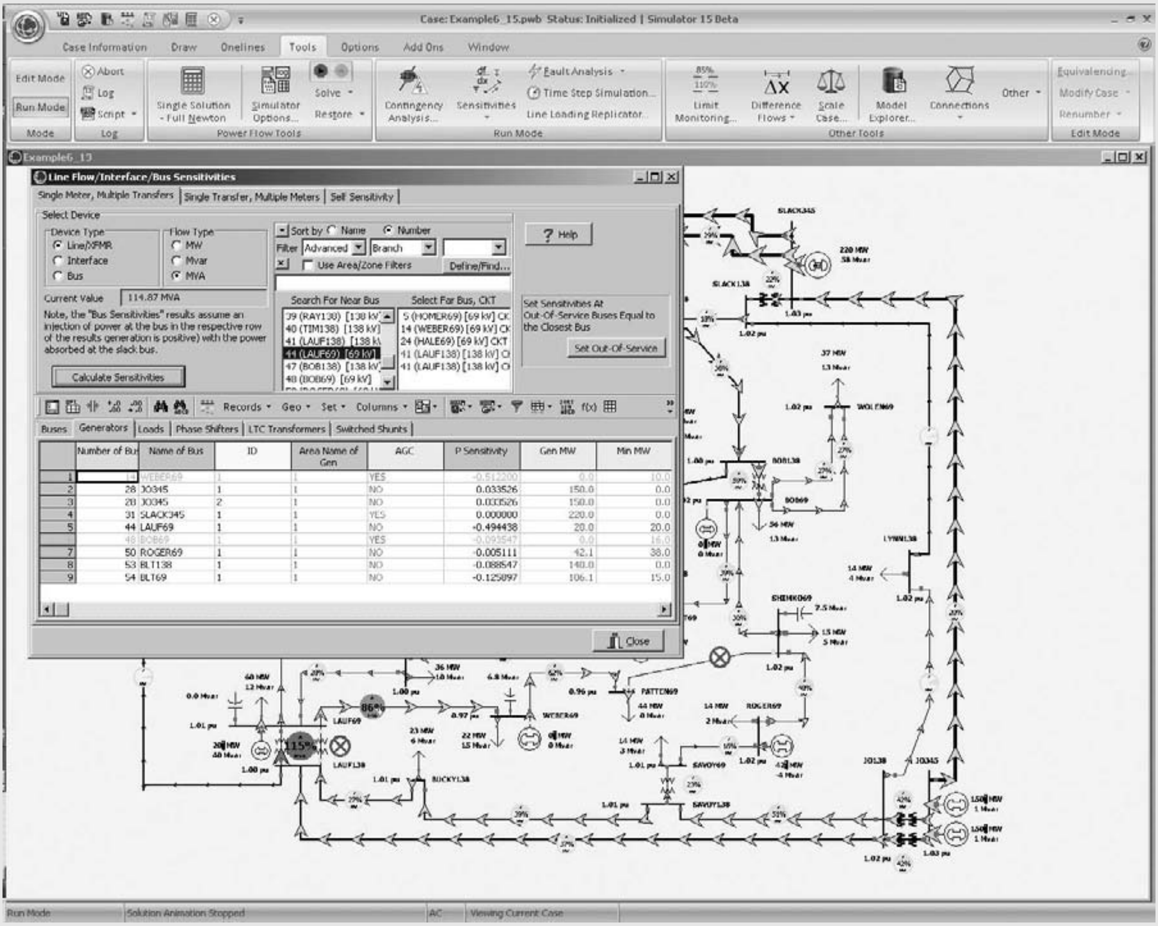

FIGURE 6.12 Example 6.15 Flow Sensitivities Dialog

An alternative possible solution is seen by noting that since the overload is caused by power flowing from the 138 kV bus, decreasing the generation at JO345 might also decrease this flow. This is indeed the case, but now the trial and error approach requires a substantial amount of work, and ultimately doesn't solve the problem. Even when we decrease the total JO345 generation from 300 MW to 0 MW, the overload is still present, albeit with its percentage decreased to 105%.

An alternative solution approach would be to first determine the generators with the most sensitivity to this violation and then adjust these (see Figure 6.12). This can be done in PowerWorld Simulator by selecting **Tools, Sensitivities, Flows and Voltage Sensitivities**. Select the LAUF 138/69 kV transformer, click on the **Calculate Sensitivities** button, and select the Generator Sensitivities tab towards the bottom of the dialog. The "P Sensitivity" field tells how increasing the output of each generator by one MW would affect the MVA flow on this transformer. Note that the sensitivity for the Lauf generator is -0.494, indicating that if we increase this generation by 1 MW the transformer MVA flow would decrease by 0.494 MVA. Hence, in order to decrease the flow by 15.2 MVA we would expect to increase the LAUF69 generator by 31 MW, exactly what we got by the trial and error approach. It is also clear that the JO345 generators, with a sensitivity of just 0.0335, would be relatively ineffective. In actual power system operation these sensitivities, known as generator shift factors, are used extensively. These sensitivities are also used in the Optimal Power Flow (introduced in Section 11.5). ■

6.8 SPARSITY TECHNIQUES

A typical power system has an average of fewer than three lines connected to each bus. As such, each row of Y_{bus} has an average of fewer than four nonzero elements, one off-diagonal for each line and the diagonal. Such a matrix, which has only a few nonzero elements, is said to be *sparse*.

Newton–Raphson power-flow programs employ sparse matrix techniques to reduce computer storage and time requirements [2]. These techniques include compact storage of Y_{bus} and $\mathbf{J}(i)$ and reordering of buses to avoid fill-in of $\mathbf{J}(i)$ during Gauss elimination steps. Consider the following matrix:

$$\mathbf{S} = \begin{bmatrix} 1.0 & -1.1 & -2.1 & -3.1 \\ -4.1 & 2.0 & 0 & -5.1 \\ -6.1 & 0 & 3.0 & 0 \\ -7.1 & 0 & 0 & 4.0 \end{bmatrix} \tag{6.8.1}$$

One method for compact storage of $\mathbf{S}$ consists of the following four vectors:

$$\mathbf{DIAG} = [1.0 \quad 2.0 \quad 3.0 \quad 4.0] \tag{6.8.2}$$

$$\mathbf{OFFDIAG} = [-1.1 \quad -2.1 \quad -3.1 \quad -4.1 \quad -5.1 \quad -6.1 \quad -7.1] \tag{6.8.3}$$

$$\mathbf{COL} = [2 \quad 3 \quad 4 \quad 1 \quad 4 \quad 1 \quad 1] \tag{6.8.4}$$

$$\mathbf{ROW} = [3 \quad 2 \quad 1 \quad 1] \tag{6.8.5}$$

DIAG contains the ordered diagonal elements and **OFFDIAG** contains the nonzero off-diagonal elements of **S**. **COL** contains the column number of each off-diagonal element. For example, the *fourth* element in **COL** is 1, indicating that the *fourth* element of **OFFDIAG**, -4.1, is located in column 1. **ROW** indicates the number of off-diagonal elements in each row of **S**. For example, the *first* element of **ROW** is 3, indicating the *first* three elements of **OFFDIAG**, -1.1, -2.1, and -3.1, are located in the *first* row. The *second* element of **ROW** is 2, indicating the next two elements of **OFFDIAG**, -4.1 and -5.1, are located in the *second* row. The **S** matrix can be completely reconstructed from these four vectors. Note that the dimension of **DIAG** and

ROW equals the number of diagonal elements of **S**, whereas the dimension of **OFFDIAG** and **COL** equals the number of nonzero off-diagonals.

Now assume that computer storage requirements are 4 bytes to store each magnitude and 4 bytes to store each phase of $\boldsymbol{Y}_{\text{bus}}$ in an N-bus power system. Also assume $\boldsymbol{Y}_{\text{bus}}$ has an average of $3N$ nonzero off-diagonals (three lines per bus) along with its N diagonals. Using the preceding compact storage technique, we need $(4+4)3N = 24N$ bytes for **OFFDIAG** and $(4+4)N = 8N$ bytes for **DIAG**. Also, assuming 2 bytes to store each integer, we need $6N$ bytes for **COL** and $2N$ bytes for **ROW**. Total computer memory required is then $(24+8+6+2)N = 40N$ bytes with compact storage of $\boldsymbol{Y}_{\text{bus}}$, compared to $8N^2$ bytes without compact storage. For a 1000-bus power system, this means 40 instead of 8000 kilobytes to store $\boldsymbol{Y}_{\text{bus}}$. Further storage reduction could be obtained by storing only the upper triangular portion of the symmetric $\boldsymbol{Y}_{\text{bus}}$ matrix.

The Jacobian matrix is also sparse. From Table 6.5, whenever $\mathrm{Y}_{kn} = 0$, $\mathrm{J1}_{kn} = \mathrm{J2}_{kn} = \mathrm{J3}_{kn} = \mathrm{J4}_{kn} = 0$. Compact storage of **J** for a 30,000-bus power system requires less than 10 megabytes with the above assumptions.

The other sparsity technique is to reorder buses. Suppose Gauss elimination is used to triangularize **S** in (6.8.1). After one Gauss elimination step, as described in Section 6.1, we have

$$\mathbf{S}^{(1)} = \begin{bmatrix} 1.0 & -1.1 & -2.1 & -3.1 \\ 0 & -2.51 & -8.61 & -7.61 \\ 0 & -6.71 & -9.81 & -18.91 \\ 0 & -7.81 & -14.91 & -18.01 \end{bmatrix} \tag{6.8.6}$$

We can see that the zeros in columns 2, 3, and 4 of **S** are filled in with nonzero elements in $\mathbf{S}^{(1)}$. The original degree of sparsity is lost.

One simple reordering method is to start with those buses having the fewest connected branches and to end with those having the most connected branches. For example, **S** in (6.8.1) has three branches connected to bus 1 (three off-diagonals in row 1), two branches connected to bus 2, and one branch connected to buses 3 and 4. Reordering the buses 4, 3, 2, 1 instead of 1, 2, 3, 4 we have

$$\mathbf{S}_{\text{reordered}} = \begin{bmatrix} 4.0 & 0 & 0 & -7.1 \\ 0 & 3.0 & 0 & -6.1 \\ -5.1 & 0 & 2.0 & -4.1 \\ -3.1 & -2.1 & -1.1 & 1.0 \end{bmatrix} \tag{6.8.7}$$

Now, after one Gauss elimination step,

$$\mathbf{S}^{(1)}_{\text{reordered}} = \begin{bmatrix} 4.0 & 0 & 0 & -7.1 \\ 0 & 3.0 & 0 & -6.1 \\ 0 & 0 & 2.0 & -13.15 \\ 0 & -2.1 & -1.1 & -4.5025 \end{bmatrix} \tag{6.8.8}$$

Note that the original degree of sparsity is not lost in (6.8.8).

Reordering buses according to the fewest connected branches can be performed once, before the Gauss elimination process begins. Alternatively, buses can be renumbered during each Gauss elimination step in order to account for changes during the elimination process.

Sparsity techniques similar to those described in this section are a standard feature of today's Newton–Raphson power-flow programs. As a result of these techniques, typical 30,000-bus power-flow solutions require less than 10 megabytes of storage, less than one second per iteration of computer time, and less than 10 iterations to converge.

EXAMPLE 6.16 Sparsity in a 37-bus system

To see a visualization of the sparsity of the power-flow Ybus and Jacobian matrices in a 37-bus system, open PowerWorld Simulator case Example 6_13.

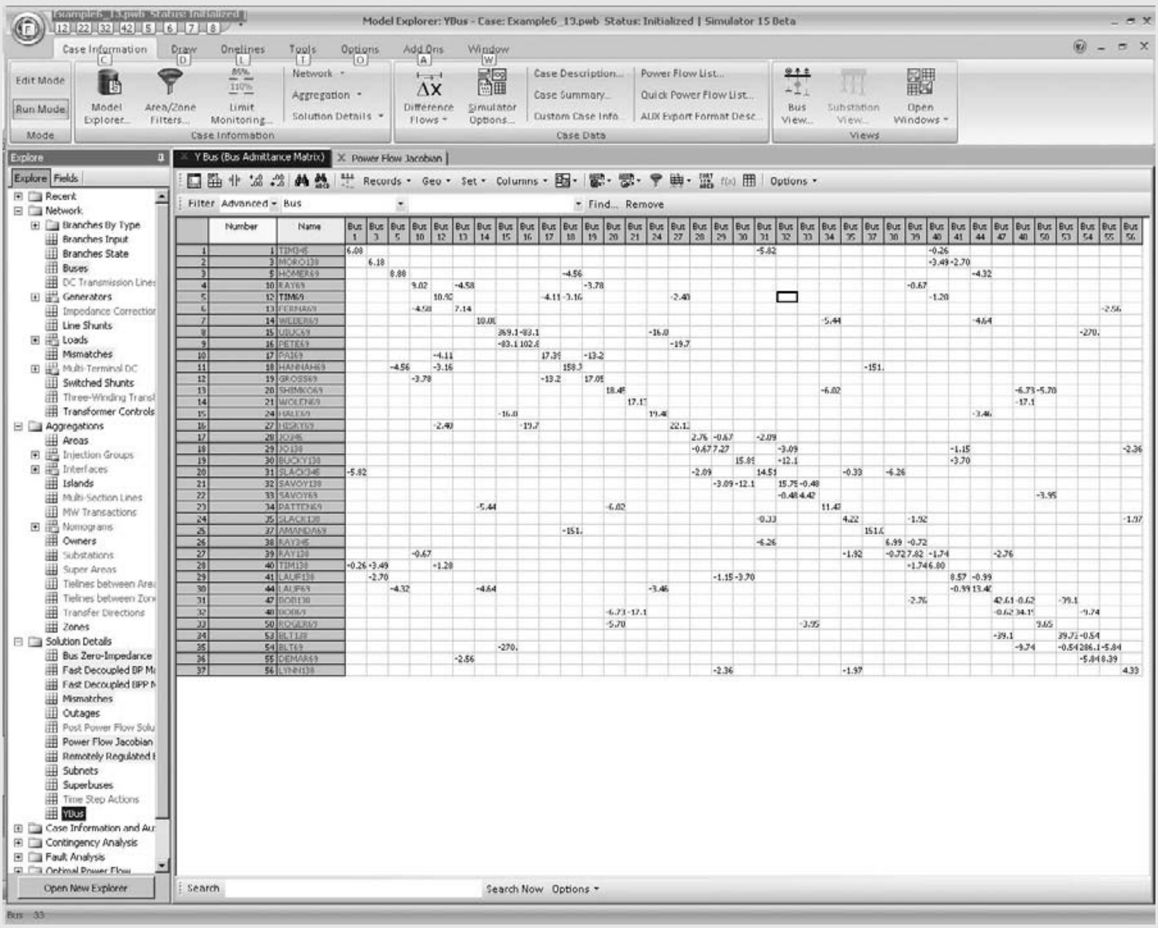

FIGURE 6.13 Screen for Example 6.16

Select **Case Information, Solution Details, Ybus** to view the bus admittance matrix. Then press ⟨ctrl⟩ Page Down to zoom the display out. Blank entries in the matrix correspond to zero entries. The 37×37 Ybus has a total of 1369 entries, with only about 10% nonzero (see Figure 6.13). Select **Case Information, Solution Details, Power Flow Jacobian** to view the Jacobian matrix. ■

6.9 FAST DECOUPLED POWER FLOW

Contingencies are a major concern in power system operations. For example, operating personnel need to know what power-flow changes will occur due to a particular generator outage or transmission-line outage. Contingency information, when obtained in real time, can be used to anticipate problems caused by such outages, and can be used to develop operating strategies to overcome the problems.

Fast power-flow algorithms have been developed to give power-flow solutions in seconds or less [8]. These algorithms are based on the following simplification of the Jacobian matrix. Neglecting $\mathbf{J}_2(i)$ and $\mathbf{J}_3(i)$, (6.6.6) reduces to two sets of decoupled equations:

$$\mathbf{J}_1(i)\Delta\boldsymbol{\delta}(i) = \Delta\mathbf{P}(i) \tag{6.9.1}$$

$$\mathbf{J}_4(i)\Delta\mathbf{V}(i) = \Delta\mathbf{Q}(i) \tag{6.9.2}$$

The computer time required to solve (6.9.1) and (6.9.2) is significantly less than that required to solve (6.6.6). Further reduction in computer time can be obtained from additional simplification of the Jacobian matrix. For example, assume $\mathrm{V}_k \approx \mathrm{V}_n \approx 1.0$ per unit and $\delta_k \approx \delta_n$. Then $\mathbf{J}_1$ and $\mathbf{J}_4$ are constant matrices whose elements in Table 6.5 are the negative of the imaginary components of $\boldsymbol{Y}_{\text{bus}}$. As such, $\mathbf{J}_1$ and $\mathbf{J}_4$ do not have to be recalculated during successive iterations.

The above simplifications can result in rapid power-flow solutions for most systems. While the fast decoupled power flow usually takes more iterations to converge, it is usually significantly faster then the Newton-Raphson algorithm since the Jacobian does not need to be recomputed each iteration. And since the mismatch equations themselves have not been modified, the solution obtained by the fast decoupled algorithm is the same as that found with the Newton-Raphson algorithm. However, in some situations in which only an approximate power-flow solution is needed the fast decoupled approach can be used with a fixed number of iterations (typically one) to give an extremely fast, albeit approximate solution.

6.10

THE "DC" POWER FLOW

The power-flow problem can be further simplified by extending the fast decoupled power flow to completely neglect the Q-V equation, assuming that the voltage magnitudes are constant at 1.0 per unit. With these simplifications the power flow on the line from bus j to bus k with reactive X_{jk} becomes

$$P_{jk} = \frac{\delta_j - \delta_k}{X_{jk}} \tag{6.10.1}$$

and the real power balance equations reduce to a completely linear problem

$$-\mathbf{B}\boldsymbol{\delta} = \mathbf{P} \tag{6.10.2}$$

where $\mathbf{B}$ is the imaginary component of the of $\mathbf{Y}_{\text{bus}}$ calculated neglecting line resistance and excepting the slack bus row and column.

Because (6.10.2) is a linear equation with a form similar to that found in solving dc resistive circuits, this technique is referred to as the dc power flow. However, in contrast to the previous power-flow algorithms, the dc power flow only gives an approximate solution, with the degree of approximation system dependent. Nevertheless, with the advent of power system restructuring the dc power flow has become a commonly used analysis technique.

EXAMPLE 6.17

Determine the dc power-flow solution for the five bus system from Example 6.9.

SOLUTION With bus 1 as the system slack, the $\mathbf{B}$ matrix and $\mathbf{P}$ vector for this system are

$$\mathbf{B} = \begin{bmatrix} -30 & 0 & 10 & 20 \\ 0 & -100 & 100 & 0 \\ 10 & 100 & -150 & 40 \\ 20 & 0 & 40 & -110 \end{bmatrix} \qquad \mathbf{P} = \begin{bmatrix} -8.0 \\ 4.4 \\ 0 \\ 0 \end{bmatrix}$$

$$\boldsymbol{\delta} = -\mathbf{B}^{-1}\mathbf{P} = \begin{bmatrix} -0.3263 \\ 0.0091 \\ -0.0349 \\ -0.0720 \end{bmatrix} \text{radians} = \begin{bmatrix} -18.70 \\ 0.5214 \\ -2.000 \\ -4.125 \end{bmatrix} \text{degrees}$$

To view this example in PowerWorld Simulator open case Example 6_17 which has this example solved using the dc power flow (see Figure 6.14). To view the dc power flow options select **Options, Simulator Options** to show the PowerWorld Simulator Options dialog. Then select the Power Flow Solution category, and the DC Options page.

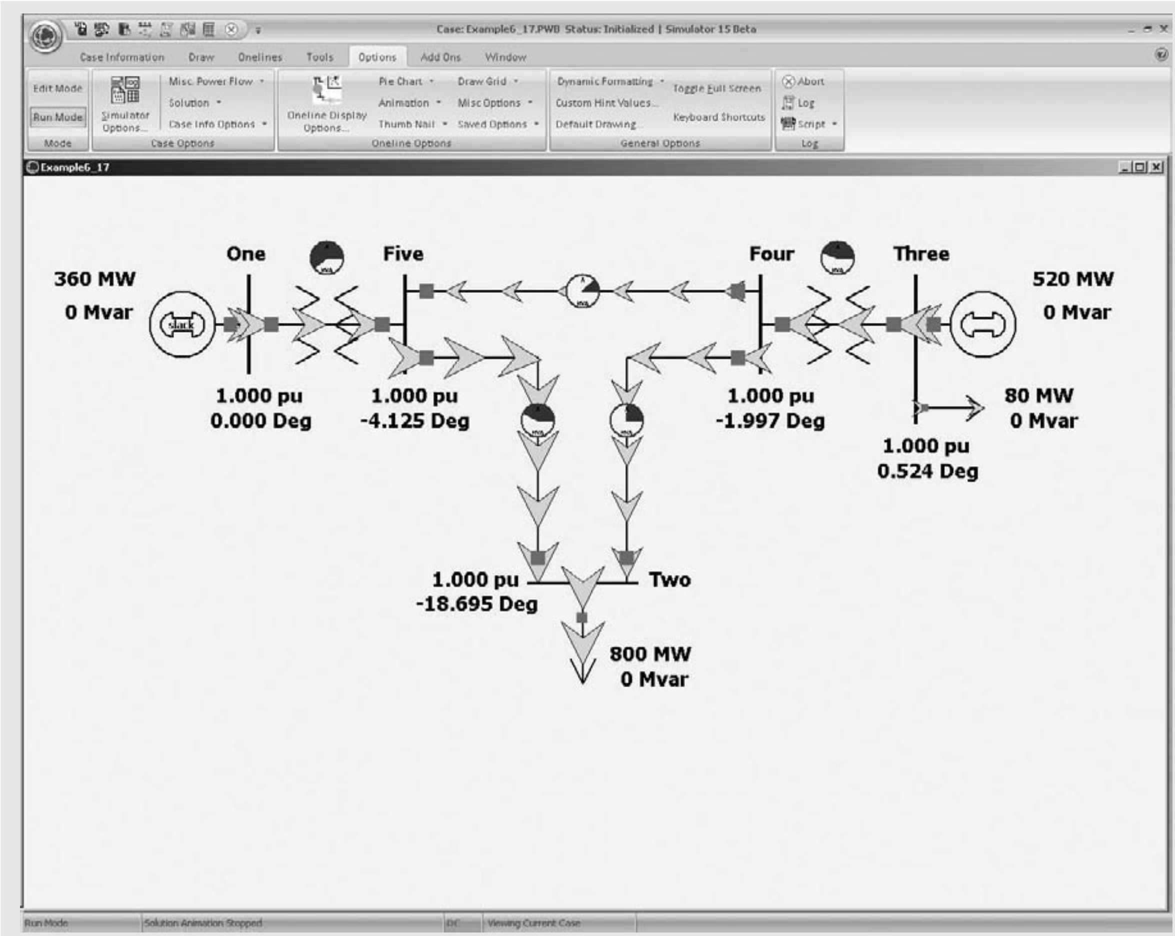

FIGURE 6.14 Screen for Example 6.17 ■

6.11 POWER-FLOW MODELING OF WIND GENERATION

As was mentioned in Chapter 1, the amount of renewable generation, particularly wind, being integrated into electric grids around the world is rapidly growing. For example, in 2008 Denmark obtained almost 20% of their total electric energy from wind while Spain was over 10%. In the United States that amount of wind capacity has been rapidly escalating from less than 2.5 GW in 2000 to more than 35 GW in 2009 (out of a total generation capacity of about 1000 GW).

Whereas most energy from traditional synchronous generators comes from large units with ratings of hundreds of MWs, comparatively speaking, individual wind turbine generator (WTG) power ratings are quite low, with

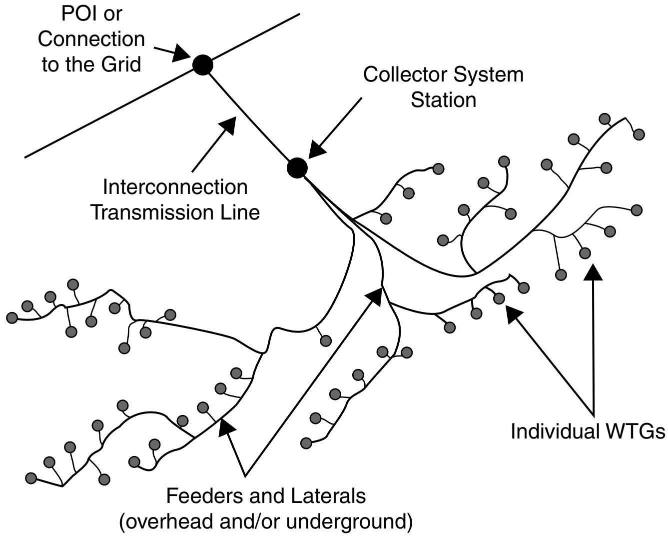

FIGURE 6.15 Wind power plant collector system topology [14] (Figure 1 from WECC Wind Generation Modeling Group, "WECC Wind Power Plant Power Flow Model Guide," WECC, May 2008, p. 2)

common values for new WTGs between one to three MWs. This power is generated at low voltage (e.g., 600 V) and then usually stepped-up with a pad-mounted transformer at the base of the turbine to a distribution-level voltage (e.g., 34.5 kV). Usually dozens or even hundreds of individual WTGs are located in wind "farms" or "parks" that cover an area of many square kilometers, with most of the land still available for other uses such as farming. An underground and/or overhead collector system is used to transmit the power to a single interconnection point at which its voltage is stepped-up to a transmission level voltage (> 100 kV). The layout of such a system is shown in Figure 6.15.

From a power system analysis perspective for large-scale studies the entire wind farm can usually be represented as a single equivalent generator which is either directly connected at the interconnection point transmission system bus, or connected to this bus through an equivalent impedance that represents the impedance of the collector system and the step-up transformers. The parameters associated with the equivalent generator are usually just scaled values of the parameters for the individual WTGs.

There are four main types of WTGs [13], with more details on each type provided in Chapter 11—here the focus is on their power-flow characteristics. As is the case with traditional synchronous generators, the real power outputs for all the WTG types are considered to be a constant value in power-flow studies. Of course how much real power a wind farm can actually produce at any moment depends upon the wind speed, with a typical wind speed versus power curve shown in Figure 6.16.

Type 1 WTGs are squirrel-cage induction machines. Since induction machines consume reactive power and their reactive power output cannot be independently controlled, typically these machines are modeled as a constant power factor PQ bus. By themselves these machines have under-excited

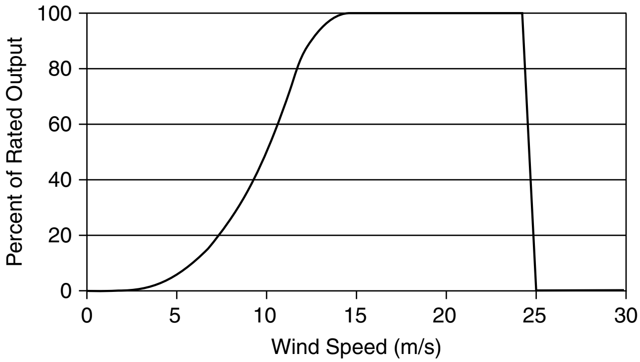

FIGURE 6.16

Typical wind speed versus power curve

(consuming reactive power) power factors of between 0.85 and 0.9, but banks of switched capacitors are often used to correct the wind farm power factor. Type 2 WTGs are wound rotor induction machines in which the rotor resistance can be controlled. The advantages of this approach are discussed in Chapter 11; from a power-flow perspective, they perform like Type 1 WTGs.

Most new WTGs are either Type 3 or Type 4. Type 3 wind turbines are used to represent doubly-fed asynchronous generators (DFAGs), also sometimes referred to as doubly-fed induction generators (DFIGs). This type models induction machines in which the rotor circuit is also connected to the ac network through an ac-dc-ac converter allowing for much greater control of the WTG. Type 4 wind turbines are fully asynchronous machines in which the full power output of the machine is coupled to the ac network through an ac-dc-ac converter. From a power-flow perspective both types are capable of full voltage control like a traditional PV bus generator with reactive power control between a power factor of up to $\pm$ 0.9. However, like traditional synchronous generators, how their reactive power is actually controlled depends on commercial considerations, with many generator owners desiring to operate at unity power factor to maximize their real power outputs.

MULTIPLE CHOICE QUESTIONS

SECTION 6.1

6.1 For a set of linear algebraic equations in matrix format, $\mathbf{Ax} = \mathbf{y}$, for a unique solution to exist, det ($\mathbf{A}$) should be ________. Fill in the Blank.

6.2 For an $N \times N$ square matrix $\mathbf{A}$, in $(N - 1)$ steps, the technique of gauss elimination can transform into an ________ matrix. Fill in the Blank.

SECTION 6.2

6.3 For the iterative solution to linear algebraic equations $\mathbf{Ax} = \mathbf{y}$, the $\mathbf{D}$ matrix in the Jacobi method is the ________ portion of $\mathbf{A}$, whereas $\mathbf{D}$ for Gauss-Siedel is the ________ portion of $\mathbf{A}$.

6.4 Is convergence guaranteed always with Jacobi and Gauss-Siedel methods, as applied to iterative solutions of linear algebraic equations?
(a) Yes (b) No

SECTION 6.3

6.5 For the iterative solutions to nonlinear algebraic equations with Newton-Raphson Method, the Jacobian Matrix **J** (i) consists of the partial derivatives. Write down the elements of first row of **J** (i).

6.6 For the Newton-Raphson method to work, one should make sure that $\mathbf{J}^{-1}$ exists.
(a) True (b) False

6.7 The Newton-Raphson method in four steps makes use of Gauss elimination and Back Substitution.
(a) True (b) False

6.8 The number of iterations required for convergence is dependent/independent of the dimension N for Newton-Raphson method. Choose one.

SECTION 6.4

6.9 The swing bus or slack bus is a reference bus for which $V_1\underline{/\delta_1}$, typically $1.0\underline{/0^\circ}$ per unit, is input data. The power-flow program computes ________. Fill in the Blank.

6.10 Most buses in a typical power-flow program are load buses, for which P_k and Q_k are input data. The power-flow program computes ________. Fill in the Blank.

6.11 For a voltage-controlled bus k, ________ are input data, while the power-flow program computes ________. Fill in the Blanks.

6.12 When the bus k is a load bus with no generation and inductive load, in terms of generation and load, $P_k =$ ________, and $Q_k =$ ________. Fill in the Blanks.

6.13 Starting from a single-line diagram of a power system, the input data for a power-flow problem consists of ________, ________, and ________. Fill in the Blanks.

SECTION 6.5

6.14 Nodal equations $\boldsymbol{I} = \boldsymbol{Y}_{\mathbf{bus}}\boldsymbol{V}$ are a set of linear equations analogous to $\boldsymbol{y} = \boldsymbol{A}\boldsymbol{x}$.
(a) True (b) False

6.15 Because of the nature of the power-flow bus data, nodal equations do not directly fit the linear-equation format, and power-flow equations are actually nonlinear. However, Gauss-Siedel method can be used for the power-flow solution.
(a) True (b) False

SECTION 6.6

6.16 The Newton-Raphson method is most well suited for solving the nonlinear power-flow equations.
(a) True (b) False

6.17 By default, PowerWorld Simulator uses ________ method for the power-flow solution. Fill in the Blank.

SECTION 6.7

6.18 Prime-mover control of a generator is responsible for a significant change in ________, whereas excitation control significantly changes ________. Fill in the Blanks.

6.19 From the power-flow standpoint, the addition of a shunt-capacitor bank to a load bus corresponds to the addition of a positive/negative reactive load. Choose the right word.

6.20 Tap-changing and voltage-magnitude-regulating transformers are used to control bus voltages and reactive power flows on lines to which they are connected.
(a) True (b) False

SECTION 6.8

6.21 A matrix, which has only a few nonzero elements, is said to be ________. Fill in the Blank.

6.22 Sparse-matrix techniques are used in Newton-Raphson power-flow programs in order to reduce computer ________ and ________ requirements. Fill in the Blanks.

6.23 Reordering buses can be an effective sparsity technique, in power-flow solution.
(a) True (b) False

SECTION 6.9

6.24 While the fast decoupled power flow usually takes more iterations to converge, it is usually significantly faster than the Newton-Raphson method.
(a) True (b) False

SECTION 6.10

6.25 The "dc" power-flow solution, giving approximate answers, is based on completely neglecting the Q–V equation, and solving the linear real-power balance equations.
(a) True (b) False

PROBLEMS

SECTION 6.1

6.1 Using Gauss elimination, solve the following linear algebraic equations:

$$-25x_1 + 5x_2 + 10x_3 + 10x_4 = 0$$
$$5x_1 - 10x_2 + 5x_3 = 2$$
$$10x_1 + 5x_2 - 10x_3 + 10x_4 = 1$$
$$10x_1 - 20x_4 = -2$$

6.2 Using Gauss elimination and back substitution, solve

$$\begin{bmatrix} 6 & 2 & 1 \\ 4 & 10 & 2 \\ 3 & 4 & 14 \end{bmatrix} \begin{bmatrix} x_1 \\ x_2 \\ x_3 \end{bmatrix} = \begin{bmatrix} 3 \\ 4 \\ 2 \end{bmatrix}$$

6.3 Rework Problem 6.2 with the value of A_{11} changed to 4.

6.4 What is the difficulty in applying Gauss elimination to the following linear algebraic equations?

$$-10x_1 + 10x_2 = 10$$
$$5x_1 - 5x_2 = -10$$

6.5 Show that, after triangularizing $\mathbf{Ax} = \mathbf{y}$, the back substitution method of solving $\mathbf{A}^{(N-1)}\mathbf{x} = \mathbf{y}^{(N-1)}$ requires N divisions, $N(N-1)/2$ multiplications, and $N(N-1)/2$ subtractions. Assume that all the elements of $\mathbf{A}^{(N-1)}$ and $\mathbf{y}^{(N-1)}$ are nonzero and real.

SECTION 6.2

6.6 Solve Problem 6.2 using the Jacobi iterative method. Start with $x_1(0) = x_2(0) = x_3(0) = 0$, and continue until (6.2.2) is satisfied with $\varepsilon = 0.01$.

6.7 Repeat Problem 6.6 using the Gauss–Seidel iterative method. Which method converges more rapidly?

6.8 Express the below set of equations in the form of (6.2.6), and then solve using the Jacobi iterative method with $\varepsilon = 0.05$, and $x_1(0), = 1, x_2(0) = 1, x_3(0) = 0$.

$$\begin{bmatrix} 10 & -2 & -4 \\ -2 & 6 & -2 \\ -4 & -2 & 10 \end{bmatrix} \begin{bmatrix} x_1 \\ x_2 \\ x_3 \end{bmatrix} = \begin{bmatrix} -2 \\ 3 \\ -1 \end{bmatrix}$$

6.9 Solve for x_1 and x_2 in the system of equations given by

$$x_2 - 3x_1 + 1.9 = 0$$
$$x_2 + x_1^2 - 3.0 = 0$$

by Gauss method with an initial guess of $x_1 = 1$ and $x_2 = 1$.

6.10 Solve $x^2 - 4x + 1 = 0$ using the Jacobi iterative method with $x(0) = 1$. Continue until (Eq. 6.2.2) is satisfied with $\varepsilon = 0.01$. Check using the quadratic formula.

6.11 Try to solve Problem 6.2 using the Jacobi and Gauss–Seidel iterative methods with the value of A_{33} changed from 14 to 0.14 and with $x_1(0) = x_2(0) = x_3(0) = 0$. Show that neither method converges to the unique solution.

6.12 Using the Jacobi method (also known as the Gauss method), solve for x_1 and x_2 in the system of equations.

$$x_2 - 3x_1 + 1.9 = 0$$
$$x_2 + {x_1}^2 - 1.8 = 0$$

Use an initial guess $x_1(0) = 1.0 = x_2(0) = 1.0$. Also, see what happens when you choose an uneducated initial guess $x_1(0) = x_2(0) = 100$.

6.13 Use the Gauss-Seidel method to solve the following equations that contain terms that are often found in power-flow equations.

$$x_1 = (1/(-20j)) * [(-1 + 0.5j)/(x_1)^* - (j10) * x_2 - (j10)]$$
$$x_2 = (1/(-20j)) * [(-3 + j)/(x_2)^* - (j10) * x_1 - (j10)]$$

Use an initial estimate of $x_1(0) = 1$ and $x_2(0) = 1$, and a stopping of $\varepsilon = 0.05$.

6.14 Find a root of the following equation by using the Gauss-Seidel method: (use an initial estimate of $x = 2$) $f(x) = x^3 - 6x^2 + 9x - 4 = 0$.

6.15 Use the Jacobi method to find a solution to $x^2 \cos x - x + 0.5 = 0$. Use $x(0) = 1$ and $\varepsilon = 0.01$. Experimentally determine the range of initial values that results in convergence.

6.16 Take the z-transform of (6.2.6) and show that $\mathbf{X}(z) = \mathbf{G}(z)\mathbf{Y}(z)$, where $\mathbf{G}(z) = (z\mathbf{U} - \mathbf{M})^{-1}\mathbf{D}^{-1}$ and $\mathbf{U}$ is the unit matrix.

$\mathbf{G}(z)$ is the matrix transfer function of a digital filter that represents the Jacobi or Gauss–Seidel methods. The filter poles are obtained by solving $\det(z\mathbf{U} - \mathbf{M}) = 0$. The filter is stable if and only if all the poles have magnitudes less than 1.

6.17 Determine the poles of the Jacobi and Gauss–Seidel digital filters for the general two-dimensional problem $(N = 2)$:

$$\left[\begin{array}{c|c} A_{11} & A_{12} \\ \hline A_{21} & A_{22} \end{array}\right] \begin{bmatrix} x_1 \\ x_2 \end{bmatrix} = \begin{bmatrix} y_1 \\ y_2 \end{bmatrix}$$

Then determine a necessary and sufficient condition for convergence of these filters when $N = 2$.

SECTION 6.3

6.18 Use Newton–Raphson to find a solution to the polynomial equation $f(x) = y$ where $y = 0$ and $f(x) = x^3 + 8x^2 + 2x - 50$. Start with $x(0) = 1$ and continue until (6.2.2) is satisfied with $\varepsilon = 0.001$.

6.19 Repeat 6.19 using $x(0) = -2$.

6.20 Use Newton–Raphson to find one solution to the polynomial equation $f(x) = y$, where $y = 7$ and $f(x) = x^4 + 3x^3 - 15x^2 - 19x + 30$. Start with $x(0) = 0$ and continue until (6.2.2) is satisfied with $\varepsilon = 0.001$.

6.21 Repeat Problem 6.20 with an initial guess of $x(1) = 4$.

6.22 For Problem 6.20 plot the function $f(x)$ between $x = 0$ and 4. Then provide a graphical interpretation why points close to $x = 2.2$ would be poorer initial guesses.

6.23 Use Newton–Raphson to find a solution to

$$\begin{bmatrix} e^{x_1 x_2} \\ \cos(x_1 + x_2) \end{bmatrix} = \begin{bmatrix} 1.2 \\ 0.5 \end{bmatrix}$$

where x_1 and x_2 are in radians. (a) Start with $x_1(0) = 1.0$ and $x_2(0) = 0.5$ and continue until (6.2.2) is satisfied with $\varepsilon = 0.005$. (b) Show that Newton–Raphson diverges for this example if $x_1(0) = 1.0$ and $x_2(0) = 2.0$.

6.24 Solve the following equations by the Newton–Raphson method:

$$2x_1^2 + x_2^2 - 10 = 0$$
$$x_1^2 - x_2^2 + x_1 x_2 - 4 = 0$$

Start with an initial guess of $x_1 = 1$ and $x_2 = 1$.

6.25 The following nonlinear equations contain terms that are often found in the power-flow equations:

$$f_1(x) = 10x_1 \sin x_2 + 2 = 0$$
$$f_2(x) = 10(x_1)^2 - 10x_1 \cos x_2 + 1 = 0$$

Solve using the Newton–Raphson method starting with an initial guess of $x_1(0) = 1$ and $x_2(0) = 0$ radians, and a stopping criteria of $\varepsilon = 10^{-4}$.

6.26 Repeat 6.25 except using $x_1(0) = 0.25$ and $x_2(0) = 0$ radians as an initial guess.

6.27 For the Newton–Raphson method the *region of attraction* (or *basin of attraction*) for a particular solution is the set of all initial guesses that converge to that solution. Usually initial guesses close to a particular solution will converge to that solution. However, for all but the simplest of multi-dimensional, nonlinear problems the region of attraction boundary is often fractal. This makes it impossible to quantify the region of attraction, and hence to guarantee convergence. Problem 6.25 has two solutions when x_2 is restricted to being between $-\pi$ and π. With the x_2 initial guess fixed at 0 radians, numerically determine the values of the x_1 initial guesses that converge to the Problem 6.25 solution. Restrict your search to values of x_1 between 0 and 1.

SECTION 6.4

6.28 Consider the simplified electric power system shown in Figure 6.17 for which the power-flow solution can be obtained without resorting to iterative techniques. (a) Compute the elements of the bus admittance matrix $\boldsymbol{Y}_{\text{bus}}$. (b) Calculate the phase angle δ_2 by using the real power equation at bus 2 (voltage-controlled bus). (c) Determine $|V_3|$ and δ_3 by using both the real and reactive power equations at bus 3 (load bus). (d) Find the real power generated at bus 1 (swing bus). (e) Evaluate the total real power losses in the system.

6.29 In Example 6.9, double the impedance on the line from bus 2 to bus 5. Determine the new values for the second row of $\boldsymbol{Y}_{\text{bus}}$. Verify your result using PowerWorld Simulator case Example 6.9.

6.30 Determine the bus admittance matrix ($\boldsymbol{Y}_{\text{bus}}$) for the following power three phase system (note that some of the values have already been determined for you). Assume a three-phase 100 MVA per unit base.

6.31 For the system from Problem 6.30, assume that a 75 Mvar shunt capacitance (three phase assuming one per unit bus voltage) is added at bus 4. Calculate the new value of Y_{44}.

FIGURE 6.17

Problem 6.27

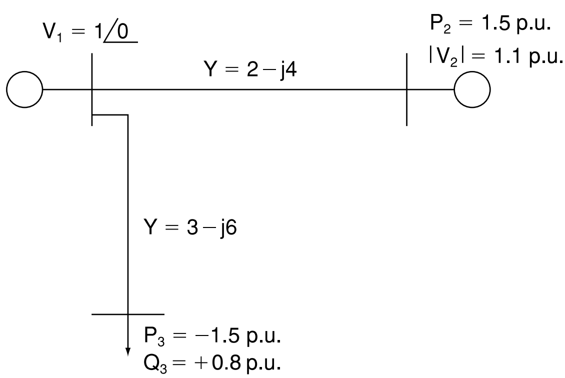

FIGURE 6.18

Sample System Diagram

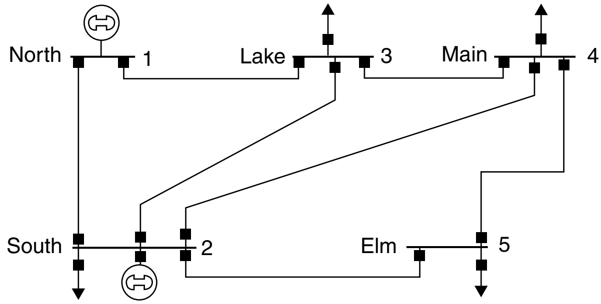

TABLE 6.9

Bus input data for Problem 6.30

Bus-to-Bus	R per unit	X per unit	B per unit
1-2	0.02	0.06	0.06
1-3	0.08	0.24	0.05
2-3	0.06	0.18	0.04
2-4	0.08	0.24	0.05
2-5	0.02	0.06	0.02
3-4	0.01	0.04	0.01
4-5	0.03	0.10	0.04

TABLE 6.10

Partially Completed Bus Admittance Matrix (Y_{bus})

$6.25 - j18.695$	$-5.00 + j15.00$	$-1.25 + j3.75$	0	0
$-5.00 + j15.00$				

SECTION 6.5

6.32 Assume a $0.8 + j0.4$ per unit load at bus 2 is being supplied by a generator at bus 1 through a transmission line with series impedance of $0.05 + j0.1$ per unit. Assuming bus 1 is the swing bus with a fixed per unit voltage of $1.0\underline{/0}$, use the Gauss-Seidel method to calculate the voltage at bus 2 after three iterations.

6.33 Repeat the above problem with the swing bus voltage changed to $1.0\underline{/30^\circ}$ per unit.

6.34 For the three bus system whose Y_{bus} is given below, calculate the second iteration value of V_3 using the Gauss-Seidel method. Assume bus 1 as the slack (with $V_1 = 1.0\underline{/0^\circ}$), and buses 2 and 3 are load buses with a per unit load of $S_2 = 1 + j0.5$ and $S_3 = 1.5 + j0.75$. Use voltage guesses of $1.0\underline{/0^\circ}$ at both buses 2 and 3. The bus admittance matrix for a three-bus system is

$$Y_{bus} = \begin{bmatrix} -j10 & j5 & j5 \\ j5 & -j10 & j5 \\ j5 & j2 & -j10 \end{bmatrix}$$

6.35 Repeat Problem 6.34 except assume the bus 1 (slack bus) voltage of $V_1 = 1.05\underline{/0^\circ}$.

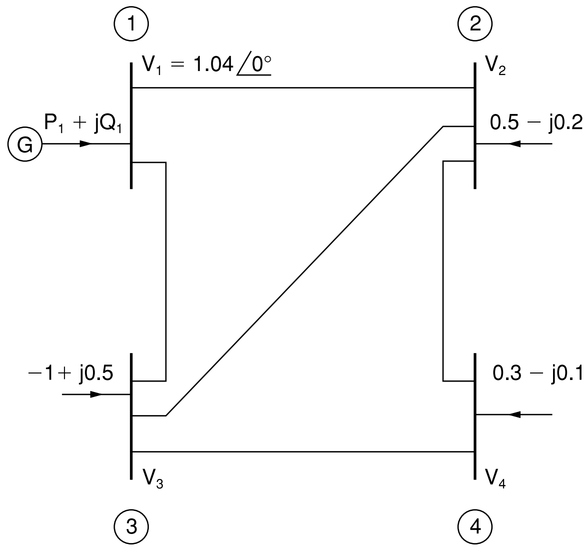

FIGURE 6.19
Problem 6.36

6.36 The bus admittance matrix for the power system shown in Figure 6.19 is given by

$$Y_{bus} = \begin{bmatrix} 3-j9 & -2+j6 & -1+j3 & 0 \\ -2+j6 & 3.666-j11 & -0.666+j2 & -1+j3 \\ -1+j3 & -0.666+j2 & 3.666-j11 & -2+j6 \\ 0 & -1+j3 & -2+j6 & 3-j9 \end{bmatrix} \text{ per unit}$$

With the complex powers on load buses 2, 3, and 4 as shown in Figure 6.19, determine the value for V_2 that is produced by the first and second iterations of the Gauss–Seidel procedure. Choose the initial guess $V_2(0) = V_3(0) = V_4(0) = 1.0\underline{/0°}$ per unit.

6.37 The bus admittance matrix of a three-bus power system is given by

$$Y_{bus} = -j\begin{bmatrix} 7 & -2 & -5 \\ -2 & 6 & -4 \\ -5 & -4 & 9 \end{bmatrix} \text{ per unit}$$

with $V_1 = 1.0\underline{/0°}$ per unit; $V_2 = 1.0$ per unit; $P_2 = 60$ MW; $P_3 = -80$ MW; $Q_3 = -60$ MVAR (lagging) as a part of the power-flow solution of the system, find V_2 and V_3 within a tolerance of 0.01 per unit, by using Gauss-Seidel iteration method. Start with $\delta_2 = 0$, $V_3 = 1.0$ per unit, and $\delta_3 = 0$.

SECTION 6.6

6.38 A generator bus (with a 1.0 per unit voltage) supplies a 150 MW, 50 Mvar load through a lossless transmission line with per unit (100 MVA base) impedance of $j0.1$ and no line charging. Starting with an initial voltage guess of $1.0\underline{/0°}$, iterate until converged using the Newton–Raphson power flow method. For convergence criteria use a maximum power flow mismatch of 0.1 MVA.

6.39 Repeat Problem 6.37 except use an initial voltage guess of $1.0\underline{/30°}$.

6.40 Repeat Problem 6.37 except use an initial voltage guess of $0.25\underline{/0°}$.

6.41 Determine the initial Jacobian matrix for the power system described in Problem 6.33.

6.42 Use the Newton–Raphson power flow to solve the power system described in Problem 6.34. For convergence criteria use a maximum power flow mismatch of 0.1 MVA.

6.43 For a three bus power system assume bus 1 is the swing with a per unit voltage of $1.0\underline{/0^\circ}$, bus 2 is a PQ bus with a per unit load of $2.0 + j0.5$, and bus 3 is a PV bus with 1.0 per unit generation and a 1.0 voltage setpoint. The per unit line impedances are j0.1 between buses 1 and 2, $j0.4$ between buses 1 and 3, and $j0.2$ between buses 2 and 3. Using a flat start, use the Newton–Raphson approach to determine the first iteration phasor voltages at buses 2 and 3.

6.44 Repeat Problem 6.42 except with the bus 2 real power load changed to 1.0 per unit.

PW **6.45** Load PowerWorld Simulator case Example 6.11; this case is set to perform a single iteration of the Newton–Raphson power flow each time **Single Solution** is selected. Verify that initially the Jacobian element J_{33} is 104.41. Then, give and verify the value of this element after each of the next three iterations (until the case converges).

PW **6.46** Load PowerWorld Simulator case Problem 6_46. Using a 100 MVA base, each of the three transmission lines have an impedance of $0.05 + j0.1$ pu. There is a single 180 MW load at bus 3, while bus 2 is a PV bus with generation of 80 MW and a voltage setpoint of 1.0 pu. Bus 1 is the system slack with a voltage setpoint of 1.0 pu. Manually solve this case using the Newton–Raphson approach with a convergence criteria of 0.1 MVA. Show all your work. Then verify your solution by solving the case with PowerWorld Simulator.

PW **6.47** As was mentioned in Section 6.4, if a generator's reactive power output reaches its limit, then it is modeled as though it were a PQ bus. Repeat Problem 6.46, except assume the generator at bus 2 is operating with its reactive power limited to a maximum of 50 Mvar. Then verify your solution by solving the case with PowerWorld Simulator. To increase the reactive power output of the bus 2 generator, select **Tools, Play** to begin the power flow simulation, then click on the up arrow on the bus 2 magenta voltage setpoint field until the reactive power output reaches its maximum.

PW **6.48** Load PowerWorld Simulator case Problem 6_46. Plot the reactive power output of the generator at bus 2 as a function of its voltage setpoint value in 0.005 pu voltage steps over the range between its lower limit of -50 Mvar and its upper limit of 50 Mvar. To change the generator 2 voltage set point first select **Tools, Play** to begin the power flow simulation, and then click on the up/down arrows on the bus 2 magenta voltage setpoint field.

SECTION 6.7

PW **6.49** Open PowerWorld Simulator case Problem 6_49. This case is identical to Example 6.9 except that the transformer between buses 1 and 5 is now a tap-changing transformer with a tap range between 0.9 and 1.1 and a tap step size of 0.00625. The tap is on the high side of the transformer. As the tap is varied between 0.975 and 1.1, show the variation in the reactive power output of generator 1, V_5, V_2, and the total real power losses.

PW **6.50** Use PowerWorld Simulator to determine the Mvar rating of the shunt capacitor bank in the Example 6_14 case that increases V_2 to 1.0 per unit. Also determine the effect of this capacitor bank on line loadings and the total real power losses (shown immediately below bus 2 on the one-line). To vary the capacitor's nominal Mvar rating, right-click on the capacitor symbol to view the Switched Shunt Dialog, and then change Nominal Mvar field.

PW **6.51** Use PowerWorld Simulator to modify the Example 6.9 case by inserting a second line between bus 2 and bus 5. Give the new line a circuit identifier of "2" to distinguish it from the existing line. The line parameters of the added line should be identical to those of the existing lines 2–5. Determine the new line's effect on V_2, the line loadings, and on the total real power losses.

PW **6.52** Open PowerWorld Simulator case Problem 6_52. Open the 69 kV line between buses HOMER69 and LAUF69 (shown toward the bottom-left). With the line open, determine the amount of Mvar (to the nearest 1 Mvar) needed from the HANNAH69 capacitor bank to correct the HANNAH69 voltage to at least 1.0 pu.

PW **6.53** Open PowerWorld Simulator case Problem 6_53. Plot the variation in the total system real power losses as the generation at bus BLT138 is varied in 20-MW blocks between 0 MW and 400 MW. What value of BLT138 generation minimizes the total system losses?

PW **6.54** Repeat Problem 6.53, except first remove the 138-69 kV transformer between BLT138 and BLT69.

SECTION 6.8

6.55 Using the compact storage technique described in Section 6.8, determine the vectors **DIAG**, **OFFDIAG**, **COL**, and **ROW** for the following matrix:

$$\mathbf{S} = \begin{bmatrix} 17 & -9.1 & 0 & 0 & -2.1 & -7.1 \\ -9.1 & 25 & -8.1 & -1.1 & -6.1 & 0 \\ 0 & -8.1 & 9 & 0 & 0 & 0 \\ 0 & -1.1 & 0 & 2 & 0 & 0 \\ -2.1 & -6.1 & 0 & 0 & 14 & -5.1 \\ -7.1 & 0 & 0 & 0 & -5.1 & 15 \end{bmatrix}$$

6.56 For the triangular factorization of the corresponding $\boldsymbol{Y}_{\text{bus}}$, number the nodes of the graph shown in Figure 6.9 in an optimal order.

SECTION 6.10

6.57 Compare the angles and line flows between the Example 6.17 case and results shown in Tables 6.6, 6.7, and 6.8.

6.58 Redo Example 6.17 with the assumption that the per unit reactance on the line between buses 2 and 5 is changed from 0.05 to 0.03.

PW **6.59** Open PowerWorld Simulator case Problem 6.58, which models a seven bus system using the dc power flow approximation. Bus 7 is the system slack. The real power generation/load at each bus is as shown, while the per unit reactance of each of the lines (on a 100 MVA base) is as shown in yellow on the one-line. (a) Determine the six by six **B** matrix for this system and the **P** vector. (b) Use a matrix package such as Matlab to verify the angles as shown on the one-line.

PW **6.60** Using the PowerWorld Simulator case from Problem 6.59, if the rating on the line between buses 1 and 3 is 65 MW, the current flow is 59 MW (from one to three), and the current bus one generation is 160 MW, analytically determine the amount this generation can increase until this line reaches 100% flow. Assume any change in the bus 1 generation is absorbed at the system slack.

SECTION 6.11

PW **6.61** PowerWorld Simulator cases Problem 6_61_PQ and 6_61_PV model a seven bus power system in which the generation at bus 4 is modeled as a Type 1 or 2 wind turbine in the first case, and as a Type 3 or 4 wind turbine in the second. A shunt capacitor is used to make the net reactive power injection at the bus the same in both cases. Compare the bus 4 voltage between the two cases for a contingency in which the line between buses 2 and 4 is opened. What is an advantage of a Type 3 or 4 wind turbine with respect to voltage regulation following a contingency? What is the variation in the Mvar output of a shunt capacitor with respect to bus voltage magnitude?

CASE STUDY QUESTIONS

A. What are some of the benefits of a high voltage electric transmission system?

B. Why is transmission capacity in the U.S. decreasing?

C. How has transmission planning changed since the mid 1990s?

D. How is the power flow used in the transmission planning process?

DESIGN PROJECT 1: A NEW WIND FARM

You've just been hired as a new power engineer with Kyle and Weber Wind (KWW), one of the country's leading wind energy developers. KWW has identified the rolling hills to the northwest of the Metropolis urban area as an ideal location for a new 200 MW wind farm. The local utility, Metropolis Light and Power (MLP), seems amenable to this new generation development taking place within their service territory. However, they are also quite adamant that any of the costs associated with transmission system upgrades necessary to site this new generation be funded by KWW. Therefore, your supervisor at KWW has requested that you do a preliminary transmission planning assessment to determine the least cost design.

Hence, your job is to make recommendations on the least cost design for the construction of new lines and transformers to ensure that the transmission system in the MLP system is adequate for any base case or first contingency loading situation when the KWW wind farm is installed and operating at its maximum output of 200 MW. Since the wind farm will be built with Type 3 DFAG wind turbines, you can model the wind farm in the power flow as a single, equivalent traditional PV bus generator with an output of 200 MW, a voltage setpoint of 1.05 per unit, and with reactive power limits of ± 100 Mvar. In keeping with KWW tradition, the wind interconnection point will be at 69 kV, and for reliability purposes your supervisor requests that there be two separate feeds into the interconnection substation.

The following table shows the available right-of-way distances for the construction of new 69 kV and/or new 138 kV lines. All existing 69 kV only substations are large enough to accommodate 138 kV as well.

Design Procedure

1. Load DesignCase1 into PowerWorld Simulator. This case contains the initial system power flow case, and the disconnected KWW generator and its interconnection bus. Perform an initial power-flow solution to determine the initial system operating point. From this solution you should find that all the line flows and bus voltage magnitudes are within their limits. Assume all line MVA flows must be at or below 100% of their limit values, and all voltages must be between 0.95 and 1.10 per unit.
2. Repeat the above analysis considering the impact of any single transmission line or transformer outage. This is known as n-1 contingency analysis. To simplify this analysis, PowerWorld Simulator has the ability to automatically perform a contingency analysis study. Select **Tools, Contingency Analysis** to show the Contingency Analysis display. Note that the 57 single line/transformer contingencies are already defined. Select **Start Run** (toward the bottom right corner of the display) to automatically see the impact of removing any single element. Without the KWW generation the system has no contingency (n-1) violations.
3. Using the available rights-of-ways and the transmission line parameters/costs given in the table, iteratively determine the least expensive system additions so that the base case and all the contingences result in reliable operation points with the KWW generation connected with an output of 200 MW. The parameters of the new transmission lines(s) need to be derived using the tower configurations and conductor types provided by the instructor. In addition, the transmission changes you propose will modify the total system losses, indicated by the yellow field on the one-line. While the system losses are not KWW's responsibility, your supervisor has asked you to consider the impact your design changes will have on the total system losses assuming the system operates in the studied condition for the next five years. Hence, you should minimize the total construction costs minus the savings associated with any decrease in system losses over the next five years.
4. Write a detailed report including the justification for your final recommendation.

Simplifying Assumptions

To simplify the analysis, several assumptions are made:

1. You need only consider the base case loading level given in DesignCase1. In a real design, typically a number of different operating points/loading levels must be considered.

2. You should consider all the generator real power outputs, including that of the new KWW generation, as fixed values. The change in the total system generation due to the addition of the 200 MW in KWW generation and any changes in the system losses are always picked up by the system slack.
3. You should not modify the status of the capacitors or the transformer taps.
4. You should assume that the system losses remain constant over the five-year period, and you need only consider the impact and new design has on the base case losses. The price for losses can be assumed to be $50/MWh.
5. You do not need to consider contingencies involving the new transmission lines and possibly any transformers you may be adding.

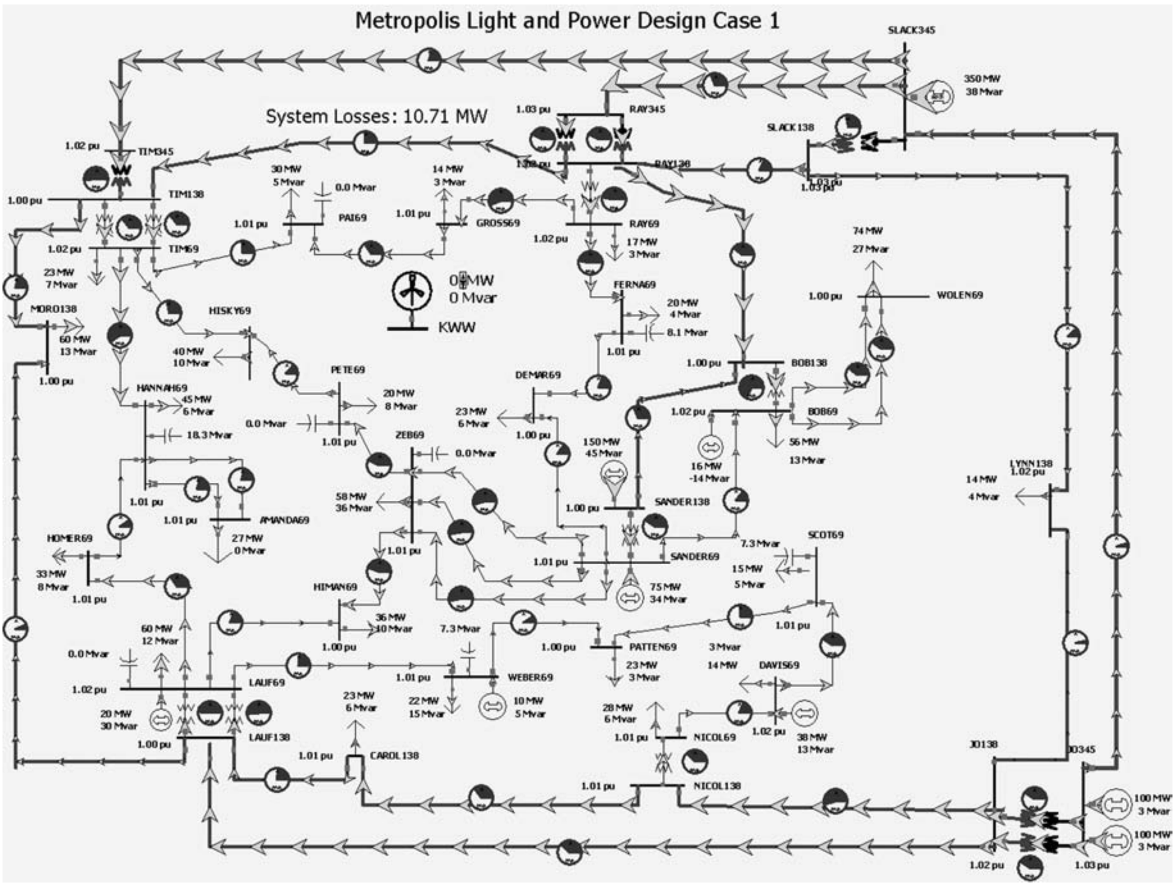

FIGURE 6.20 Design Case 1 System One-line Diagram

6. While an appropriate control response to a contingency might be to decrease the KWW wind farm output (by changing the pitch on the wind turbine blades), your supervisor has specifically asked you not to consider this possibility. Therefore the KWW generator should always be assumed to have a 200 MW output.

Available New Rights-of-Ways for Design Case 1

Right-of-Way/Substation	Right-of-Way Mileage(km)
KWW to PAI	9.66
KWW to PETE	11.91
KKWW to DEMAR	19.31
KKWW to GROSS	7.24
KKWW to HISKY	18.02
KKWW to TIM	20.92
KKWW to RAY	24.14
KWW to ZEB	17.7

DESIGN PROJECT 2: SYSTEM PLANNING FOR GENERATION RETIREMENT

After more than 70 years of supplying downtown Metropolis with electricity it is time to retire the SANDERS69 power plant. The city's downtown revitalization plan, coupled with a desire for more green space, make it impossible to build new generation in the downtown area. At the same time, a booming local economy means that the city-wide electric demand is still as high as ever, so this impending plant retirement is going to have some adverse impacts on the electric grid. As a planning engineer for the local utility, Metropolis Light and Power (MLP), your job is to make recommendations on the construction of new lines and transformers to ensure that the transmission system in the MLP system is adequate for any base case or first contingency loading situation. The below table shows the right-of-way distances that are available for the construction of new 69 kV and/or new 138 kV lines. All existing 69 kV only substations are large enough to accommodate 138 kV as well.

Design Procedure

1. Load DesignCase2 into PowerWorld Simulator which contains the system dispatch without the SANDERS69 generator. Perform an initial power flow solution to determine the initial system operating point. From this solution you should find that all the line flows and bus voltage magnitudes are within their limits. Assume all line MVA

flows must be at or below 100% of their limit values, and all voltages must be between 0.95 and 1.10 per unit.

2. Repeat the above analysis considering the impact of any single transmission line or transformer outage. This is known as n-1 contingency analysis. To simplify this analysis, PowerWorld Simulator has the ability to automatically perform a contingency analysis study. Select **Tools, Contingency Analysis** to show the Contingency Analysis display. Note that the 57 single line/transformer contingencies are already defined. Select **Start Run** (toward the bottom right corner of the display) to automatically see the impact of removing any single element. Without the SANDERS69 generation this system is insecure for several contingencies, including at least one that has nothing to do with the power plant retirement (but it still needs to be fixed).

3. Using the rights-of-way and the transmission line parameters/costs given in the table, iteratively determine the least expensive system additions so that the base case and all the contingences result in secure operation points. The parameters of the new transmission lines(s) need to be derived using the tower configurations and conductor types provided by the instructor. The total cost of an addition is defined as the construction costs minus the savings associated with any decrease in system losses over the next five years.

4. Write a detailed report discussing the initial system problems, your approach to optimally solving the system problems and the justification for your final recommendation.

Simplifying Assumptions

To simplify the analysis, several assumptions are made:

1. You need only consider the base case loading level given in DesignCase2. In a real design, typically a number of different operating points/loading levels must be considered.

2. You should consider the generator outputs as fixed values; any changes in the losses are always picked up by the system slack.

3. You should not modify the status of the capacitors or the transformer taps.

4. You should assume that the system losses remain constant over the five-year period and need only consider the impact and new design has on the base case losses. The price for losses can be assumed to be $50/MWh.

Available New Rights-of-Ways

Right-of-Way/Substation	Right-of-Way Mileage (km)
BOB to SCOT	13.68
BOB to WOLEN	7.72
FERNA to RAY	9.66
LYNN to SCOT	19.31
LYNN to WOLEN	24.14
SANDER to SCOTT	9.66
SLACK to WOLEN	18.51
JO to SCOT	24.14

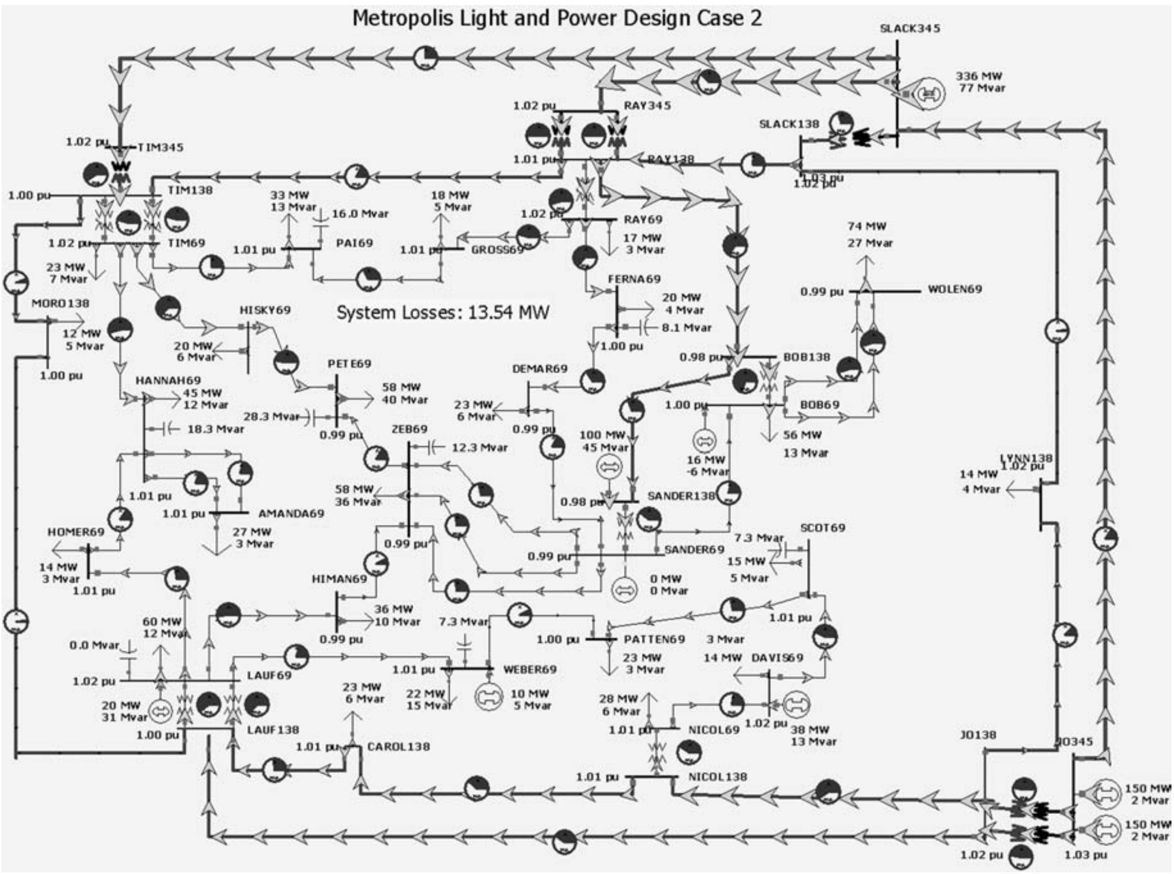

FIGURE 6.21 Design Case 2 System One-line Diagram

DESIGN PROJECTS 1 AND 2: SAMPLE TRANSMISSION SYSTEM DESIGN COSTS

Transmission lines (69 kV and 138 kV) New transmission lines include a fixed cost and a variable cost. The fixed cost is for the design work, the purchase/installation of the three-phase circuit breakers, associated relays, and changes to the substation bus structure. The fixed costs are **$200,000** for a 138-kV line and **$125,000** for a 69-kV line.

The variable costs depend on the type of conductor and the length of the line. The assumed cost in $/km are given here.

Conductor Type	Current Rating (Amps)	138-kV Lines	69-kV Lines
Rook	770	$250,000/km	$200,000/km
Crow	830	$270,000/km	$220,000/km
Condor	900	$290,000/km	$240,000/km
Cardinal	1110	$310,000/km	

Lined impedance data and MVA ratings are determined based on the conductor type and tower configuration. The conductor characteristics are given in Table A.4 of the book. For these design problems assume a symmetric tower configurations with the spacing between the conductors student specific. To find your specific value consult the table at the end of this design project.

Transformers (138 kV/69 kV) Transformer costs include associated circuit breakers, relaying and installation.

101 MVA	$950,000
187 MVA	$1,200,000

Assume any new 138/69 kV transformer has 0.0025 per unit resistance and 0.04 per unit reactance on a 100-MVA base.

Bus work

Upgrade 69-kV substation to 138/69 kV $200,000

DESIGN PROJECT 3: SYSTEM PLANNING*

Time given: 11 weeks
Approximate time required: 40 hours
Additional references: [10, 11]

*This case is based on a project assigned by Adjunct Professor Leonard Dow at Northeastern University, Boston, Massachusetts.

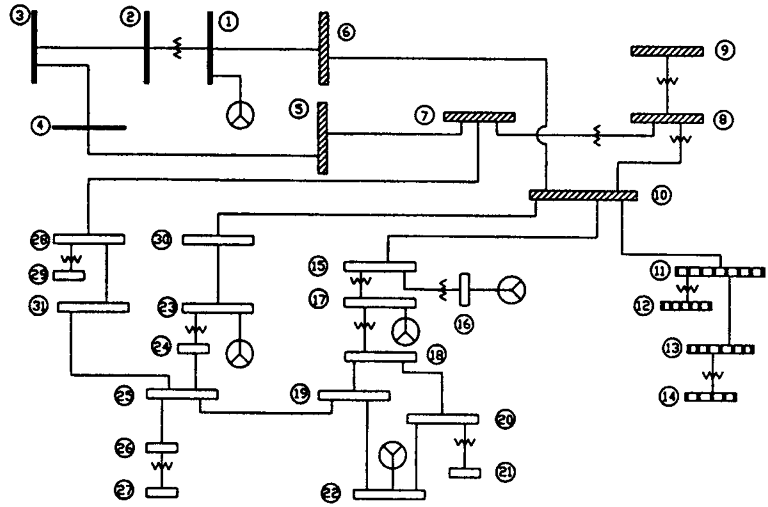

FIGURE 6.22

Design Project 3: Single-line diagram for 31-bus interconnected power system

Figure 6.22 shows a single-line diagram of four interconnected power systems identified by different graphic bus designations. The following data are given:

1. There are 31 buses, 21 lines, and 13 transformers.
2. Generation is present at buses 1, 16, 17, 22, and 23.
3. Total load of the four systems is 400 MW.
4. Bus 1 is the swing bus.
5. The system base is 100 MVA.
6. Additional information on transformers and transmission lines is provided in [10, 11].

Based on the data given:

1. Allocate the total 400-MW system load among the four systems.
2. For each system, allocate the load to buses that you want to represent as load buses. Select reasonable load power factors.
3. Taking into consideration the load you allocated above, select appropriate transmission-line voltage ratings, MVA ratings, and distances necessary to supply these loads. Then determine per-unit transmission-line impedances for the lines shown on the single-line diagram (show your calculations).
4. Also select appropriate transformer voltage and MVA ratings, and determine per-unit transformer leakage impedances for the transformers shown on the single-line diagram.
5. Develop a generation schedule for the 5 generator buses.

6. Show on a copy of the single-line diagram per-unit line impedances, transformer impedances, generator outputs, and loads that you selected above.
7. Using PowerWorld Simulator, run a base case power flow. In addition to the printed input/output data files, show on a separate copy of the single-line diagram per-unit bus voltages as well as real and reactive line flows, generator outputs, and loads. Flag any high/low bus voltages for which $0.95 \le V \le 1.05$ per unit and any line or transformer flows that exceed normal ratings.
8. If the base case shows any high/low voltages or ratings exceeded, then correct the base case by making changes. Explain the changes you have made.
9. Repeat (7). Rerun the power-flow program and show your changes on a separate copy of the single-line diagram.
10. Provide a typed summary of your results along with your above calculations, printed power-flow input/output data files, and copies of the single-line diagram.

DESIGN PROJECT 4: POWER FLOW/SHORT CIRCUITS

Time given: 3 weeks
Approximate time required: 15 hours

Each student is assigned one of the single-line diagrams shown in Figures 6.23 and 6.24. Also, the length of line 2 in these figures is varied for each student.

Assignment 1: Power-Flow Preparation

For the single-line diagram that you have been assigned (Figure 6.23 or 6.24), convert all positive-sequence impedance, load, and voltage data to per unit using the given system base quantities. Then using PowerWorld Simulator, create three input data files: bus input data, line input data, and transformer input data. Note that bus 1 is the swing bus. Your output for this assignment consists of three power-flow input data files.

The purpose of this assignment is to get started and to correct errors before going to the next assignment. It requires a knowledge of the per-unit system, which was covered in Chapter 3, but may need review.

Assignment 2: Power Flow

Case 1. Run the power flow program and obtain the bus, line, and transformer input/output data files that you prepared in Assignment 1.

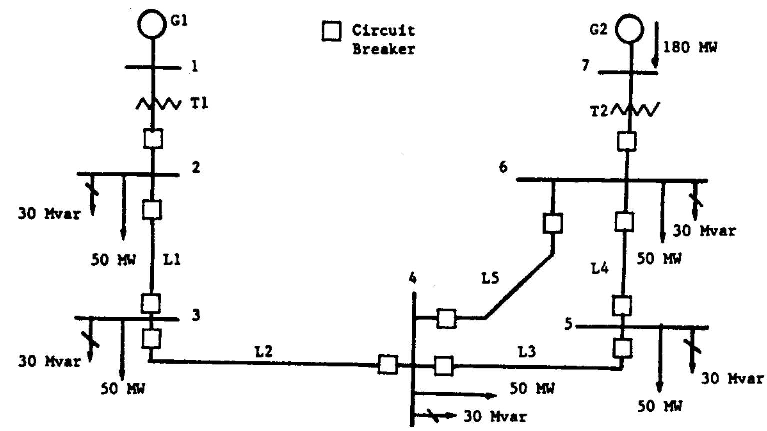

<u>Generator Ratings</u>
G1: 100 MVA, 13.8 kV, $x'' = 0.12, x_2 = 0.14, x_0 = 0.05$ per unit
G2: 200 MVA, 15.0 kV, $x'' = 0.12, x_2 = 0.14, x_0 = 0.05$ per unit
The generator neutrals are solidly grounded
<u>Transformer Ratings</u>
T1: 100 MVA, 13.8 kVΔ/230 kVY, x=0.1 per unit
T2: 200 MVA, 15 kVΔ/230 kVY, x=0.1 per unit
The transformer neutrals are solidly grounded
<u>Transmission Line Ratings</u>
All Lines: 230 kV, $z_1 = 0.08 + j0.5$ Ω/km,
$z_0 = 0.2 + j1.5$ Ω/km, $y_1 = j3.3$ E-6 S/km,
Maximum MVA = 400
Line Lengths: $L_1 = 15$ km, L_2 assigned by the instructor (20 to 50 km), $L_3 = 40$ km, $L_4 = 15$ km, $L_5 = 50$ km.

<u>Power Flow Data</u>
Bus 1 : Swing bus, $V_1 = 13.8$ kV, $\delta_1 = 0°$
Bus 2,3,4,5,6 : Load buses
Bus 7 : Constant voltage magnitude bus, $V_7 = 15$ kV, $P_{G7} = 180$ MW, -87 Mvar < Q_{G7} < $+87$ Mvar
<u>System Base Quantities</u>
$S_{base} = 100$ MVA (three-phase)
$V_{base} = 13.8$ kV (line-to-line) in the zone of G1

FIGURE 6.23 Single-line diagram for Design Project 4—transmission loop

Case 2. Suggest one method of increasing the voltage magnitude at bus 4 by 5%. Demonstrate the effectiveness of your method by making appropriate changes to the input data of case 1 and by running the power flow program.

Your output for this assignment consists of 12 data files, 3 input and 3 output data files for each case, along with a one-paragraph explanation of your method for increasing the voltage at bus 4 by 5%.

During this assignment, course material contains voltage control methods, including use of generator excitation control, tap changing and regulating transformers, static capacitors, static var systems, and parallel transmission lines.

This project continues in Chapters 7 and 9.

DESIGN PROJECT 5: POWER FLOW*

Time given: 4 weeks
Approximate time required: 25 hours

*This case is based on a project assigned by Adjunct Professor Richard Farmer at Arizona State University, Tempe, Arizona.

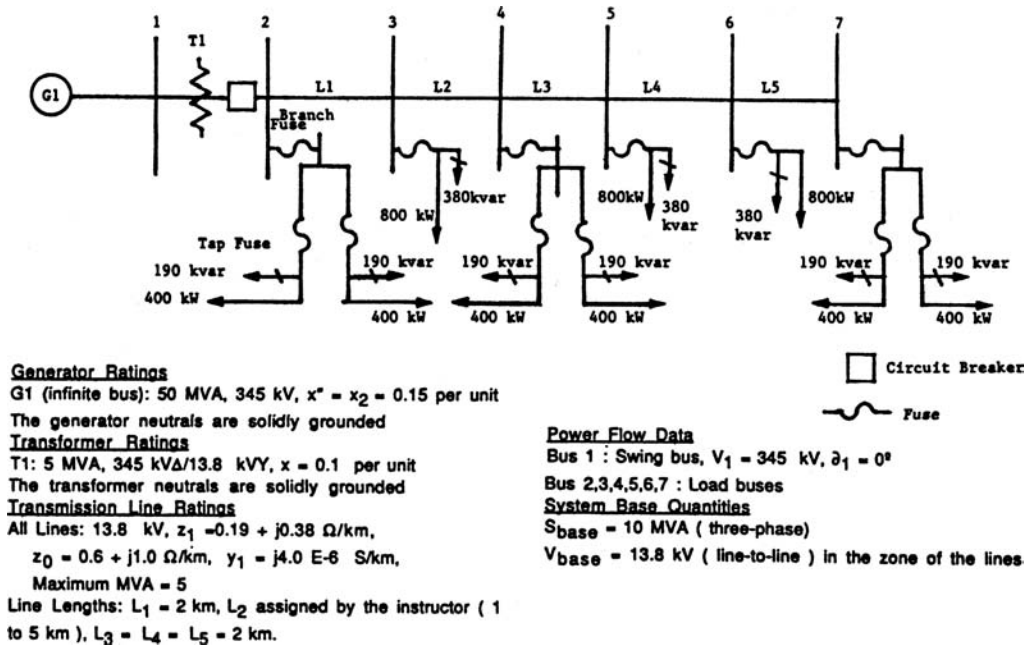

FIGURE 6.24 Single-line diagram for Design Project 4—radial distribution feeder

Figure 6.25 shows the single-line diagram of a 10-bus power system with 7 generating units, 2 345-kV lines, 7 230-kV lines, and 5 transformers. Per-unit transformer leakage reactances, transmission-line series impedances and shunt susceptances, real power generation, and real and reactive loads during heavy load periods, all on a 100-MVA system base, are given on the diagram. Fixed transformer tap settings are also shown. During light load periods, the real and reactive loads (and generation) are 25% of those shown. Note that bus 1 is the swing bus.

Design Procedure

Using PowerWorld Simulator (convergence can be achieved by changing load buses to constant voltage magnitude buses with wide var limits), determine:

1. The amount of shunt compensation required at 230- and 345-kV buses such that the voltage magnitude $0.99 \leq V \leq 1.02$ per unit at all buses during both light and heavy loads. Find two settings for the compensation, one for light and one for heavy loads.
2. The amount of series compensation required during heavy loads on each 345-kV line such that there is a maximum of 40° angular displacement between bus 4 and bus 10. Assume that one 345-kV line is

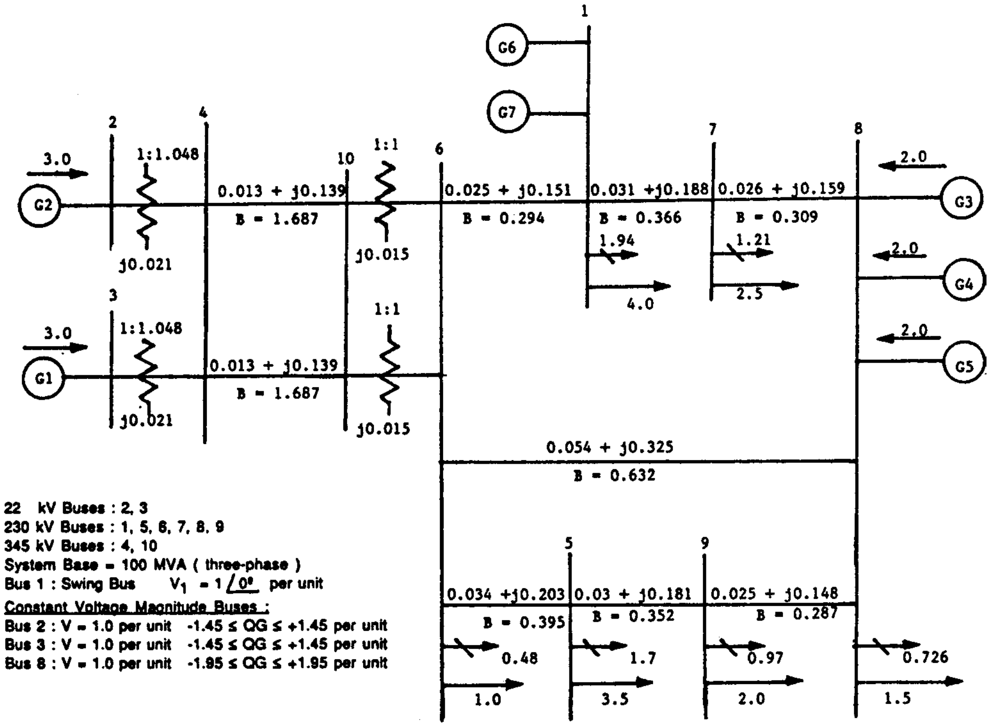

FIGURE 6.25 Single-line diagram for Design Project 5—10-bus power system

out of service. Also assume that the series compensation is effectively distributed such that the net series reactance of each 345-kV line is reduced by the percentage compensation. Determine the percentage series compensation to within $\pm 10\%$.

REFERENCES

1. W. F. Tinney and C. E. Hart, "Power Flow Solutions by Newton's Method," *IEEE Trans. PAS*, *86* (November 1967), p. 1449.
2. W. F. Tinney and J. W. Walker, "Direct Solution of Sparse Network Equations by Optimally Ordered Triangular Factorization," *Proc. IEEE*, *55* (November 1967), pp. 1801–1809.
3. Glenn W. Stagg and Ahmed H. El-Abiad, *Computer Methods in Power System Analysis* (New York: McGraw-Hill, 1968).
4. N. M. Peterson and W. S. Meyer, "Automatic Adjustment of Transformer and Phase Shifter Taps in Newton Power Flow," *IEEE Trans. PAS*, *90* (January–February 1971), pp. 103–108.

5. W. D. Stevenson, Jr., *Elements of Power Systems Analysis*, 4th ed. (New York: McGraw-Hill, 1982).

6. A. Bramellar and R. N. Allan, *Sparsity* (London: Pitman, 1976).

7. C. A. Gross, *Power Systems Analysis* (New York: Wiley, 1979).

8. B. Stott, "Fast Decoupled Load Flow," *IEEE Trans. PAS*, Vol. PAS 91 (September–October 1972), pp. 1955–1959.

9. T. Overbye and J. Weber, "Visualizing the Electric Grid," *IEEE Spectrum*, 38, 2 (February 2001), pp. 52–58.

10. Westinghouse Electric Corporation, *Transmission and Distribution Reference Book*, 4th ed. (Pittsburgh: Westinghouse, 1964).

11. Aluminum Association, *The Aluminum Electrical Conductor Handbook* (Washington, D.C.: Aluminum Association).

12. A. J. Wood and B. F. Wollenberg, *Power Generation, Operation and Control*, 2nd ed. (New York: John Wiley & Sons, 1996).

13. A. Ellis, "Wind Power Plant Models for System Studies," Tutorial on Fundamentals of Wind Energy, Section V, *IEEE PES GM* (Calgary, AB: July 2009).

14. WECC Wind Generator Modeling Group, "WECC Wind Power Plant Power Flow Modeling Guide," *WECC*, May 2008.

15. E.H. Camm, et. al., "Characteristics of Wind Turbine Generators for Wind Power Plants," *Proc. IEEE* 2009 General Meeting (Calgary, AB: July 2009).